New Insights into *Leishmania* Stress Tolerance: The Impact of the Small Heat Shock Protein 23 and Casein Kinase 1.2

Dissertation

For the award of the degree

"*doctor rerum naturalium*"

(Dr. rer. nat.)

at the Faculty of

Mathematics, Informatics, and Natural Science

Department of Biology

University of Hamburg

submitted by

Constanze Kröber-Boncardo

from Aachen, Germany

Hamburg, 2020

Genehmigt vom Fachbereich der Biologie
der Fakultät für Mathematik, Informatik und Naturwissenschaften
der Universität Hamburg
auf Antrag von PD Dr. Joachim Clos
Weitere Gutachter der Dissertation: Prof. Dr. Tim.Gilberger
Prof. Dr. Gabriele Pradel
Tag der Disputation: 12. Februar 2021
Vorsitzende der Prüfungskommission: Prof. Dr. Esther Schnettler
Hamburg, 28. Februar 2021

This work has been conducted from October 2017 to September 2020 in the research group of PD Dr. Joachim Clos at the Bernhard-Nocht-Institute for Tropical Medicine in Hamburg.

1st Evaluator:

PD Dr. Joachim Clos

Bernhard-Nocht-Institut für Tropenmedizin
Bernhard-Nocht-Straße 74, 20359 Hamburg

2nd Evaluator:

Prof. Dr. Tim-Wolf Gilberger

Center for Structural Systems Biology (CSSB)
Notkestraße 85, 22607 Hamburg

Eidesstattliche Versicherung

Hiermit erkläre ich an Eides statt, dass ich die vorliegende Dissertationsschrift selbst verfasst und keine anderen als die angegebenen Quellen und Hilfsmittel benutzt habe.

Hamburg, den 08.09.2020

Abstract

Protozoa of the genus *Leishmania* are the causative agents of a spectrum of diseases, collectively known as leishmaniases. Depending on the *Leishmania* species and the immune status of the host, the clinical manifestations range from spontaneously healing ulcerated skin lesions to disseminated visceral infections. To date, there are no effective vaccines and the current antileishmanial treatments are limited to expensive and toxic chemo-therapies.

During its life cycle, *Leishmania* parasites alternate between two distinct developmental stages: the extracellular, flagellated promastigote in the insect vector and the intracellular, aflagellated amastigote form inside the mammalian host. The transition from promastigotes to amastigotes is induced by an increase of temperature and the acidic pH, which the parasites encounter within the phagolysosome of the host macrophages. At the same time, the temperature shift also induces a classic cellular stress response, with increased synthesis of several heat shock protein families including the small heat shock protein 23. This protein was recently characterised in *L. donovani,* the causative agent of visceral leishmaniasis, and was found to be essential at mammalian tissue temperature (37°C) as demonstrated by a *bona fide* temperature-sensitive (TS) phenotype of HSP23$^{-/-}$ null mutants [1]. Since HSP23 has no homologues in humans and is structurally different from human small heat shock proteins, it was proposed as a potential drug target.

In this thesis, I analysed the suitability of HSP23 as drug target by addressing two questions: (i) is the essential function of HSP23 conserved among *Leishmania* and closely related *Trypanosoma* species and (ii) is there a bypass for the lack of HSP23 that can restore parasite fitness and viability at both ambient and mammalian temperatures?

Indeed, generation and subsequent phenotype analysis of *L. major* HSP23$^{-/-}$ null mutants revealed the same stress and TS phenotype as observed previously for *L. donovani* HSP23$^{-/-}$ null mutants. Furthermore, the conserved functionality of HSP23 was confirmed by complementation studies showing that *L. donovani* and *L. major* HSP23$^{-/-}$ null mutants could be complemented phenotypically with HSP23 transgenes from a range of trypanosomatids.

I further report the spontaneous emergence of an LdHSP23$^{-/-}$ escape variant named LdHSP23$^{-/-}$ esc0. This mutant was characterised by (i) a wild type-like growth at permissive temperatures, (ii) restored tolerance to ethanol and (iii) increased resistance to hydrogen peroxide. A preselection at non-permissive temperatures followed by a recovery period at permissive temperatures further allowed to select for two temperature-tolerant LdHSP23$^{-/-}$ mutant populations. To gain further insights into the compensatory molecular mechanisms, I resorted to comparative genomics which revealed major strain-specific differences associated with the loss of HSP23. Particularly interesting was the selective, either partial or complete, amplification of chromosome 35 that was observed for all investigated LdHSP23$^{-/-}$ mutant lines. I confirmed that somy and gene copy number variations, but in particular the massive amplification of a six-gene cluster on chromosome 35 in the temperature-tolerant

LdHSP23$^{-/-}$ mutant lines, correlated well with elevated transcript and protein abundance. To identify the genes involved in rescuing the TS phenotype of HSP23$^{-/-}$ null mutants, I implemented a functional cloning approach in which the respective candidates were collectively over expressed as transgenes in TS HSP23$^{-/-}$ mutants. Following a continuous selection at either permissive or non-permissive temperatures, over expression plasmids were again recovered from the selected parasite cultures and analysed for the presence of transgenes by PCR. This revealed that over expression of a protein kinase, namely casein kinase 1.2 (LdBPK_351030), is responsible and sufficient to rescue the TS phenotype of HSP23$^{-/-}$ null mutants. In addition, *in vitro* phosphorylation experiments established both HSP23 and the related P23 co-chaperone as substrates and modulators of casein kinase 1.2.

In summary, I showed that spontaneous genetic adaptations can overcome the loss of HSP23 function, ruling out HSP23 as a therapeutic target against *Leishmania* infections. Also, this study provides evidence for a crucial link between chaperones and signal transduction protein kinases in this early-branching eukaryote and contributes to the understanding of how trypanosomatids adapt to changing conditions.

Zusammenfassung

Protozoen der Gattung *Leishmania* sind die Erreger verschiedener Krankheiten, die kollektiv als Leishmaniosen bezeichnet werden. Je nach *Leishmania*-Art und Immunstatus des Wirts kommt es zu unterschiedlichen Krankheitsformen, die von spontan heilenden ulzerierenden Hautläsionen bis hin zu disseminierten viszeralen Verläufen reichen. Bis heute stehen keine wirksamen Impfstoffe zur Verfügung und die gegenwärtigen Leishmaniose-Therapien beschränken sich auf teure und/oder toxische Chemotherapien.

Während ihres Lebenszyklus durchlaufen *Leishmania* Parasiten zwei unterschiedliche Entwicklungsstadien: die extrazelluläre, begeißelte Promastigote in der Sandmücke und die intrazelluläre, unbegeißelte Amastigote innerhalb des Säugetierwirts. Die Differenzierung von Promastigoten zu Amastigoten wird durch die höhere Temperatur und den sauren pH-Wert innerhalb des Phagolysosoms der Wirtsmakrophage induziert. Gleichzeitig kommt es zu einer klassischen zellulären Stressantwort, also einer erhöhten Synthese mehrerer Hitzeschockproteine, darunter auch des kleinen Hitzeschockproteins 23. Dieses Protein wurde zuvor in *L. donovani*, dem Erreger der viszeralen Leishmaniose, charakterisiert und ist, wie durch den temperatursensitiven (TS) Phänotyp von HSP23$^{-/-}$ Nullmutanten gezeigt wurde [1], essenziell für das Überleben des Parasiten bei erhöhten Temperaturen (37°C). Da keine HSP23 Homologe im Menschen existieren und HSP23 sich zudem strukturell von kleinen Hitzeschockproteinen des Menschen unterscheidet, stellt es einen potenziellen Angriffspunkt für Wirkstoffe dar.

In dieser Arbeit habe ich anhand zweier Fragen die Eignung von HSP23 als möglichen Angriffspunkt für Medikamente analysiert: (i) Ist die essenzielle Funktion von HSP23 in Leishmanien- und den nah verwandten *Trypanosoma*-Spezies konserviert und (ii) gibt es einen *Bypass* für das Fehlen von HSP23, der die Fitness und Lebensfähigkeit der Parasiten sowohl bei Umgebungs- als auch bei Säugetiertemperaturen wiederherstellen kann?

Tatsächlich zeigte die Phänotypanalyse von *L. major* HSP23$^{-/-}$ Nullmutanten den gleichen Stress- und TS Phänotyp wie bereits zuvor die *L. donovani* HSP23$^{-/-}$ Nullmutanten. Darüber hinaus wurde die konservierte Funktionalität von HSP23 durch Komplementationsstudien bestätigt, die zeigten, dass *L. donovani* und *L. major* HSP23$^{-/-}$ Nullmutanten phänotypisch mit HSP23 Transgenen von anderen Trypanosomatiden kompensiert werden können.

Zudem berichte ich über die spontane Entstehung einer LdHSP23$^{-/-}$ *escape*-Variante, LdHSP23-/- esc0. Diese Mutante zeigte (i) ein Wildtyp-ähnliches Wachstum bei permissiven Temperaturen, (ii) eine wiederhergestellte Toleranz gegenüber Ethanol und (iii) eine erhöhte Resistenz gegenüber Wasserstoffperoxid. Eine Selektion bei nicht-permissiven Temperaturen, gefolgt von einer Inkubation bei permissiven Temperaturen, ermöglichte die Selektion von zwei temperaturtoleranten LdHSP23$^{-/-}$ Populationen. Für die Identifizierung der zugrunde liegenden kompensatorischen molekularen Mechanismen führte ich eine vergleichende Analyse der Genome durch, die wesentliche stammspezifische Unterschiede

im Zusammenhang mit dem Verlust von HSP23 aufzeigte. Besonders interessant war die selektive, partielle oder vollständige Amplifikation von Chromosom 35, die in allen untersuchten LdHSP23$^{-/-}$ Mutanten zu beobachten war. Ich konnte bestätigten, dass Veränderungen der Chromosomen- und Genkopienzahl, insbesondere aber die massive Amplifikation eines sechs Gene umfassenden Bereichs auf Chromosom 35 in den temperaturtoleranten LdHSP23$^{-/-}$ Mutantenlinien, mit einer erhöhten Transkript- und Proteinabundanz korrelierten. Um die Gene zu identifizieren, die den TS Phänotyp von HSP23$^{-/-}$ Nullmutanten kompensieren, habe ich einen Komplementations-genetischen Ansatz verfolgt, bei dem die jeweiligen Kandidaten kollektiv als Transgene in TS HSP23$^{-/-}$ Mutanten überexprimiert wurden. Nach einer Selektion bei permissiven oder nicht-permissiven Temperaturen wurden aus den selektierten Parasitenkulturen die Überexpressionsplasmide reisoliert und mittels PCR auf das Vorhandensein von Transgenen analysiert. Dabei zeigte sich, dass die Überexpression einer Proteinkinase, der Kaseinkinase 1.2 (LdBPK_351030), notwendig und ausreichend ist, um den TS Phänotyp der HSP23$^{-/-}$ Nullmutanten zu kompensieren. Darüber hinaus wurde durch *in vitro* Phosphorylierungsexperimente sowohl HSP23 als auch das verwandte P23-Co-Chaperon als Substrate und Modulatoren der Kaseinkinase 1.2 nachgewiesen.

Zusammenfassend konnte ich zeigen, dass spontane genetische Anpassungen den Funktionsverlust von HSP23 aufheben können, was HSP23 als Ziel für eine therapeutische Intervention gegen *Leishmania*-Infektionen ausschließt. Zudem liefert diese Studie Belege für eine entscheidende Verbindung zwischen Chaperonen und Signaltransduktionsproteinkinasen in diesen frühen Eukaryoten und trägt zum Verständnis bei, wie die Trypanosomatida sich an veränderte Bedingungen anpassen.

Table of Content

List of Figures

List of Tables

Abbreviations and Symbols

∅	Diameter
®	Registered trademark
™	Trademark
µg	Microgram
µL	Microlitre
µM	Micromolar
A	Adenine
aa	Amino acid
ACD	Alpha-crystallin domain
Aha-I	Activator of Hsp90 ATPase
Ala	Alanine
Amp	Ampicillin
ANOVA	Analysis of variance
AP	Alkaline phosphatase
APS	Ammonium persulfate
Arg	Arginine
Asp	Aspartic acid
ATP	Adenosinetriphosphate
BM	Blood meal
BLAST	Basic Local Alignment Search Tool
Bp	Base pair
BSA	Bovine serum albumin
C	Cytosine
°C	Degrees Celsius
Cas9	CRISPR-associated protein 9
cDNA	Complementary DNA
CL	Cutaneous leishmaniasis
cl.	Clone
cm	Centimetre
CNV	Copy number variation
CRISPR	Clustered regulatory interspaced short palindromic repeats
C-terminus	Carboxy-terminus
Cys	Cysteine
d	Day
DAPI	4′,6-Diamidin-2-phenylindol
ddH_2O	Double-distilled water

DMSO	Dimethyl sulfoxide
DNA	Deoxyribonucleic acid
DNase	Deoxyribonuclease
dNTP	Deoxynucleoside triphosphate
DSB	Double strand breaks
DTT	Dithiothreitol
DR	Downstream Reverse
E. coli	*Escherichia coli*
EDTA	Ethylenediaminetetraacetic acid
e.g.	*Exempli gratia*
EGTA	Ethylene glycol-bis β-aminoethyl ether-tetraacetic acid
ER	endoplasmatic reticulum
EtBr	Ethidium bromide
EtOH	Ethanol
fs	Frameshift
fwd	Forward
G	Guanine
g	Gram
gDNA	Genomic DNA
Gene ID	Gene identity
GRP94	Single glucose regulated protein 94 kDa
GCN	Gene copy number
Glu	Glutamic acid
Gln	Glutamine
Gly	Glycine
GOI	Gene of interest
h	Hours
HEPES	2-[4-(2-hydroxyethyl)piperazin-1-yl]ethanesulfonic acid
His	Histidine
HR	Homologous recombination
HSF	Heat shock factor
HSP	Heat shock protein
HT	High temperature
IFA	Immunofluorescence assay
IgY, IgG	Immunoglobulin Y, G
Ile	Isoleucine
IPTG	Isopropyl-β-D-thiogalactopyranoside
Kb	Kilobase
kDa	Kilo Dalton
L	Litre

L.	*Leishmania*
LB	Lysogeny broth
Leu	Leucine
LT	Low temperature
Lys	Lysine
M	Molar
mA	Milliampere
MAPK	Mitogen-activated protein kinase
Mb	Megabase
MBP	Myelin basic protein
MCL	Mucocutanous leishmaniasis
MCS	Multiple cloning site
Met	Methionine
MeOH	Methanol
mg	Milligram
min	Minutes
mL	Millilitre
mM	Millimolar
mRNA	Messenger RNA
ng	Nanogram
NGS	Next generation sequencing
ns	Non-significant
nt	Nucleotide
N-terminus	Amino-terminus
O/N	Over night
PCR	Polymerase chain reaction
PBS	Phosphate buffered saline
pH	Power of hydrogen
Phe	Phenylalanine
PKDL	Post-kala-azar dermal leishmaniasis
Pro	Proline
PVDF	Polyvinylidene fluoride
qRT-PCR	Quantitative real-time PCR
rev	Reverse
RNA	Ribonucleic acid
RNase	Ribonuclease
rpm	Revolutions per minute
RT	Room temperature or reverse transcriptase (context)
s	Seconds
SAT1	Streptothricin acetyl transferase 1

SDS	Sodium dodecyl sulfate
SDS-PAGE	SDS-polyacrylamide gel electrophoresis
SEM	Standard error of the mean
Ser	Serine
sgRNA	Single guide RNA
SGT	Small, glutamine-rich tetratricopeptide repeat protein
sHSP(s)	Small heat shock protein(s)
SIDER	Short interspersed degenerated retroposons
SNP	Single nucleotide polymorphism
spp.	Species pluralis
STI-1	Stress-inducible protein 1
T	Thymine
T.	*Trypanosoma*
T7RNAP	T7 RNA-Polymerase
TAE	Tris/acetic acid/EDTA buffer
TEMED	Tetramethylethylendiamine
Thr	Threonine
TRAP1	TNF Receptor Associated Protein 1
TS	temperature-sensitive
Tyr	Tyrosine
U	Units
UF	Upstream Forward
UTR	Untranslated regions
V	Volt
v	Volume
Val	Valine
Vol.	Volume
w/	With
w	Weight
WB	Western blot
WHO	World Health Organisation
WT	Wild type

1 Introduction

1.1 Leishmaniases

Leishmaniases encompass a range of vector-borne neglected tropical diseases caused by more than 20 species of intracellular protozoan parasites of the *Leishmania* genus. These diseases are endemic in 88, mostly tropical and subtropical countries, and affect more than 12 million people around the globe with an annual incidence of 1.6 million new infections and 20,000 deaths [2-5]. So far, there are no vaccines against *Leishmania* infections and current antileishmanial treatments are limited by their toxicity, lack of efficacy, high costs and the widespread drug resistance observed in important endemicity regions [6-8]. Climate and environmental changes may further expand the geographic range and distribution of the sandfly vectors and endemic regions of leishmaniasis [9, 10].

Depending on the *Leishmania* species (spp.) and the host immune status, leishmaniases present a variety of clinical manifestations, e.g. cutaneous (CL), mucocutaneous (MCL) and visceral leishmaniasis (VL). The latter may be followed by a highly disfiguring skin complication called post-kala-azar dermal leishmaniasis (PKDL) [11].

CL, also known as the oriental sore, is the most common form of leishmaniasis and accounts for 600,000-1,200,000 new cases each year. It is caused by *Leishmania* spp. such as *L. major*, *L. tropica*, and *L. aethiopica* in the Old World (Southern Europe, the Middle East, Asia, and Africa), and *L. amazonensis*, *L. mexicana, L. peruviana*, *L. braziliensis*, and *L. guyanensis* in the New World (South and Central America)(Fig 1A). These *Leishmania* spp. are dermotropic and adapted to slightly lower temperatures of ~34°C than their viscerotropic counterparts [12]. CL leads to the development of self-resolving ulcerated lesions at the site of infection often associated with permanent scarring and social stigmatisation [13].

Clinical progression to MCL, also known as Espundia, occurs in 1–10% of patients infected by *L. braziliensis* (90%), *L. panamensis* and *L. guyanensis*. This disease manifests in facial disfigurement and tissue destructions of the mucous membranes of the nose, mouth and throat. Although not life-threatening *per se*, secondary infections frequently lead to complications and death.

VL, also known as kala-azar, is the most severe form of leishmaniasis and is caused by infections with *L. donovani* and *L. infantum*. These species are viscerotropic and able to survive temperatures of over 37°C [12, 14]. Over 90% of the cases are observed in six countries: India, Bangladesh, Sudan, South Sudan, Brazil, and Ethiopia [2, 4] (Fig.1B). Clinical manifestations of VL include prolonged fever, cachexia, hepatosplenomegaly and pancytopenia. Without treatment, this form of the disease is fatal in more than 95% of the cases usually due to secondary infection and/or coagulopathy [15]. The mortality rate is also associated with jaundice, bleeding and anaemia or HIV co-infection [16-19].

In 10% (South Asia) to 60% (East Africa) of apparently cured VL patients, the disease may lead to PKDL. This is characterised by a skin rash consisting of macules, papules or nodules that harbour persisting parasites from the previous VL infection, thereby increasing the risk for parasite transmission by sandflies in endemic regions [20, 21].

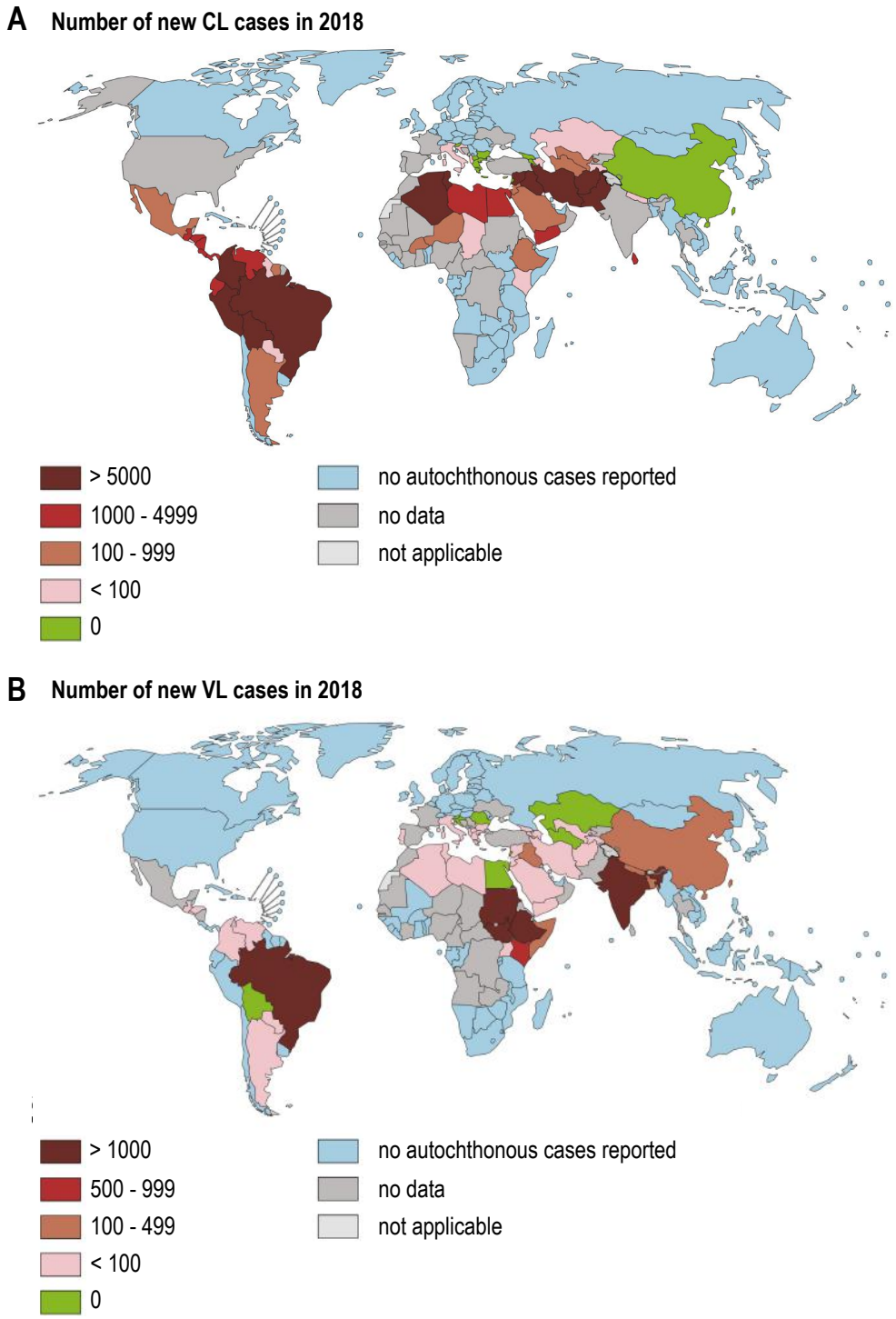

Figure 1 Worldwide geographical distribution of leishmaniases in 2018. The number of new cases of cutaneous (CL) (A) and visceral (VL) (B) leishmaniasis are indicated by colour codes. Non-endemic regions are shown in light blue, grey denotes countries with no data available. Adapted and modified from https://www.who.int/leishmaniasis/burden/en/.

1.2 The Taxonomy and Life Cycle of *Leishmania*

Parasites of the genus *Leishmania* belong to the taxon Euglenozoa, the class Kinetoplastea and the order Trypanosomatida. Based on the location of the parasite inside the sandfly intestine, they are further classified into two subgenera, namely *Leishmania* and *Viannia.* To date, approximately 53 species have been identified, of which 31 are pathogenic for mammals and 20 are categorised as human pathogens [22]. Mammalian reservoirs include rodents, canids, edentates, marsupials and primates. In general, humans are considered accidental hosts [23].

Leishmania spp. are mostly transmitted by female sandflies of the genera *Phlebotomus* and *Lutzomyia*. Thirty-one out of the 500 known phlebotomine species are currently known to transmit pathogenic species of *Leishmania* to humans [24]. Due to host specificity, the geographical distribution of the vector(s) determine(s) the geographical distribution of the cognate parasites and the associated diseases [25, 26].

During its digenetic life cycle (Fig 2), *Leishmania* parasites switch between two life cycle stages: the flagellated promastigote within sandflies and the intracellular, aflagellated amastigote within the mammalian host [27]. The transmission cycle starts when an infected female sandfly takes a blood meal from a vertebrate host, inoculating promastigotes into the subcutaneous tissues. In the skin, promastigotes are rapidly phagocytosed by diverse types of local or recruited immune cells such as neutrophils, macrophages, dendritic cells or fibroblasts [28-30]. Inside the phagolysosome of macrophages, which are considered the main host cells, promastigotes eventually differentiate into the amastigote stage. This differentiation is triggered mainly by a drop of pH (pH 5.5) and the increase of temperature (37°C) which the parasites encounter during the transmission from poikilothermic insect vectors to warm-blooded mammalian hosts [31]. The intracellular amastigote undergoes multiple rounds of binary fission until the host cell ruptures and releases parasites into the reticulo-endothelial system, allowing reinfection of other phagocytes. This phase of infection is associated with the clinical symptoms of the disease, as frequent cell rupture induces fever and anaemia. In the case of *L. donovani* infections, parasites further disseminate from the skin to the liver, spleen and bone marrow, where they cause damage, immune cell influx and induce typical symptoms of VL.

After ingestion of infective phagocytes by another sandfly, amastigotes are released from macrophages and convert back into the proliferative procyclic promastigotes (flagellum shorter than cell body) inside the sandfly's midgut. During metacyclogenesis, *Leishmania* develop through various non-infectious stages (nectomonad, leptomonad and haptomonad promastigotes) into the infective metacyclic promastigotes (flagellum longer than the cell body) [32, 33]. This stage of the infection involves massive replication and colonisation of the sandfly’s midgut which leads to the formation of parasite clusters at the anterior midgut. The parasite-mediated blockage of the gut is supposed to alter the feeding behaviour of the vector in favour of parasite transmission [34, 35]. More recently, reverse metacyclogenesis

was described, in which metacyclic promastigotes inside the sandfly midgut convert back to the highly proliferative leptomonad forms after every subsequent blood meal increasing parasite burden and sandfly infectiousness [36, 37].

The parasite's life cycle is completed when the highly motile metacyclic promastigotes migrate to the proboscis of the sandfly and are inoculated into a vertebrate host during the next blood meal.

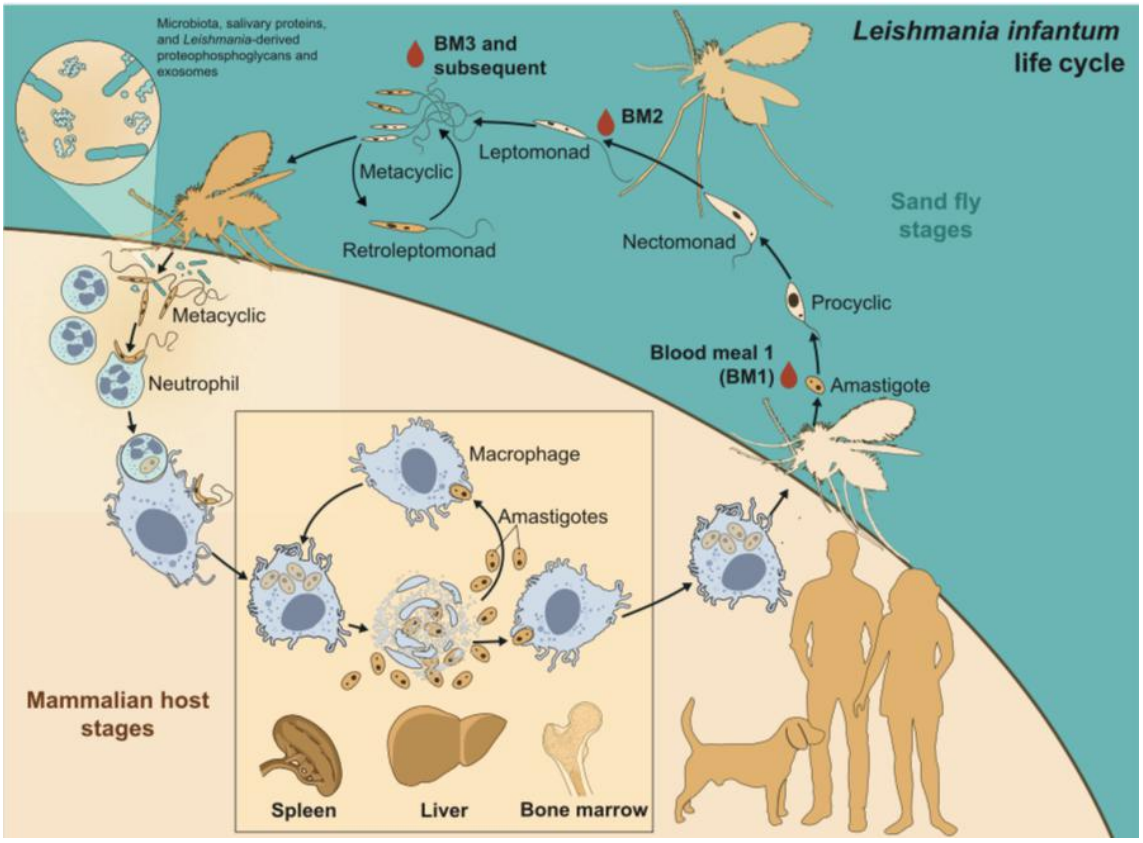

Figure 2 The *Leishmania* life cycle. During an infective blood meal, a female sandfly injects metacyclic promastigotes into the skin of the mammalian host where they are rapidly phagocytosed by immune cells. Within the phagolysosome of macrophages, promastigotes differentiate into the intracellular amastigote form. Amastigotes multiply until the cell ruptures and releases amastigotes into the blood. These can infect new macrophages or are taken up by another sandfly. Once in the sandfly midgut, the amastigotes differentiate into the proliferative procyclic promastigotes. These undergo several morphological stages transforming from the nectomonad to leptomonad promastigotes. The latter further differentiate into either haptomonad promastigotes which attach to the stomodeal valve or metacyclic promastigotes that are transmitted to the mammalian host. Sequential blood meals (BM) can induce redifferentiation from non-proliferative metacyclic promastigotes into the proliferative retroleptomonad form. Proliferative stages are indicated by a circular arrow. Figure was taken from [37].

1.3 Therapy of Leishmaniases

To date, there are no effective vaccines or drugs that can induce long-term protection against *Leishmania* infections. Furthermore, existing chemo-therapies are problematic due to high treatment costs, toxicity and invasive routes of administration.

Since 1945, **pentavalent antimonials** such as sodium stibogluconate (pentosan) and meglumine antimoniate are used as first-line drugs to treat both visceral and cutaneous leishmaniases. Antimony is thought to act as prodrug being reduced from its pentavalent form (Sb^{V}) to a more toxic trivalent form (Sb^{III}). The reduced form, in turn, is supposed to target the thiol redox metabolism, primarily of *Leishmania* amastigotes [38, 39]. Still, the exact mode of action remains largely unknown. Furthermore, the occurrence of drug resistance has limited the use of antimonials in several endemic regions, especially Bihar in India [40]. Beginning in the 1980s, patients refractory to pentavalent antimony were therefore treated with the second-line drugs **pentamidine** [41] and later with **amphotericin B**. While pentamidine was rapidly removed from the list of antileishmanial treatments due to its high toxicity and associated complications (e.g. shock, hypoglycaemia and death), amphothericin B is one of the most effective antileishmanial drugs that disrupts the parasite plasma membrane [42]. It was first approved as amphotericin B deoxycholate (AmBD) in 1959 for use against fungal infections and was later optimised as lipid formulation (AmBisome) to reduce toxicity [43]. However, the requirement for patient hospitalisation and associated high costs is a major drawback limiting its use in most affected countries [44, 45]. Health authorities in India, Bangladesh and Nepal are now using single-dose treatment with AmBisome in a large-scale *Leishmania* elimination program [46-48].

The alkylphosphocholine analogue **miltefosine**, originally used in anticancer therapy, was the first oral drug approved for the treatment against visceral and cutaneous leishmaniasis [49]. Proposed targets of miltefosine are the fatty acid and sterol metabolism as well as the biosynthesis of phospholipids leading to apoptosis-like death in *Leishmania* [50-52]. Advantages over standard antimonial treatments are only moderate side effects and the oral application of the drug. However, the main safety issues are the teratogenic potential and the long half-life (150-200 h) of the compound that may additionally potentiate the emergence of resistance [53-55].

Paromomycin is an aminoglycoside broad-spectrum antibiotic isolated from *Streptomyces rimosus*, effective against several gram-negative and gram-positive bacteria, some protozoa and cestodes [56, 57]. Since 2006, it has also been used successfully against visceral leishmaniasis being administered by intramuscular injections for 21 days [58, 59]. Paromomycin inhibits protein synthesis by binding to the 16S ribosomal RNA [60, 61]. Main advantages are the high efficacy, low price, shorter course of treatment and good safety profile.

Because drug monotherapies are related to emerging drug resistance, combination therapies have been applied for leishmaniasis treatment [62, 63], especially in endemic areas or in

case of HIV co-infection [64], since they provide several advantages: (i) they shorten treatment durations, (ii) reduce the risk of drug resistance and (iii) limit side effects due to lower dosage of the drugs [65, 66].

1.4 Regulation of the *Leishmania* Stress Response

During their complex life cycle involving the transmission from the insect vector to the mammalian host, *Leishmania* parasites encounter sudden changes of environmental conditions including an increase of temperature and oxidative stress, a drop of pH, and nutrient deprivation. Also, natural parasite populations are often exposed to periods of drug pressure which may lead to the development of drug resistance [67, 68]. To allow short and long-term adaptation to these changing conditions, *Leishmania* parasites rely on a variety of unique genetic features and regulatory mechanisms.

1.4.1 Regulation of Gene Expression

The genome of *Leishmania* has a size of 32 Mb harbouring ~8300 coding genes [69] that are distributed over 34 and 35 for *L. mexicana* and *L. braziliensis*, respectively [70] or 36 pairs of chromosomes for *L. donovani*, *L. infantum*, *L. major*, *L. tropica* and *L. aethiopica* [71]. As is common for trypanosomatids, *Leishmania* are devoid of conventional promoter-mediated transcriptional control as demonstrated by the lack of defined RNA Polymerase II promoters and general transcription factors [72]. Another unique feature is the organisation of genes into large polycistronic transcription units that are co-transcribed by RNA polymerase II [69, 73, 74]. Precursor RNAs are further processed by concomitant trans-splicing and polyadenylation yielding the mature monocistronic mRNAs [75, 76]. As a result of polycistronic RNA synthesis, most of the *Leishmania* genes are constitutively transcribed with little fluctuations of mRNA levels throughout the parasite life cycle, mostly due to pre-mRNA maturation, mRNA stability and/or decay [77-80]. Since mRNA steady-state levels and the proteome are only poorly correlated (20-40%), short-term regulation of *Leishmania* gene expression is thought to be mainly modulated by translational and post-translational control mechanisms such as translational efficiency and protein half-life [81].

More recently, several studies provided compelling evidence for another peculiar way of *Leishmania* to modulate transcript abundance. In the absence of transcriptional initiation control, strain-specific gene expression patterns were shown to rely mostly on changes in gene dosage rather than post-transcriptional mechanisms [82]. *Leishmania* parasites have a highly plastic genome with frequent amplifications of single genes (often present as tandem repeats), gene clusters [83-85] or even of whole chromosomes (aneuploidy) [86, 87]. The gene amplification may be intrachromosomal or occur as extrachromosomal circular or linear amplified DNA. They often appear at the sites of homologous direct or inverted repeated sequences [88, 89] as well as at short interspersed degenerated retrotransposons (SIDERs)

[85]. Apart from their implication in DNA rearrangements, SIDER elements are also involved in the regulation of gene expression at both the post-transcriptional (SIDER2) and translational (SIDER1) level [90, 91].
Moreover, gene copy number variations are often linked to drug resistance mechanisms in natural isolates as well as in laboratory strains by regulating the expression of drug targets (e.g. drug transporters) [67, 92]. Interestingly, most of the gene amplifications selected under drug pressure were shown to be already present within *Leishmania* populations in the absence of selection. This pre-existing genetic diversity among *Leishmania* populations is also termed as 'genetic mosaicism' and provides a strong adaptive advantage by selecting the fittest and best adapted mutants in response to rapidly changing environmental conditions [85, 86].
Altogether, the genetic structure of *Leishmania* parasites has a substantial impact on gene expression especially in response to stress conditions and represents an important evolutionary adaptation to the absence of transcriptional control.

1.4.2 The *Leishmania* Heat Shock Response

Members of the HSP family are evolutionarily conserved molecular chaperones that are found expressed in all prokaryotes and eukaryotes [93]. They are implicated in diverse cellular processes such as protein synthesis, folding and assembly of newly synthesised proteins, protein trafficking, and turn-over, thereby playing a central role in maintaining the proteostasis of the cell.
In more detail, molecular chaperones facilitate the correct folding of native polypeptides, both in the presence and absence of stress, by binding to and shielding hydrophobic residues of their client proteins [94-96]. Hydrophobic residues are often exposed during the folding and damaging of proteins and may induce irreversible protein aggregations. These protein aggregates are often detrimental to the cells and have been associated with many diseases such as ALS, Alzheimer's, Parkinson's, prion disease and cancer [97-100]. Beyond their ability to prevent protein aggregation, some chaperones are involved in the active folding of proteins into their native conformations utilising the free energy from ATP hydrolysis. The ATPase activity of the major chaperones itself is often regulated by the binding of co-chaperones [101].
Given the peculiar life cycle of a variety of digenetic protozoan parasites (section 1.2) which alternate between a poikilothermic arthropod vector and a homeothermic mammalian host, heat shock proteins are considered a crucial component of the parasite stress responses as well as integral, evolutionarily adapted parts of parasite biology. Hence, HSPs have been implicated in diverse cellular processes such as development, pathogen-host interaction, virulence and differentiation [102].
In the particular case of *Leishmania* parasites, both the increase of temperature and the drop of pH, which the parasites encounter within the acidified phagolysosome of the host macrophages, are key triggers of the stage differentiation both *in vivo* and *in vitro*, to which

the parasites respond with rapid induction of heat shock proteins (HSPs) [103]. However, in contrast to other organisms, HSP synthesis in *Leishmania* is only induced by elevated temperatures, but, except for radicicol, not by most other chemical stressors such as ethanol (EtOH), acidic pH, cadmium, copper, arsenite or pentavalent antimony [104].
In *Leishmania* and most other trypanosomatids, six major chaperone families have been described and grouped based on their molecular weight: HSP100, HSP90, HSP70, HSP60, HSP40 and small HSPs (sHSPs). The structures and functions of these chaperone families are highly diverse and adapted to the environmental conditions of the life cycle stages [105, 106].

1.4.2.1 Major Heat Shock Protein Families

HSP100 belongs to the superfamily of AAA+ domain-containing ATPases [107]. Members of this protein family are also referred to as 'disaggregases', as they can recognise misfolded proteins within aggregates and subsequently catalyse the active unfolding [108]. Eventually, this allows the rerouting of client substrates into the refolding pathways by acting in concert with the HSP70/DnaK chaperone machinery. In the *Leishmania* genome, HSP100 is encoded by a single-copy gene. Its expression was shown to be induced upon heat stress and increases during the stage conversion into the intracellular amastigotes [109]. The loss of HSP100 indeed led to attenuated virulence in *ex vivo* macrophages for both *L. major* and *L. donovani* as well as in mice for *L. major* [110, 111]. The fact that HSP100$^{-/-}$ null mutants did not display any considerable phenotype in *in vitro* axenic amastigotes, however, argued against a predominant role of HSP100 in thermotolerance, as shown for other organisms [112, 113]. Comparative proteomic analyses of *L. donovani* wild type and HSP100$^{-/-}$ null mutants rather indicate a role of HSP100 in promoting parasite-host interactions, mainly by determining the composition of the exosomal cargo [114]. HSP100 itself, as well as a variety of other HSPs and virulence factors, are packaged into exosomes that are shed off the flagellar pocket membrane into the host cell, in turn modulating the host immune response [114-116]. The observed phenotype of HSP100$^{-/-}$ null mutants inside the host, thus, may be ascribed to the involvement of HSP100 in the exosomal protein sorting.
HSP90 is an evolutionarily conserved ATP-dependent chaperone and represents one of the most abundant proteins in eukaryotic cells. It is implicated in the chaperoning of a defined set of client proteins, including transcription factors and protein kinases that are mainly involved in cell-cycle control, proliferation, apoptosis and signal transduction [117-119]. HSP90 activity is dependent on its interaction with a wide variety of co-chaperones and cofactors resulting in a large multi-protein complex, also known as the 'foldosome' [120]. Apart from HSP90, this complex comprises HSP70, HOP/Sti1, HSP40 and p23.
The *Leishmania* genome harbours up to 18 tandemly arrayed HSP90 genes and two single-copy HSP90 paralogues, namely GRP94 (single glucose-regulated protein 94 kDa (Grp94) protein) and TRAP1 (TNF Receptor Associated Protein 1; also known as HSP75) [105, 121], which in other organisms are localised at the endoplasmatic reticulum (ER) and

mitochondrion, respectively. Apart from the reported immunoprotective potential of GRP94 [122], the function of the HSP90 paralogues in *Leishmania*, however, remains largely unknown.

In contrast, the role of HSP90 has been the subject of extensive studies. Inhibition of HSP90 using the specific inhibitor geldanamycin [123] or radicicol [124] results in a G2/M cell cycle arrest of promastigotes and concomitantly induces a morphological differentiation towards amastigote-like axenic forms [125-127]. Similar to other organisms, *Leishmania* HSP90 activity is modulated by co-chaperones such as P23, Ahal, Stil as well as post-translational modifications (section 1.4.3). Whether HSP90 activity is similarly coupled to the HSP70/ HSP40 chaperone machinery in *Leishmania* is still unknown, but HSP70 was found in HSP90 foldosome complexes [128].

HSP70 is the most conserved protein in all organisms with essential functions in stressed and non-stressed cells [129]. Its activity is intimately linked to the DNAj domain-containing protein HSP40 which recognises misfolded and unfolded proteins and delivers them to the substrate-binding domain of HSP70 [130, 131]. Either alone or in concerted action with other ATP-dependent chaperones including HSP100, HSP90 and chaperonins, HSP70 is involved in the folding and refolding of proteins and the prevention and dissolution of protein aggregates [132]. Relatively little is known about the functional implications of HSP70 and its co-chaperone HSP40 in *Leishmania*. Like HSP90, both proteins are encoded by multi-copy genes varying in number between species. HSP70 was found to be highly abundant in *L. major* promastigotes accounting for 2.1% of the total cellular protein extract [133], while protein synthesis is further increased under higher temperatures. Over expression studies in *L. chagasi* additionally pointed towards a role of HSP70 in intracellular survival [134].

CPN60 (60 kDa chaperonin, also known as HSP60 and GroEL) is also highly conserved. In general, chaperonins are involved in preventing intermolecular aggregation in an ATP-dependent fashion [135]. In Leishmania and other Trypanosomatida, CPN60 and its co-chaperonin CPN10 reside in the mitochondrion [136, 137]. A total of four HSP60 orthologues and two HSP10 genes, a co-chaperonin of HSP60, have been identified in the *Leishmania* genome [137]. Apart from being a component of the exosomal payload [138], the role of the different HSP60s throughout the parasite life cycle, however, remains largely unknown.

1.4.2.2 Small Heat Shock Proteins and the Role of HSP23

Small heat shock proteins (sHSPs) comprise the most poorly conserved family of molecular chaperones, reflected in a wide size range between 15-40 kDa. They are found in all kingdoms and have been implicated in the response to diverse stresses, e.g. temperature upshift or oxidative stress, apoptosis and immune responses [139-142]. Hence, sHSP dysfunction is linked to several diseases, e.g. eye cataracts, myopathies and neurological degenerative disorders [143-145]. In addition to their low molecular size, sHSPs are characterised by an ancient, structurally conserved alpha-crystallin domain (ACD) which was first identified in the eye lens protein, α-crystallin [146]. This domain consists of

approximately 80-90 residues and folds into six to seven β-strands organised in two large β-sheets that are linked by a short loop [147] (Fig 3A).

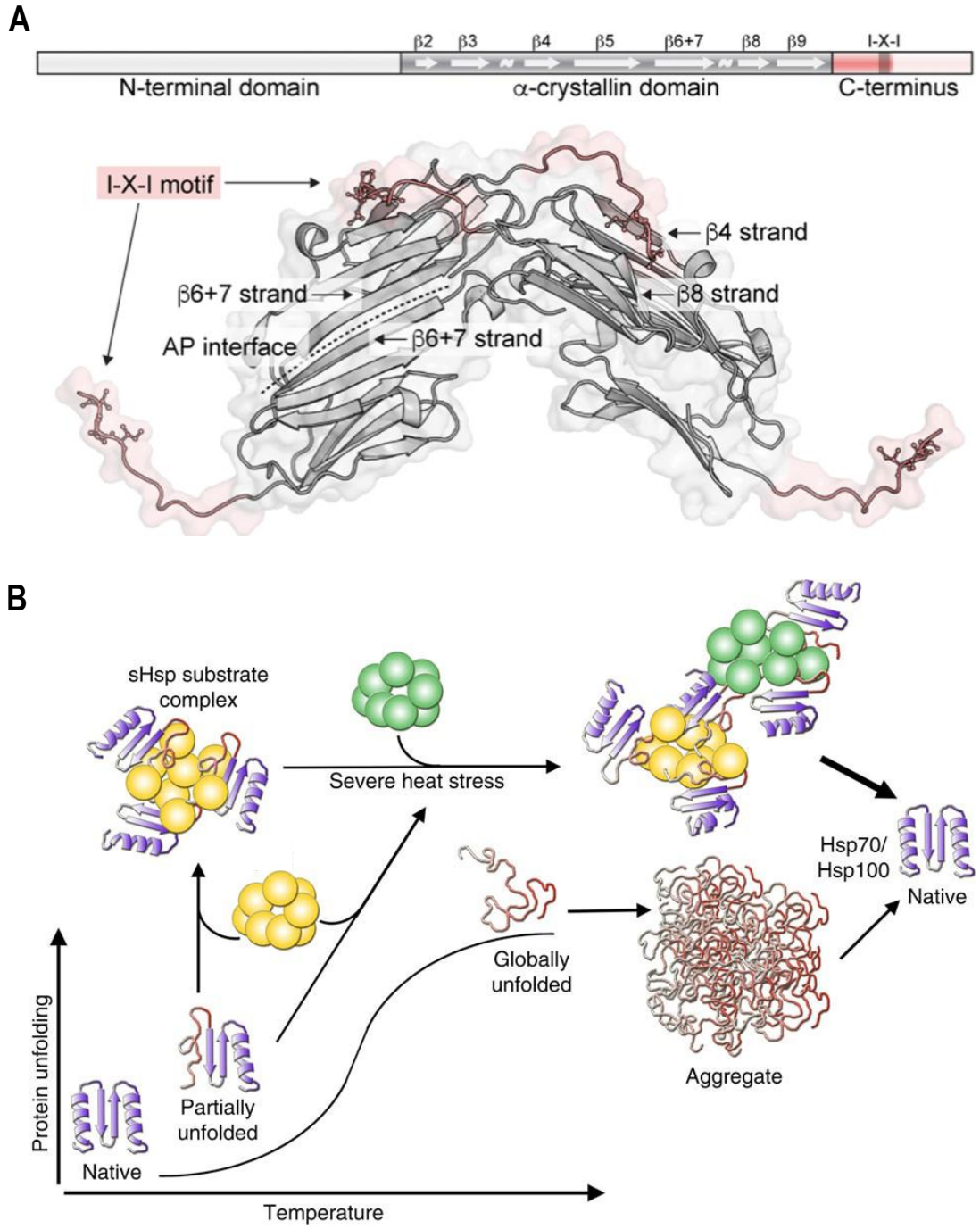

Figure 3 The structure and function of small heat shock proteins. (A) Schematic representation and X-ray structure of the human small heat shock protein HspB5. The primary sequence encodes a central alpha-crystallin domain (ACD) which folds into six to seven β-sheets and is flanked by N- and C-terminal regions. The ACD dimerises via an antiparallel (AP) interface between strands β6 + 7. Figure modified from [147] (B) Mode of action of small heat shock proteins. Cellular stress (e.g. high temperatures, chemical stress) cause native proteins to misfold. During these stress conditions, sHSPs bind to partially unfolded proteins to prevent their aggregation. Additional chaperone complexes (including HSP40, HSP70, and HSP100) allow refolding in an ATP-dependent manner. Figure taken from [154].

In addition, the ACD is flanked by amino- and carboxy-terminal extensions that modulate the oligomerisation state, substrate binding and chaperoning function [141]. The dynamic oligomerisation of sHSPs is believed to regulate the binding to non-native and misfolded proteins.

It can be influenced by post-translational modifications, including phosphorylation which was shown to induce oligomer dissociation [148-151]. As 'holdases', sHSPs bind to their client proteins and keep them in a near-native state [152-154]. The release of substrates and the subsequent refolding is facilitated with the concerted action of other ATP-dependent chaperones (e.g. HSP70, HSP100) (Fig 3B).

The number of sHSPs varies depending on the organism, ranging from one in yeast, four in Drosophila, eleven in humans (hspB1-B10), 14 in *C. elegans* to more than 30 in plants [141] [155]. sHSPs have been also identified in the genomes of protozoan protists: e.g. five and six genes are present in the apicomplexan parasites *Toxoplasma* and *Plasmodium*, respectively, while only three sHSPs, namely HSP20, HSP23 and P23, are encoded in the genomes of trypanosomatidic parasites [156]. The first sHSP identified in *Leishmania* was HSP20 that was found to be antigenic during natural *L. amazonensis* infections of dogs [157]. The immunoprotective properties of HSP20 as DNA vaccine, however, turned out to be rather low; similarly, the protein showed no immunogenicity in humans [157].

The orthologues of P23 and HSP23 were identified in the genomes of most Trypanosomatida and are, with a few exceptions, encoded by single-copy genes [156]. In *L. donovani*, P23 is encoded on chromosome 35 while *HSP23* was found to be located on chromosome 34 within a telomeric cluster of genes, comprising *ARM56* and *ARM58*, that have been implicated in antimony resistance [158, 159].

P23 and HSP23 share a relatively low sequence identity of only 30%, with rather low structural conservation. Recombinant *L. braziliensis* P23 and HSP23 (named Lbp23A and Lbp23B) were shown to negatively affect the HSP90 ATPase activity, suggesting a co-chaperoning function of both proteins [160]. This is consistent with the general role of P23 proteins which bind to HSP90 in its ATP-bound state, thereby preventing the ATP-hydrolysis required for the release of substrates [161, 162].

Reverse genetic analyses in *L. donovani* indeed identified P23 as a functional HSP90 co-chaperone, as P23$^{-/-}$ null mutants displayed an increased sensitivity against the HSP90-specific inhibitors geldanamycin and radicicol [163]. In contrast, hypersensitivity against either inhibitor was not observed upon disruption of the HSP23 gene providing first evidence for distinct functions of these ACD proteins [1].

Instead, phenotype analysis of *L. donovani* HSP23$^{-/-}$ null mutants revealed a predominant role of HSP23 in thermotolerance demonstrated by the following observations [1] (i) The loss of *HSP23* renders null mutants non-viable at mammalian tissue temperatures, abrogates *in vitro* stage differentiation into axenic amastigotes and reduces the infectivity of *ex vivo* macrophages. Also, (ii) exposure to 37°C results in a complete destruction of the cellular

membrane (Fig 4), (iii) in contrast to P23, HSP23 expression is heat-inducible and up-regulated during axenic amastigote differentiation both at mRNA and protein levels [1, 127, 164], (iv) recombinant HSP23 forms large oligomeric complexes which are enhanced at mammalian tissue temperatures, and (v) HSP23 shows a differential localisation throughout the life cycle stages: while it is predominantly cytoplasmic in promastigotes, it relocates to the nuclear periphery in mature amastigotes.

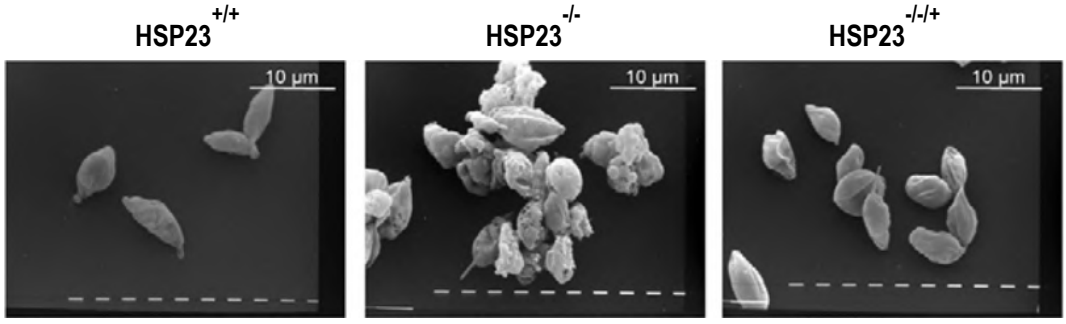

Figure 4 Scanning electron microscopy images of axenic amastigotes of HSP23$^{+/+}$, HSP23$^{-/-}$ null mutants and add-back lines. Figure was modified from [1].

Besides its involvement in heat tolerance, HSP23 was shown to be implicated in the tolerance against other chemical stresses such as exposure to EtOH, acidic pH, and trivalent antimony (Sb^{III}). The observed sensitivity to antimony treatment and the fact that *HSP23* is located within the known antimony resistance gene cluster on chromosome 34 implicates it in resistance against antimony-based antileishmanial drugs [159]. The involvement of HSP23 in response to chemical and/or temperature stress is not restricted to *Leishmania*, but has been reported for orthologous proteins in *Drosophila* [165, 166], *Trichoderma virens* [167] and plants [168, 169]. Importantly, as HSP23 is structurally different from human small HSPs, it may constitute a potential therapeutic target for the treatment of leishmaniasis.

1.4.3 Regulation of Heat Shock Proteins

The regulation of the heat shock proteins, the main effectors of protein folding homeostasis, substantially influences the cellular fate under stress and non-stress conditions. In most eukaryotes, the heat shock response is regulated at the transcriptional level by heat shock factors (HSFs) [170-172]. Under homeostatic conditions, HSFs are bound to major chaperones. In the presence of chronic or acute proteotoxic stress, however, HSFs dissociate from the chaperones and translocate to the nucleus [173]. Inside the nucleus, HSFs form homotrimers and bind to structurally conserved heat shock elements within the promoters of heat shock genes or enhancers of HSP genes, thereby inducing the transcription of HSP genes.

Given the absence of transcriptional control, the regulation of *Leishmania* HSPs is independent of HSFs, but relies on multiple other mechanisms including (i) regulated expression, (ii) coordinated co-chaperone networks and (iii) post-translational modifications.

First, transcript abundance of several HSPs seems to be regulated via gene dosage. As described before (section 1.4.2.1), several *Leishmania* HSPs, e.g. HSP40, HSP70 and HSP90, are encoded by tandemly arrayed multi-copy genes allowing for high transcript levels upon polycistronic transcription. Differences in gene copy numbers were shown to account for differential transcript abundances among *Leishmania* strains [82]. However, their impact on the stage-specific differences observed between promastigotes and amastigotes seems to be negligible as HSP transcript levels do not correlate with HSP synthesis [127]. Hence, the increased synthesis of several HSPs during stage differentiation (e.g. HSP70, mtHSP70, HSP90, HSP100 and chaperonins) [79, 174] is ascribed predominantly to post-transcriptional mechanisms.

It was shown that the stability and translation efficiency of various HSP transcripts of *Leishmania,* but also *Trypanosoma* is regulated by trans-acting RNA-binding proteins that bind to cis-acting elements within the 3' untranslated region (UTR) of mRNAs. Such regulatory units were identified within the 3'UTR of HSP70 [175, 176] and HSP90 [177-179].

An additional layer of regulation occurs at the post-translational level. The activity of the major heat shock proteins is commonly regulated by a broad variety of co-chaperones [180, 181]. These cofactors bind to distinct domains of the heat shock proteins, thereby modulating the ATPase activity and substrate turnover. In addition, other co-chaperones determine HSP specificity by acting as adaptor proteins to promote client interactions. In *Leishmania*, several co-chaperones have been implicated in the HSP90 foldosome complex including two essential tetratricopeptide domain-containing proteins named stress-inducible protein 1 (STI-1)[126] and small, glutamine-rich tetratricopeptide repeat protein (SGT)[128] as well as the two non-essential co-chaperones P23 [163] and the Activator of Hsp90 ATPase (AhaI) [182].

Furthermore, the activity of both HSPs as well as co-chaperones is intimately coupled to post-translational modifications including phosphorylation, acetylation, methylation, and S-nitrosylation, as well as ubiquitination [183, 184]. In particular, phosphorylation has been linked to stage differentiation in *Leishmania* as measured by increased phosphoprotein abundance in amastigotes [164]. Stress-induced phosphorylation during stage differentiation was reported for several HSPs such as HSP70 and HSP90 [164, 185, 186] and for the co-chaperone STI-1 [187]. To date, two kinases are known to phosphorylate HSP70 and HSP90 *in vitro* including *L. donovani* MAPK1 and casein kinase 1.2 [185, 186, 188]. The latter plays an essential role in intracellular survival [189].

To conclude, the multifactorial regulation of HSPs in *Leishmania* links stress adaptation and stage-specific survival mechanisms [190, 191] and may, in part, compensate for the absence of transcriptional control.

1.5 Aims of the Study

Small HSPs have essential functions in diverse organisms and are part of the protein quality system of the cell. Recently, the small heat shock protein 23 was characterised in *L. donovani,* the causative agent of visceral leishmaniasis, and was found to be essential for the parasite's stress tolerance as demonstrated by a *bona fide* TS phenotype of HSP23$^{-/-}$ null mutants [1]. As HSP23 is specific to trypanosomatids with no homologues in humans, it represents a potential drug target.

Here, I aim to further analyse the function of HSP23 in parasite biology with special emphasis on its suitability as a drug target.

Leishmaniasis is caused by a wide spectrum of *Leishmania* spp., which display differences in tissue and tropism and disease manifestation (section 1.1). Therefore, one aim of this study was to investigate whether the function of HSP23 is conserved throughout the genus *Leishmania*. To address this question, HSP23$^{-/-}$ null mutants are to be generated in the dermotropic species *L. major* which causes the cutaneous form of the disease using a CRISPR-Cas9 strategy that was recently developed by Beneke and colleagues for use in *Leishmania* [192]. Phenotype analysis of *L. major* HSP23$^{-/-}$ null mutants is planned, including assays on cell morphology, growth under different conditions, and may provide further insights into the general role of HSP23. In a second approach, I plan to perform complementation studies in both *L. donovani* and *L. major* HSP23$^{-/-}$ null mutants by introducing HSP23 transgenes from other leishmaniae and *Trypanosoma* spp.. In more detail, I will test the ability of the different HSP23 transgenes to rescue the TS phenotype of null mutant lines at elevated temperatures.

The high genome plasticity of *Leishmania* provides an evolutionary mechanism to adapt to fast-changing environmental conditions. However, it also poses major difficulties for reverse genetics and the analysis of mutant phenotypes as they might be rapidly lost and compensated by genome changes. In view of drug development, the investigation of compensatory genetic adaptation is critical as it can lead to drug resistance. To identify genomic alterations compensating for the loss of HSP23, I plan to perform whole-genome sequencing, comparing the genomes of *L. donovani* 1SR or *L. major* 5ASKH wild type to HSP23$^{-/-}$ null mutant strains. A detailed bioinformatic analysis of resulting aneuploidy patterns, gene copy numbers and single nucleotide polymorphisms (SNPs) is expected to provide clues about selective genetic alterations and may even allow the identification of novel candidate drug targets or pathways involved in the parasite stress response.

2 Results

2.1 Generation of HSP23$^{-/-}$ Null Mutants

Targeted gene replacement was proven to be a powerful tool to characterise the biological role of individual genes. A first *L. donovani* HSP23$^{-/-}$ mutant was successfully obtained via homologous recombination (HR) [1]. Characterisation of the HSP23$^{-/-}$ mutant phenotype revealed an important role of *L. donovani* HSP23 in heat and stress tolerance. Yet, the function of HSP23 orthologues in other *Leishmania* spp. remained largely unknown. To investigate whether HSP23 is functionally conserved, I opted to generate and characterise HSP23$^{-/-}$ mutants in the dermotropic spp. *L. major*.

2.1.1 Generation of *L. major* HSP23$^{-/-}$ via CRISPR/Cas9

For a long time, the use of reverse genetics in *Leishmania* was restricted to the HR-based strategy, but could recently be extended by the CRISPR/Cas9 system [193]. This technology is based on a CRISPR-associated endonuclease Cas9 that is directed by specific single guide RNAs (sgRNAs) to the target locus where it introduces DNA double strand breaks (DSBs)[194, 195]. In *Leishmania*, DSBs are usually repaired by microhomology-mediated end-joining or single-strand annealing [196, 197]. However, due to a relatively low efficiency of these gene repair mechanisms, CRISPR/Cas9 gene editing in *Leishmania* has been facilitated by the additional introduction of donor repair cassettes. These harbour antibiotic resistance marker genes flanked by short homology arms to the target locus and are inserted by homology-directed repair, thereby improving the efficiency and specificity of gene editing. Given the high propensity of *Leishmania* to undergo genetic adaptations in response to diverse stresses (section 1.4.1), the rapid and simultaneous disruption of alleles using the CRISPR/Cas9 system provides major advantages over HR. Most importantly, it limits possible compensatory effects, e.g. gene or chromosome amplifications that may occur during the selection of viable null mutants, especially when targeting genes contributing to parasite survival and growth.

2.1.1.1 Generation of *L. major*:Cas9 Parental Cells

To implement the CRISPR/Cas9 system in *L. major*, I first generated a parental cell line, ectopically expressing the Cas9 nuclease and the T7-RNA-Polymerase (T7RNAP). The latter is required for sgRNA transcription *in vivo* from PCR-generated DNA templates (section 2.1.1.2). For this, I transfected *L. major* 5ASKH promastigotes with the pT007 plasmid [193] bearing the humanised *Streptococcus pyogenes* Cas9 nuclease gene (*hSpCas9*) fused to a FLAG tag, T7RNAP and a hygromycin B resistance cassette.

Following hygromycin B selection and limiting dilution, five putative *L.maj*:Cas9 clones (1-5) were tested for Cas9 expression by Western blot using an anti-FLAG antibody. As shown in Figure 5A, a band with an approximate size of 170 kDa was visible for all Cas9-expressing clones, as well as for the *L. donovani:*Cas9 [198] cell lysate used as a positive control, while it was absent in the *L. major* WT sample.

To address whether Cas9 has toxic effects on parasites' viability, growth of *L. maj*:Cas9 cl.1 was tested at 25°C as well as 34°C (Fig 5B,C). Similar growth rates were observed for both wild type and transgenic cells indicating that ectopic Cas9 expression is well tolerated by *L. major* promastigotes.

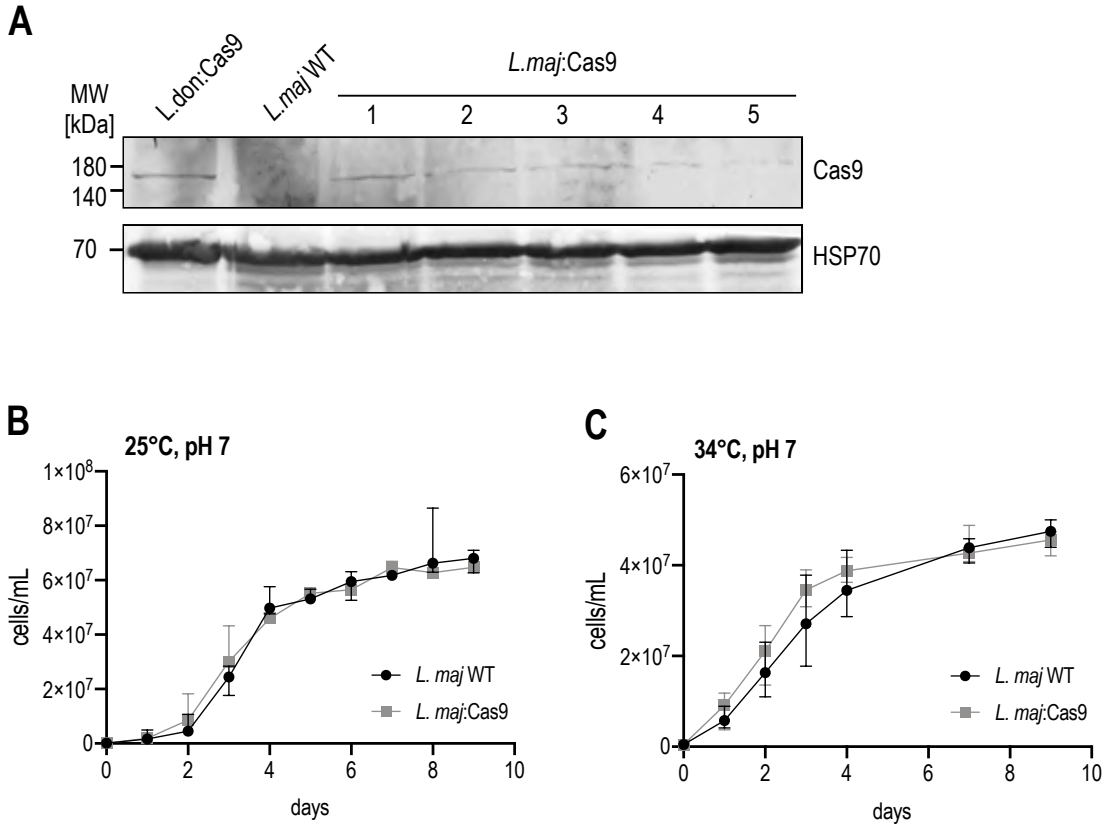

Figure 5 Generation and phenotype analysis of Cas9 expressing *L. major* cells. (A) Western blot analysis of whole cell lysates of five Cas9 expressing *L. major* clones (*L. maj*:Cas9) and *L. major* 5ASKH WT (*L. maj* WT). A previously generated *L. donovani* Cas9 expressing clone (*L. don*:Cas9) [198] served as positive control. Samples were probed with an anti-FLAG (1/500) or anti-HSP70 (1/500; loading control) antibody. MW = molecular weight. (B) Growth comparison between *L.maj* WT and *L. maj*:Cas9. Promastigotes of *L. maj* WT and *L. maj*:Cas9 were seeded at a density of 1 × 10^6 cells/mL into 10 mL of complete M199 medium. The cell density was measured over a period of nine days. The data represent the median +/- range (n=4).

2.1.1.2 Generation of sgRNAs and Replacement Constructs

Primer design for the generation of 5' sgRNA and 3' sgRNA targeting *LmjHSP23* was done as described in section 4.2.3.5. As mentioned before, a special feature of the optimised CRISPR/Cas9 system for *Leishmania* is the *in vivo* transcription of PCR-amplified sgRNA templates. For this, the "sgRNA" primers consist of a T7 RNA polymerase promoter, a 20-nt sequence homologous to the target locus and a 20-nt overlap to the CRISPR-Cas9 backbone sequence allowing generation of sgRNA templates by PCR.

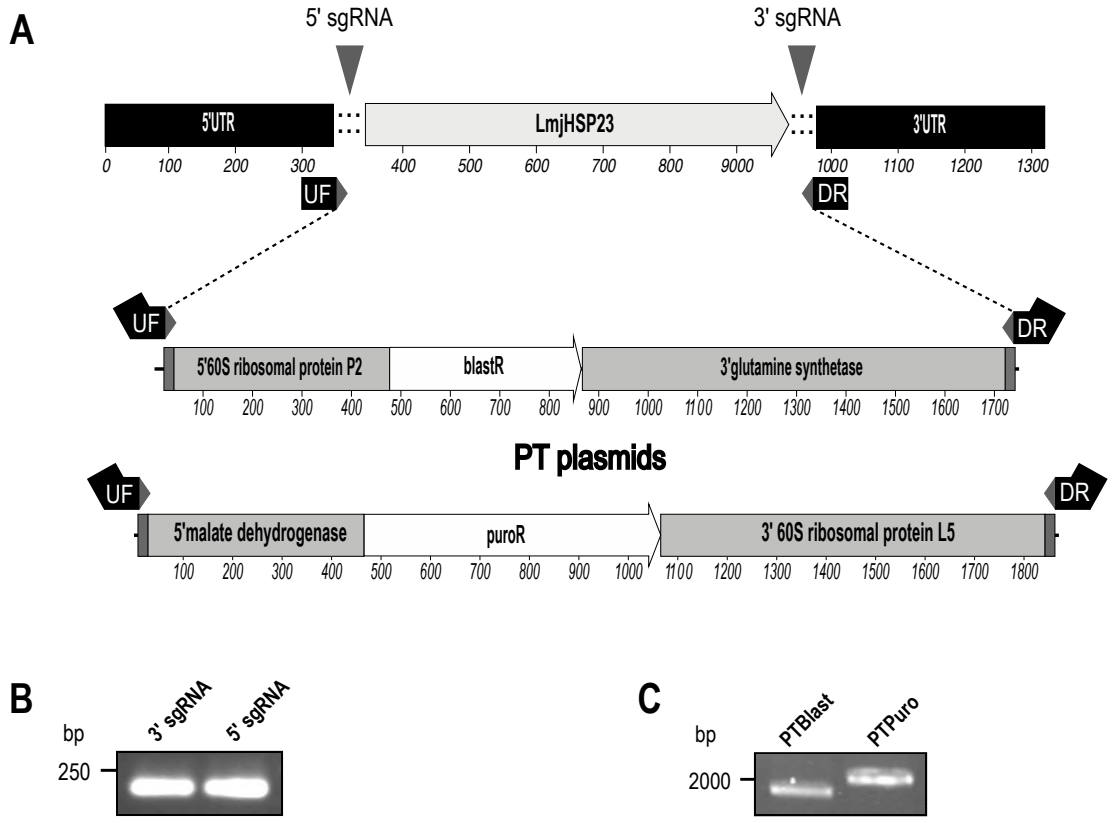

Figure 6 CRISPR/Cas9 mediated gene replacement of *L. major HSP23*. (A) Schematic representation of the PCR-based CRISPR-Cas9 method established by Beneke et al. [192]. The *L. major HSP23* endogenous locus and binding positions of 5' and 3' sgRNA primers are shown. Upstream Forward (UF) and Downstream Reverse (DR) primers used to amplify the resistance marker cassettes (blastR=Blasticidin resistance; puroR=Puromycin resistance) from PT plasmids contain short homology arms to the 5' and 3' untranslated regions (UTRs) of *HSP23*. (B) PCR products of 3' and 5' sgRNA templates that are transcribed *in vivo* by T7 RNA Polymerase. (C) PCR products of BlastR and PuroR replacement constructs. bp = base pairs

Replacement constructs were PCR-amplified from pT plasmids that harbour either a Puromycin or Blasticidin resistance marker gene that is flanked by unrelated UTRs. The amplification was done using an Upstream Forward (UF) and a Downstream Reverse (DR) primer (Table 10) that contain 30-nt homologous flanks to the 5'UTR or 3'UTR of *HSP23* required for HR-repair after Cas9 induced DSBs. A schematic representation of the PCR

amplification strategy is depicted in Figure 6A. Successful amplification of sgRNAs and replacement constructs was confirmed by agarose gel electrophoresis (Fig 6B,C).
After verification of the correct PCR product sizes, the *L. major* Cas9/T7 parental clone 1 was co-transfected with the sgRNA and donor DNA templates. One day post-transfection, transfectants were subjected to puromycin and blasticidin selection. To reduce possible Cas9 off-target effects, at this point, hygromycin B pressure for the maintenance of the pT007 episome encoding Cas9 and T7 RNAP was stopped. Viable double drug-resistant cell populations emerged in culture at day six to ten post-transfection, suggesting that the *L. major* HSP23 gene is not essential in promastigotes at ambient temperature.

2.1.2 Generation of *L. donovani* HSP23$^{-/-}$ by Homologous Recombination

For a better comparative analysis of *L. major* and *L. donovani* HSP23$^{-/-}$ null mutant phenotypes, I generated additional *L. donovani* HSP23$^{-/-}$ null mutants applying the same homologous recombination strategy as before [1].
Briefly, to obtain double-allele null mutants, two different targeting constructs were used. These included the selective resistance marker genes, puroR or neoR, flanked by sequences homologous to the 5' (1023 bp) and 3' UTR (779 bp) of the LdHSP23 gene (Fig 7). After linearisation, the first targeting construct was transfected into *L. donovani* promastigotes and positively selected with the cognate antibiotic (puromycin or neomycin). Putative single-allele null mutants were raised and thereafter transfected with the second targeting construct. Transfection was followed by dual drug selection yielding two putative double-allele LdHSP23$^{-/-}$ null populations. After limiting dilution, genomic DNA (gDNA) of a panel of LdHSP23$^{-/-}$ clones was analysed by diagnostic PCR using *HSP23*-specific primers. PCR analysis confirmed that the LdHSP23 ORF was undetectable in these clones (data not shown). Two of these clones, LdHSP23$^{-/-}$ cl.2 and cl.3, were additionally subjected to NGS (section 2.2.1).

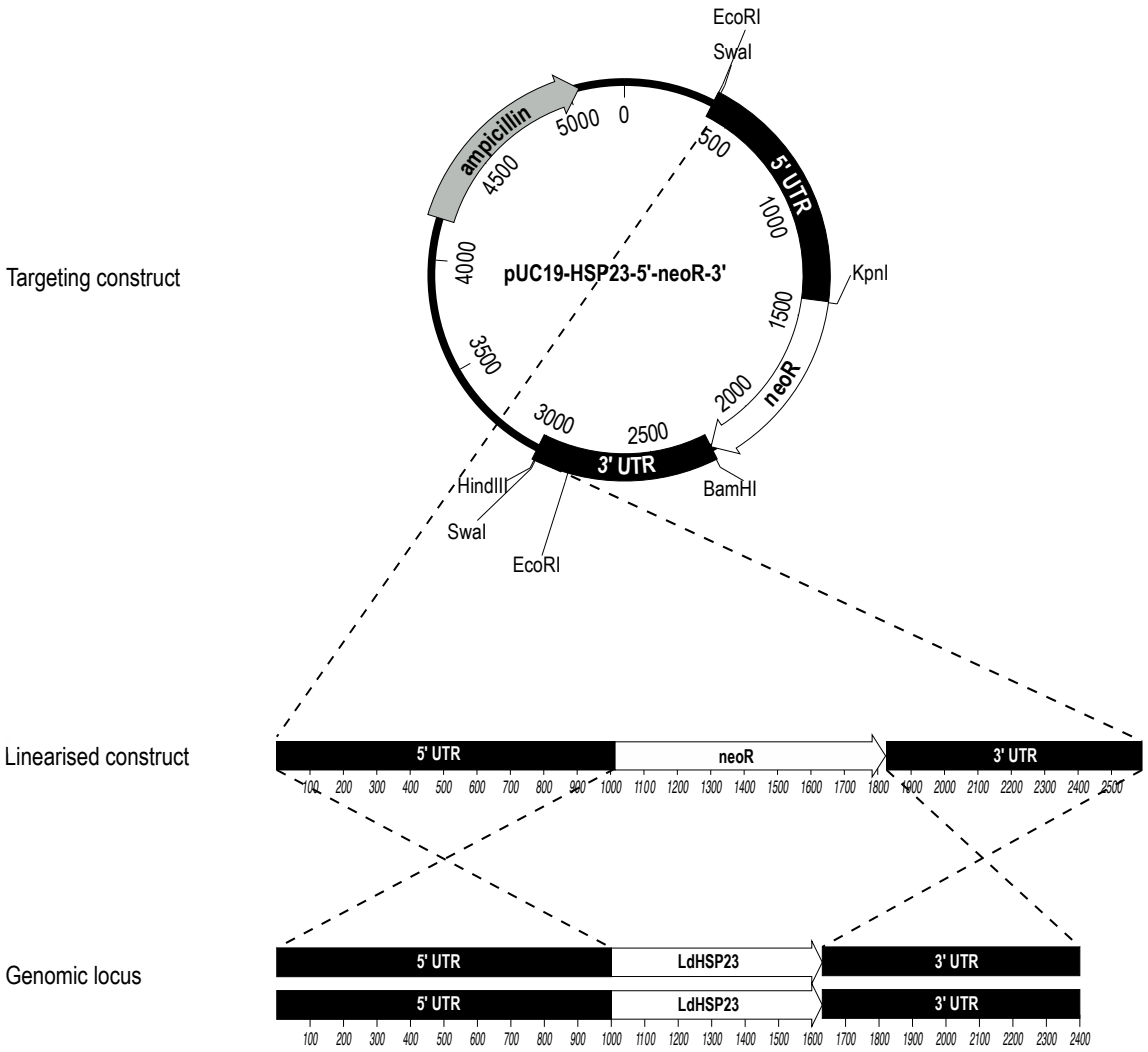

Figure 7 Schematic representation of the double cross-over homologous recombination strategy used for the generation of *L. donovani* HSP23$^{-/-}$. An exemplary targeting construct (pUC19-HSP23-5'-neoR-3') bearing the neomycin resistance gene (neoR) flanked by the *LdHSP23*-specific 5' and 3' untranslated regions (UTRs) is shown. The ampicillin resistance gene (β-lactamase) for plasmid amplification in *E. coli* is indicated. The linearised plasmid is transfected into *L. donovan*i promastigotes followed by positive selection with the respective antibiotic yielding single-allele null mutants. In a second step, the procedure is repeated using a targeting construct with a different resistance marker gene. Numbers indicate nucleotide sequence positions.

2.2 Verification of Gene Replacement

To validate the generation of HSP23$^{-/-}$ null mutants, the presence of HSP23 was investigated at three different levels: (i) at DNA level by PCR or whole genome sequencing (WGS), (ii) at transcript level by quantitive real-time PCR (qRT-PCR), and (iii) at protein level by Western blot analysis using an HSP23-specific antibody.

2.2.1 Verification at the DNA Level

After limiting dilution, genomic DNA of putative *L. major* and *L. donovani* HSP23$^{-/-}$ clones was first examined by diagnostic PCR confirming a complete loss of the HSP23 gene (data not shown). The genomic DNA of two *L. major* and *L. donovani* HSP23$^{-/-}$ clones each was further subjected to WGS. Bioinformatic analysis indeed verified a lack of sequence reads for the targeted gene regions for both *L. major* (Fig 8A) and *L. donovani* (Fig 8B) HSP23$^{-/-}$ null mutants confirming the excision of *HSP23*. In both CRISPR/Cas9-generated *L. major* HSP23$^{-/-}$ clones, gene disruption occurred at the sgRNA binding sites resulting in a loss of 700 bp (Fig 8A). To analyse the integration of the respective resistance marker cassettes, I additionally aligned the sequence reads to *in silico* designed target chromosomes containing the integrated replacement constructs. Indeed, reads for the full length replacement constructs were detected in *L. major* (Fig 9) and *L. donovani* (Fig 10) HSP23$^{-/-}$ mutants, while being absent in HSP23$^{+/+}$ WT cells, demonstrating the on-target integration of the respective drug resistance cassettes.

Alignment to the pT007 plasmid harbouring the Cas9 and T7 transgenes revealed the presence of sequence reads for the full length plasmid in the LmjHSP23$^{+/+}$ Cas9 sample while only the tubulin homology regions were detectable in LmjHSP23$^{-/-}$ cl.1 and cl.2 samples, where HygB pressure for the maintenance of the pT007 plasmid had been removed (Fig 11).

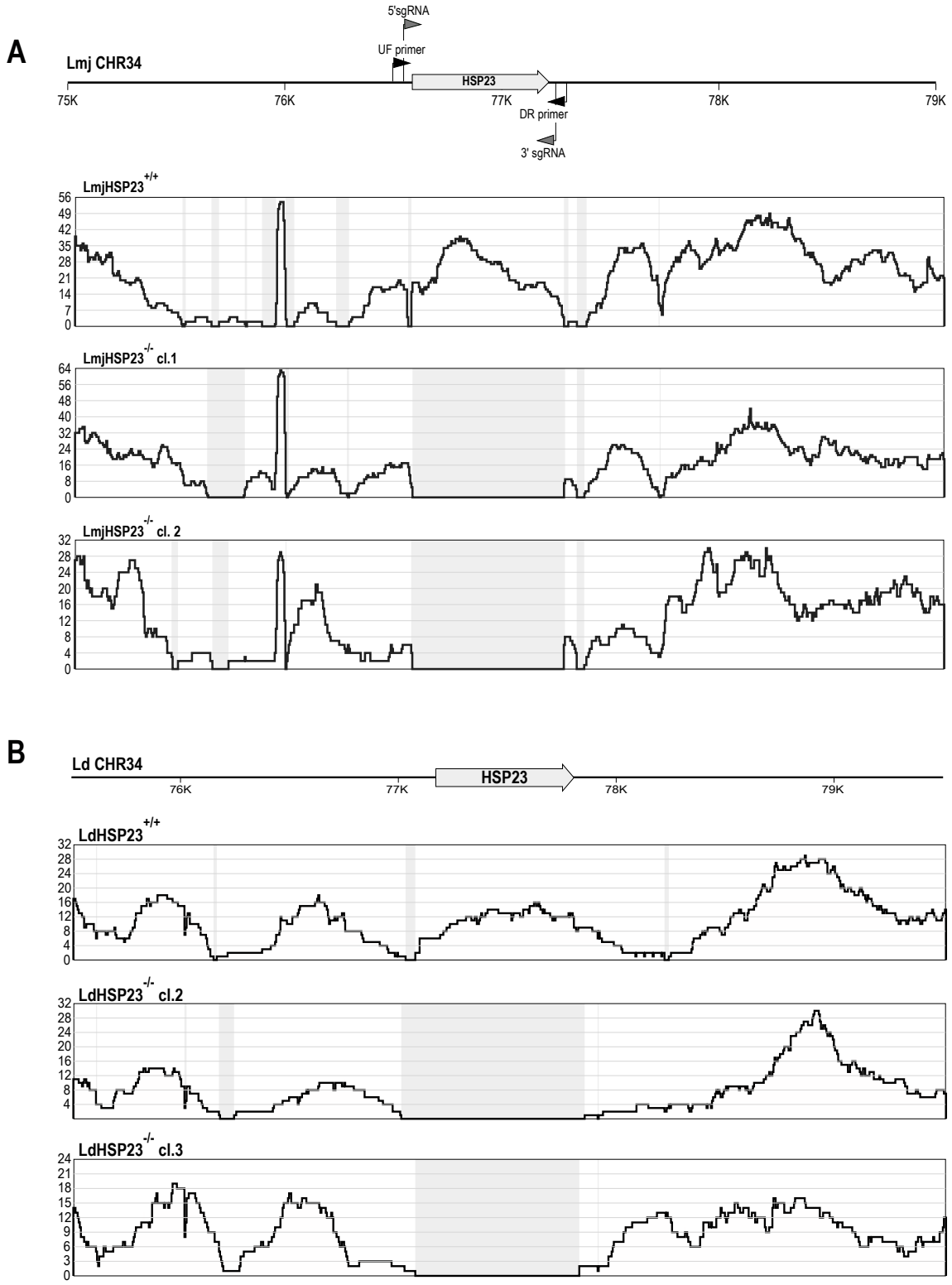

Figure 8 Whole genome sequencing of HSP23$^{-/-}$ null mutants. Sequence reads from *L. major* (A) or *L. donovani* (B) HSP23$^{-/-}$ null mutants were aligned to the reference DNA sequence consisting of chromosome 34 of *L. major* LV39c5 reference genome or *L. donovani* BPK282A1 reference genome using Bowtie 2 software. The Y-axis represents the number of reads and the X-axis shows the nucleotide position (bp) on chromosome 34. Grey shaded areas denote a complete lack of aligned reads. Upstream forward (UF), downstream reverse (DR) and both sgRNA primer binding sites are indicated with arrows.

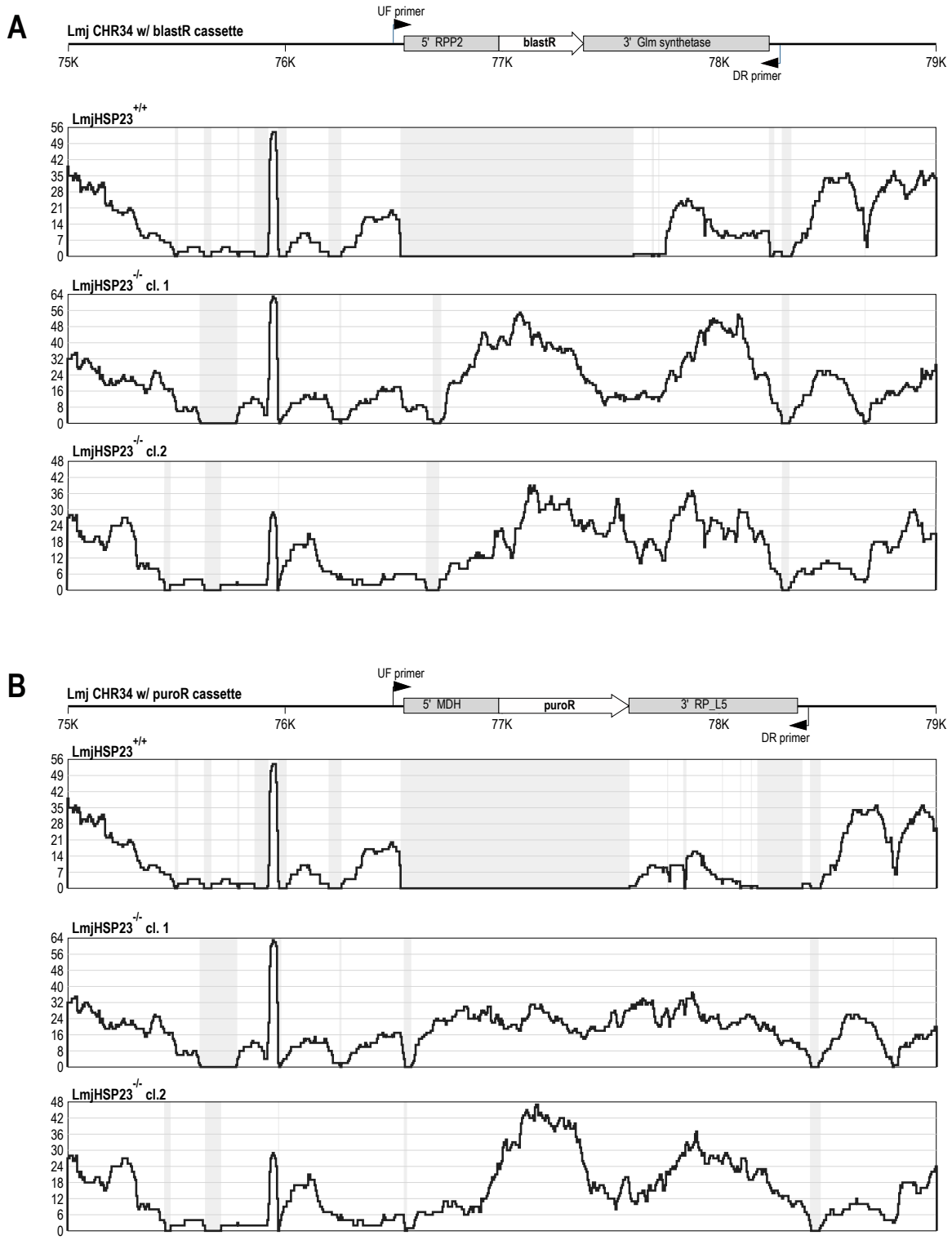

Figure 9 Verification of the *L. major* HSP23 gene replacement by the respective resistance cassettes. Sequence reads from the analysed LmjHSP23$^{-/-}$ null mutant clones were aligned to the *in silico*-designed reference DNA sequences consisting of the *L. major* genome (DNA) sequence of chromosome 34 (LV39c5) with the expected insertion of antibiotic resistance cassettes (blastR = blasticidin; PuroR = Puromycin). The Y-axis represents the number of reads and the X-axis shows the nucleotide position (bp) on chromosome 34. Grey shaded areas denote a complete lack of aligned reads. Upstream forward (UF) and Downstream reverse (DR) primer binding are depicted as arrows. MDH = malate dehydrogenase; RPP2= 60S ribosomal protein P2; Glm = glutamine; RP_L5= 60S ribosomal protein L5

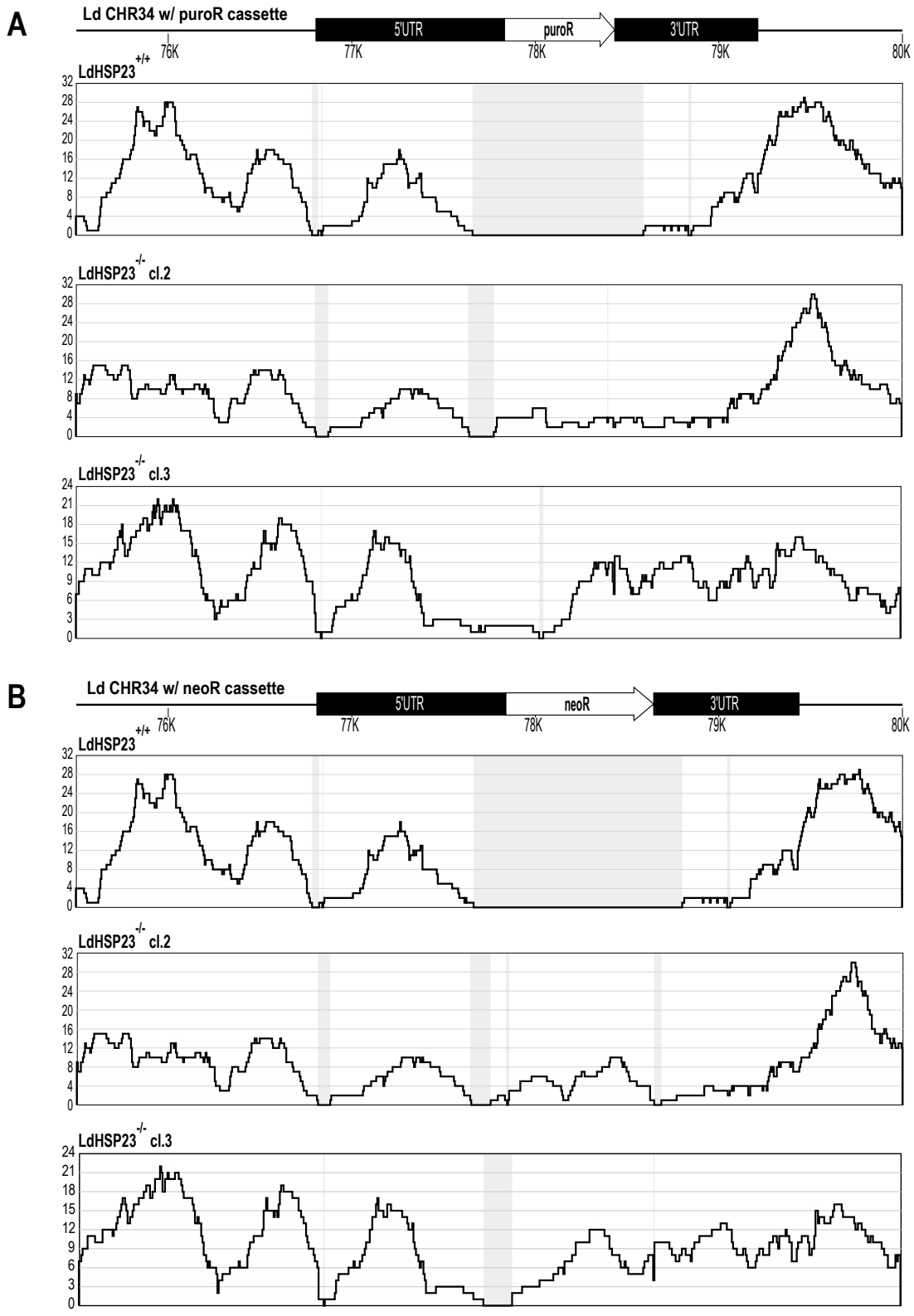

Figure 10 Verification of the *L. donovani* HSP23 gene replacement by the respective resistance cassettes. Sequence reads from each analysed strain were aligned to the *in silico*-designed reference DNA sequences consisting of the *L. donovani* genome (DNA) sequence of chromosome 34 (TriTrypDB-46_LdonovaniBPK282A1_Genome.fasta) with the expected insertion of antibiotic resistance cassettes (NeoR = Neomycin; PuroR = Puromycin). The Y-axis represents the number of reads and the X-axis shows the nucleotide position (bp) on chromosome 34. Grey shaded areas denote a complete lack of aligned reads.

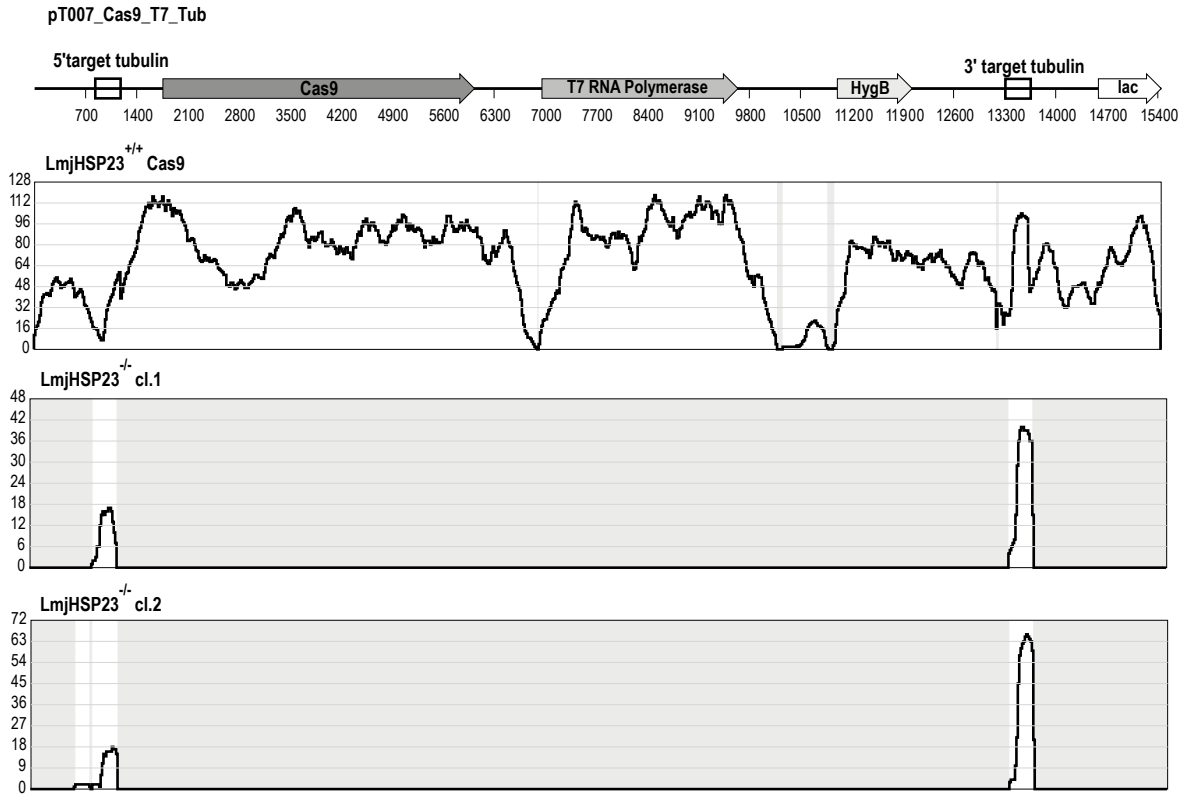

Figure 11 Bowtie alignment of sequence reads against the pT007 plasmid. The Y-axis represents the number of reads and the X-axis shows the nucleotide position (bp) on the pT007 plasmid. Grey shaded areas denote a complete lack of aligned reads. HygB= Hygromycin B

2.2.2 Verification at the mRNA Level and Protein Level

Next, I analysed the loss of HSP23 at the transcript and protein level by performing quantitative real-time PCR (qRT-PCR) and Western blot analyses, respectively. While HSP23-specific mRNA was detectable in HSP23$^{+/+}$ WT cells (set to 1), it was absent in all HSP23$^{-/-}$ mutants analysed (Fig 12A,B). Furthermore, I confirmed the absence of Cas9 mRNA in all LmjHSP23$^{-/-}$ mutants (Fig 12A). Western blot analysis using HSP23-specific antibodies also verified the absence of the HSP23 protein in these HSP23$^{-/-}$ mutant lysates (Fig 12C,D). These results indicate that I successfully obtained double-allelic *L. major* and *L. donovani* HSP23$^{-/-}$ null mutants.

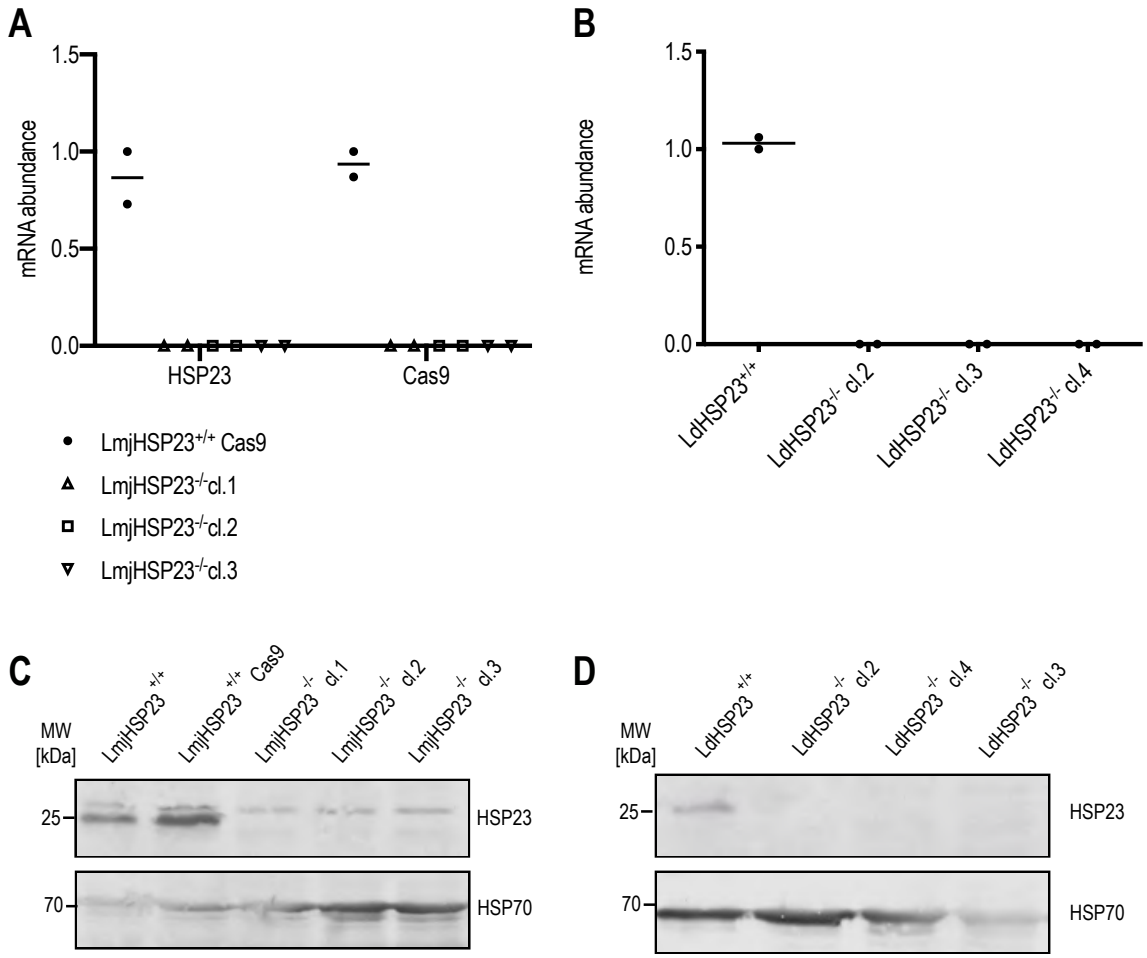

Figure 12 Verification of HSP23 gene replacement at the mRNA and protein level. HSP23 mRNA abundance was quantified in *L. major* (A) and *L. donovani* (B) strains by qRT-PCR using *HSP23*-specific primers. CT values were normalised to actin levels and then to the cognate WT (HSP23$^{+/+}$) sample (set to 1). HSP23 protein abundance in *L. major* (C) and *L. donovani* (D) strains was tested by Western blot analysis. 1 × 10^7 cells of the respective strains were lysed under denaturing conditions, the cell lysates were separated by SDS-PAGE and subjected to Western blot using an anti-HSP23 (1/500) antibody. An anti-HSP70 (1/1000) antibody was used as loading control. MW = Molecular weight in kilodalton.

2.3 Phenotype Analysis

2.3.1 *L. major* HSP23$^{-/-}$

The loss of HSP23 in *L. donovani* was previously shown to render parasites more sensitive towards chemical stressors and incapable of surviving at mammalian tissue temperatures [1]. To investigate the role of the *L. major* HSP23, the phenotype of *L. major* HSP23$^{-/-}$ mutants was assessed under different *in vitro* growth conditions and compared with wild type cells.

Cell density on day 4 (stationary phase) was analysed and expressed as percentage of growth relative to the wild type (set at 100%). At optimal growth conditions for promastigotes

(25°C, pH 7.4), all LmjHSP23$^{-/-}$ clones analysed showed a 50% reduction of growth when compared to wild type cells (Fig 13A).

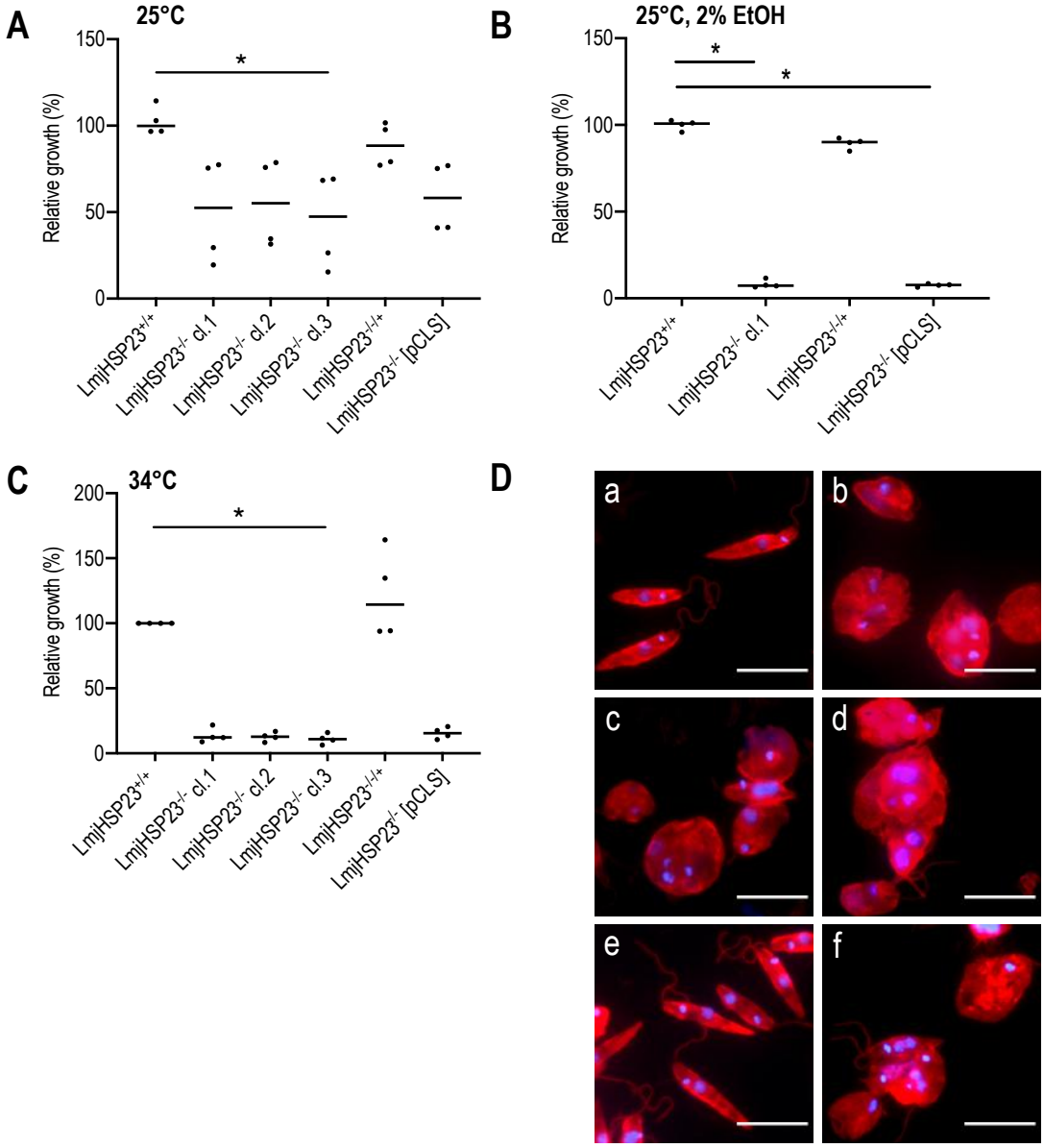

Figure 13 Phenotype analysis of *L. major* HSP23$^{-/-}$ mutants. 1 × 10^6 or 5 × 10^6 parasites were seeded in 10 mL complete M199 medium and parasite density was assessed at day 4. Parasites were grown at 25°C (A), 25°C with 2% EtOH (B), and 34°C (C). Cell density is shown as percentage of HSP23$^{+/+}$ WT (set at 100%). Statistical testing was carried out by Kruskal-Wallis test; *=p < 0.05 (n=4) (D) The *L.maj* HSP23$^{-/-}$ clones incubated for 4 days at 34°C were stained with mouse anti-tubulin antibody (1/4000) and DAPI (1/50). Images were taken on an EVOS FL Auto Cell Imaging System and processed using the ImageJ Software. a = LmjHSP23$^{+/+}$; b = LmjHSP23$^{-/-}$ cl.1; c = LmjHSP23$^{-/-}$ cl.2; d = LmjHSP23$^{-/-}$ cl.3; e = LmjHSP23$^{-/-/+}$; f = LmjHSP23$^{-/-}$ [pCLS]. Scale bar: 10µm.

As expected, growth can be restored by episomal expression of the LmjHSP23 transgene (LmjHSP23$^{-/-/+}$), but not by the expression vector alone (LmjHSP23$^{-/-}$ [pCLS]).

I also tested LmjHSP23$^{-/-}$ cl.1 for tolerance to sublethal EtOH, a trigger to induce the unfolded protein response. Addition of 2% EtOH to the cell culture medium led to a complete growth

arrest of LmjHSP23$^{-/-}$ and LmjHSP23$^{-/-}$ [pCLS] mutants, while the add-back cells showed a similar growth rate to the wild type (Fig 13B). Next, I assessed the ability of LmjHSP23$^{-/-}$ clones to survive temperature stress by incubating the cells at 34°C for four days. In line with previous work, the LmjHSP23$^{-/-}$ and LmjHSP23$^{-/-}$ [pCLS] mutants were temperature-sensitive and did not proliferate (Fig 13C). As assayed by immunofluorescence, high temperatures also induced typical morphological changes such as the rounding of the normally elongated WT promastigotes (Fig 13D). Again, ectopic expression of the *L. major* HSP23 transgene abrogated these heat-induced effects (Fig 13D, panel e).

2.3.2 *L. donovani* HSP23$^{-/-}$

To verify the previously reported *L. donovani* HSP23$^{-/-}$ phenotype, I also analysed the growth behaviour of the newly generated LdHSP23$^{-/-}$ null mutants. For comparison, the previously characterised LdHSP23$^{-/-}$ null mutant [1], hereinafter named esc0, was included in the analysis. At 25°C, HSP23 deficient clones 2, 3 and 4 displayed a 65% reduced proliferative capacity at day 4 compared to WT cells (Fig 14A). The growth phenotype could be partially rescued by ectopic over expression of the HSP23 transgene but not by the empty expression vector alone. An unexpected growth behaviour was found for the LdHSP23$^{-/-}$ esc0. This clone appeared to have lost the growth phenotype at 25°C and exhibited comparable growth to that of wild type cells.

Next, I tested whether the cell growth is similarly affected by protein folding stress. For this, LdHSP23$^{-/-}$ cl.2 was treated with 2% EtOH over a period of 4 days. In agreement with previous results, treatment with 2% EtOH resulted in severe growth inhibition, which was partially reversed by ectopic over expression of the HSP23 transgene, but not by the empty expression vector alone (Fig 14B). Again, the LdHSP23$^{-/-}$ esc0 was less sensitive to EtOH when compared to LdHSP23$^{-/-}$ cl.2 showing similar growth rates as the add-back strain (LdHSP23$^{-/-/+}$). I also tested the growth behaviour under H_2O_2 addition (Fig 14C). While LdHSP23$^{-/-}$ cl.2 showed a 60% reduced growth, the LdHSP23$^{-/-}$ esc0 grew even slightly better than LdHSP23$^{+/+}$. Unexpectedly, introduction of an LdHSP23 transgene (LdHSP23$^{-/-/+}$) did not rescue the observed growth phenotype. LdHSP23$^{-/-/+}$ and LdHSP23$^{-/-}$ [pCLS] grew at similar, reduced rates.

These results strongly indicate the spontaneous emergence of an LdHSP23$^{-/-}$ escape variant with increased resistance towards several stressors, hence designated as LdHSP23$^{-/-}$ esc0.

Based on this finding, I next questioned whether LdHSP23$^{-/-}$ esc0 also displays increased tolerance to high temperatures. For this, proliferation and survival of the HSP23$^{+/+}$ WT cells, the LdHSP23$^{-/-}$ esc0 and the three newly generated LdHSP23$^{-/-}$ clones were investigated at non-permissive temperatures monitoring cell density daily over a period of four days (Fig 14D). Since viscerotropic *Leishmania* spp. like *L. donovani* are able to tolerate higher temperatures than their dermotropic counterparts such as *L. major,* growth was measured at 37°C. Here, only the LdHSP23$^{+/+}$ WT and the LdHSP23$^{-/-/+}$ add-back strain were able to

proliferate reaching a cell density of 5 × 10^7 cells/mL and 3.5 × 10^7 cells/mL at day 4, respectively (Fig 14D).

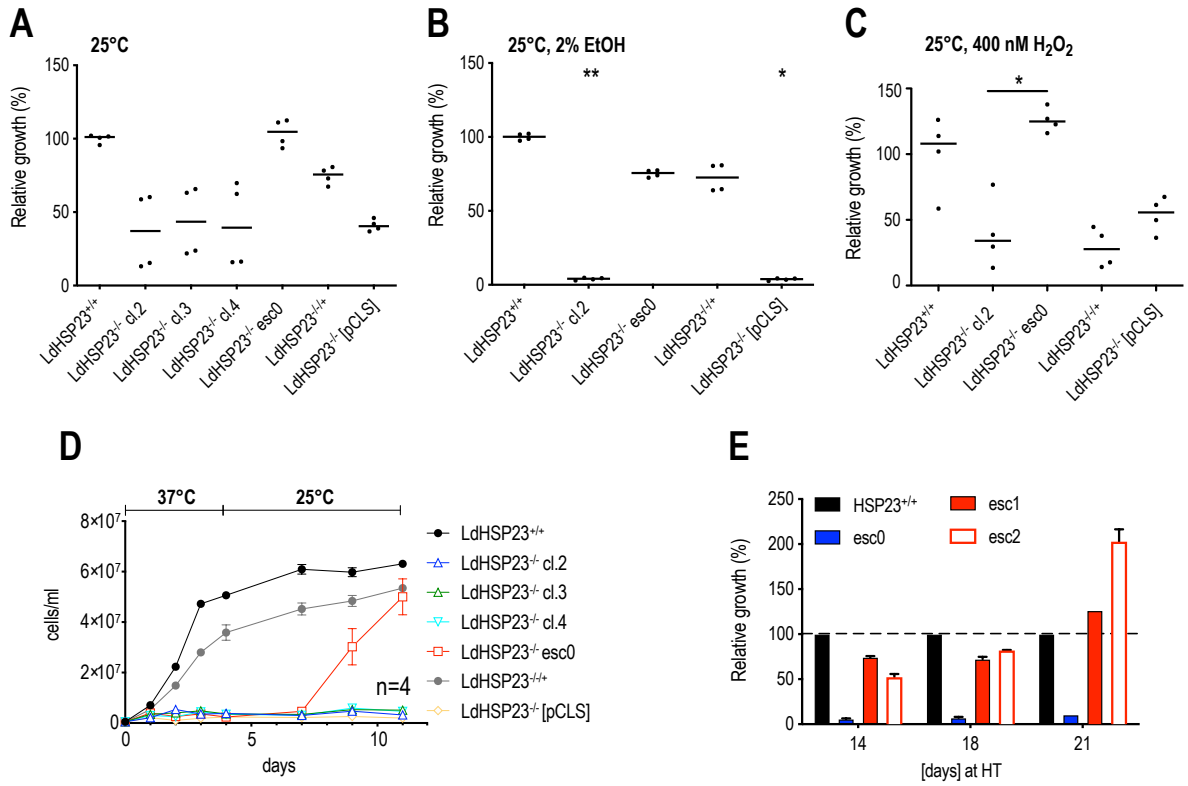

Figure 14 Phenotype analysis of *L. donovani* HSP23$^{-/-}$ mutants. 1 × 10^6 cells were seeded into 7 mL of supplemented M199$^+$ medium. Parasites were cultured at LT (25°C) (A), 2% EtOH at LT (B) or 400 nM H_2O_2 at LT (C). Cell density was assessed on day 4 and was normalised to wild type (HSP23$^{+/+}$) cell density (set at 100%). The previously generated LdHSP23$^{-/-}$ clone [1], renamed as LdHSP23$^{-/-}$ esc0, was included in the analysis. Differences were tested for significance using the Kruskal–Wallis test: *=p<0.05, **=p<0.01 (n=4) (D) Growth analysis at non-permissive temperatures (37°C). 5 × 10^5 cells/mL were seeded into 10 mL of M199$^+$ medium and incubated for four days at HT (37°C). The cultures were shifted back to LT and grown for seven days. (E) Growth comparison of parent non-selected LdHSP23$^{-/-}$ esc0, two LdHSP23$^{-/-}$ esc0 populations, that were incubated for four days at 37°C and then shifted back to 25°C (see D), and HSP23$^{+/+}$ wild type cells (set as 100%). Cells were cultured until day 21, and were diluted twice weekly to 5 × 10^5 cells/mL. Error bars represent the standard error of the mean (SEM).

In contrast, all LdHSP23$^{-/-}$ null mutant lines, including the LdHSP23$^{-/-}$ esc0 mutant, did not grow at the elevated culture temperature. To distinguish between parasite death and growth inhibition, the cultures were shifted back to 25°C at day 4. While no outgrowth was observed for LdHSP23$^{-/-}$ clones 2, 3 and 4, indicating that the four-day exposure to heat stress had been indeed lethal, the LdHSP23$^{-/-}$ esc0 mutant quickly entered logarithmic growth and reached a similar cell density as the WT at day 11 (Fig 14D). This indicated that a part of the LdHSP23$^{-/-}$ esc0 population had survived the high temperature selection.

Next, two independent outgrowth populations, obtained after the recovery period at 25°C shown in Fig 14D, were tested again for their ability to tolerate high temperatures (Fig 14E). While the parent LdHSP23$^{-/-}$ esc0 population did not grow over a period of 21 days at 37°C,

the two preselected outgrowth populations esc1 and esc2 showed restored thermotolerance reaching similar growth rates as wild type cells.

In summary, phenotype analysis of newly generated LdHSP23$^{-/-}$ confirmed the data of previous work. However, I identified an LdHSP23$^{-/-}$ escape variant esc0 that displayed restored stress tolerance at 25°C and the ability to survive short-term heat periods. Furthermore, preselection at HT followed by a recovery period at permissive temperatures allowed to select and expand two fully temperature-tolerant LdHSP23$^{-/-}$ mutant populations esc1 and esc2. A deeper investigation of underlying compensatory mechanisms will be described in section 2.5.

2.4 Complementation Studies

The use of reverse genetics and subsequent phenotype analysis of HSP23$^{-/-}$ null mutant strains in two different *Leishmania* spp. has pointed towards a functional conservation of HSP23. To further address this, I implemented a functional cloning approach by over expressing various putative HSP23 homologues in the *L. major* and *L. donovani* HSP23$^{-/-}$ null mutant background.

2.4.1 Identification of HSP23 Orthologues

Firstly, to identify HSP23 orthologues in other *Leishmania* and *Trypanosoma* spp., a BLASTP search was performed using the *L. donovani* HSP23 amino acid sequence as reference. In line with already published phylogenetic analyses, a single HSP23 orthologue was found in all *Leishmania* spp., as well as in the related *Trypanosoma* spp..

Table 1 Phylogenetic analysis of *Leishmania* and *Trypanosoma* HSP23 proteins. A multiple sequence alignment of HSP23 amino acid sequences was performed using the ClustalW algorithm. The resulting sequence identity scores of HSP23s between *Leishmania* and *Trypanosoma* species are indicated in (%).

	L. donovani	*L. infantum*	*L. major*	*L. braziliensis*	*T. brucei*	*T. cruzi*
L. donovani	100.0					
L. infantum	99.5	100.0				
L. major	95.2	94.7	100.0			
L. braziliensis	85.2	85.2	84.2	100.0		
T. brucei	36.3	36.3	37.3	36.3	100.0	
T. cruzi	38.7	38.7	39.2	39.2	51.5	100.0

Next, I performed a multiple sequence alignment with a selected panel of HSP23 orthologues using the ClustalW algorithm. As shown in Table 1, protein sequence identities among *Leishmania* HSP23s range from 84% to 99% with *L. braziliensis* HSP23 being the most divergent protein. An even lower sequence conservation of 36%-39% was found between the different *Leishmania* and the two *Trypanosoma* orthologues reflecting the phylogenetic divergence of *Leishmania* and *Trypanosoma* spp. during evolution, but also the high sequence variability of small heat shock proteins.

2.4.2 Generation and Verification of Complementation Lines

To generate complementation lines, the *L. major* HSP23$^{-/-}$ cl.1 and *L. donovani* HSP23$^{-/-}$ cl.2 were transfected with an episomal plasmid pCLS bearing the HSP23 orthologues of *L. donovani*, *L. infantum*, *L. major, L. braziliensis*, *T. brucei* and *T. cruzi,* respectively. After selection of nourseothricine-resistant populations, ectopic over expression of HSP23 was first tested at the RNA level by qRT-PCR using *HSP23* species-specific primers.

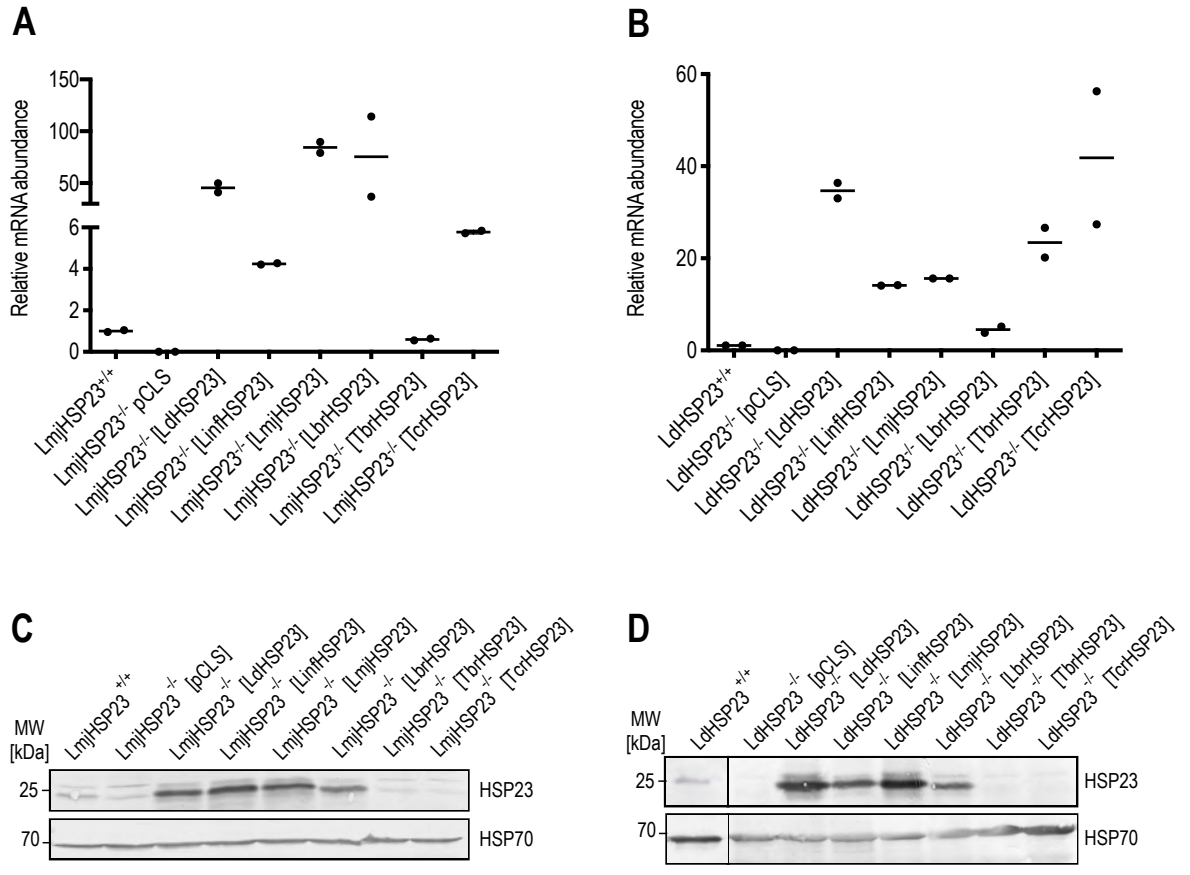

Figure 15 Verification of LmjHSP23$^{-/-}$ and LdHSP23$^{-/-}$ complementation lines. Relative mRNA abundance of orthologous HSP23 transcripts (*L. donovani, L. major, L. infantum, L. braziliensis, T. brucei* and *T. cruzi.)* was quantified for *L. major* (A) and *L. donovani* (B) complementation lines by qRT-PCR using transgene-specific primers. CT values were first normalised to actin used as internal control and then to the WT sample (set to 1). (C,D) Western blot of whole cell lysates of *L. major* (C) and *L. donovani* (D) complementation lines probed with an anti-HSP23 antibody (1/500) and anti-HSP70 (1/1000) antibody. MW = molecular weight in kilodalton.

As expected, HSP23 mRNA was detected in all transgenic over expression lines, while it was absent in the HSP23$^{-/-}$ [pCLS] parasites transfected with the empty plasmid only (Fig 15A,B). Notably, the level of HSP23 mRNA varied strongly between the different transgenic lines and appeared to be dependent on the parental strain used for transfection. For example, in the *L. major* HSP23$^{-/-}$ null mutant background (Fig 15A), the highest mRNA abundance was observed for the *L. major* and *L. braziliensis* HSP23 transgene, as demonstrated by a 70- to 80-fold increase of mRNA when compared to *L. major* HSP23$^{+/+}$ WT cells. In contrast, transfection of the same transgenes in *L. donovani* HSP23$^{-/-}$ null mutants only resulted in a 16-fold (LmjHSP23) and 4.5-fold (LbrHSP23) increase of mRNA abundance (Fig 15B).
Since transcript and protein levels in *Leishmania* are poorly correlated, all transgenic lines were also tested for the presence of HSP23 protein by Western blot analysis using specific antibodies raised against recombinantly expressed *L. donovan*i HSP23 (Fig 15C,D). Ectopic over expression was confirmed for all *Leishmania* HSP23s including *L. donovani*, *L. infantum*, *L. major* and *L. braziliensis*, but not for *T. brucei* and *T. cruzi*.

2.4.3 Phenotype Analysis of Complementation Lines

To assess whether ectopic expression of different trypanosomatid HSP23 transgenes in LdHSP23$^{-/-}$ or LmjHSP23$^{-/-}$ mutants can complement for the loss of the endogenous HSP23 protein, I first tested the growth of transgenic lines at 25°C. While LmjHSP23$^{-/-}$ [pCLS] and LmjHSP23$^{-/-}$ [LinfHSP23] showed a severe growth defect as previously demonstrated for the parental HSP23$^{-/-}$ null mutant clones (Fig 13A), ectopic expression of all other transgenes fully restored growth to WT levels (Fig 16A). Similarly, the significant growth reduction observed for LdHSP23$^{-/-}$ [pCLS] was reversed upon ectopic expression of all different transgenes (Fig 16B), though to a lesser extent than in *L. major*.
Next, I tested sensitivity to heat stress monitoring *in vitro* growth at 34°C or 37°C, for the *L. major* and *L. donovani* complementation lines, respectively. Again, ectopic expression of the HSP23-encoding orthologous genes of all *Leishmania* species and the phylogenetically closely related *Trypanosoma brucei* rescued the TS phenotype of both LmjHSP23$^{-/-}$ and LdHSP23$^{-/-}$ null mutants (Fig 16C,D). However, the degree of complementation substantially differed in *L. major* and *L. donovani* complementation lines: While ectopic over expression of HSP23 homologues in *L. major* HSP23$^{-/-}$ allowed almost complete reversal of the HSP23$^{-/-}$ TS phenotype (Fig 16C), only partial complementation was observed in *L. donovani* lines (Fig 16D). Also, expression of the TcrHSP23 transgene only partially complemented for the lack of the *L. major* HSP23 at 34°C, and did not restore growth of *L. donovani* HSP23$^{-/-}$ null mutants which grew at the same growth rate as the vector control line LdHSP23$^{-/-}$ [pCLS].
Next, I questioned whether HSP23 may determine the differences in temperature tropism of dermotropic and viscerotropic *Leishmania* spp.. To analyse possible differences in the capacity of transgenes to confer temperature tolerance, I also tested the growth of the dermotropic *L. major* complementation lines at 37°C. Similar cell densities were observed at

day four for all complementation lines showing that HSP23 transgenes from viscerotropic *Leishmania* spp. do not provide a fitness advantage when compared with transgenes from dermotropic species (data not shown).

These data show that the trypanosomatid HSP23 homologues, except for TcrHSP23, share functionality, enhancing proliferation at ambient temperatures and conferring protection against heat stress.

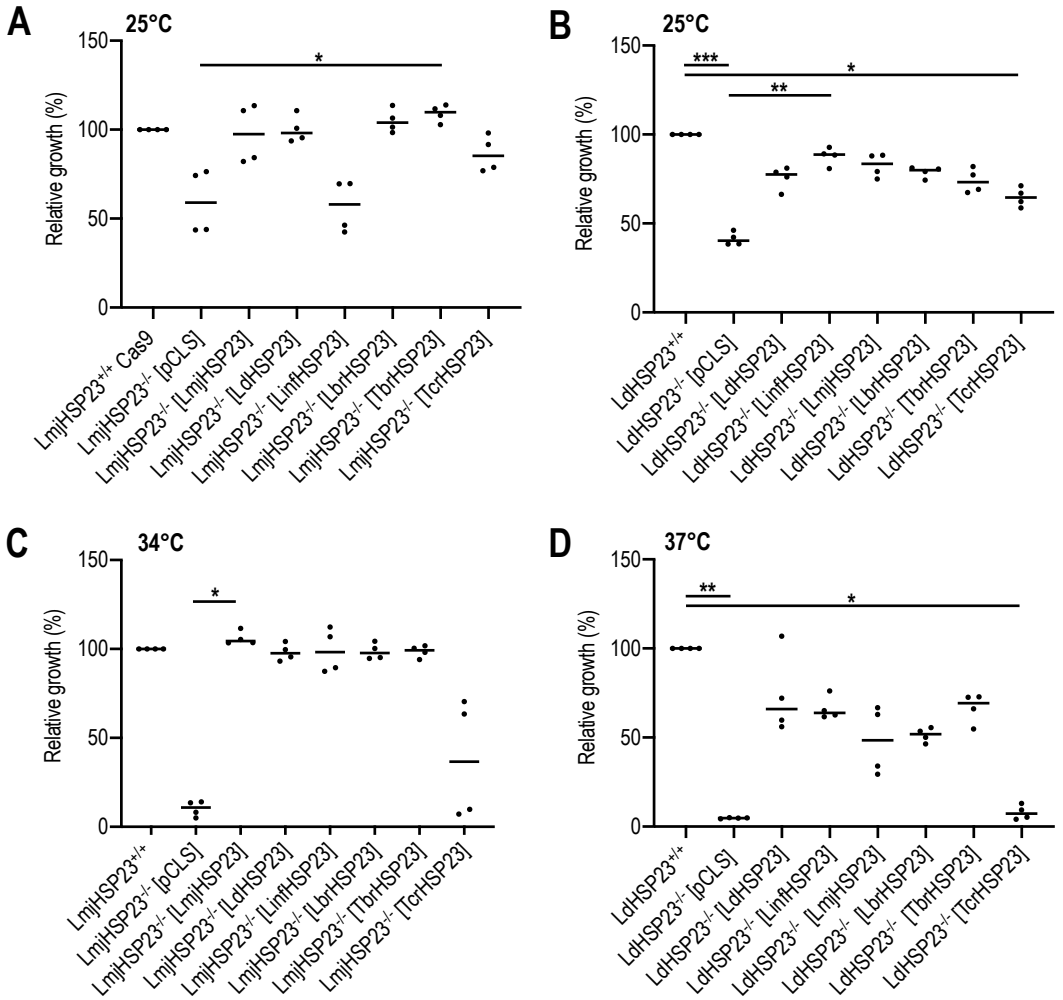

Figure 16 Phenotype analysis of *L. major* and *L. donovani* complementation lines. LmjHSP23$^{-/-}$ and LdHSP23$^{-/-}$ complementation lines were seeded at a cell density of 1 × 10^5 or 5 × 10^5 cells/mL and were either grown at permissive (A, B) or non-permissive temperatures (C, D). Cell density was assessed at day 4 and is shown normalised to LmjHSP23$^{+/+}$ WT growth (set at 100%). Statistical testing was carried out by Kruskal-Wallis test; *=$p < 0.05$, **=$p < 0.01$; (n=6): ***=$p < 0.001$ (n=4).

2.5 Compensatory Mechanisms for the Loss of HSP23

As described before, phenotype analysis of LdHSP23$^{-/-}$ null mutants revealed the emergence of an LdHSP23$^{-/-}$ escape variant named LdHSP23$^{-/-}$ esc0, showing WT-like growth at 25°C, restored tolerance to EtOH stress, and increased survival at high temperatures compared to

the other LdHSP23$^{-/-}$ clones (Fig 14). Subjecting these LdHSP23$^{-/-}$ esc0 to a four-day incubation at high temperature, followed by a recovery period at ambient temperature, yielded two fully temperature-tolerant LdHSP23$^{-/-}$ null mutant populations (esc1 and esc2) (Fig 14 D,E).

2.5.1 Genetic Adaptations

Due to the lack of transcriptional control, *Leishmania* adaptive gene expression is thought to be mainly modulated through chromosomal or gene copy number variations (aneuploidy, gene amplification, or gene deletion) [83-85]. Importantly, these genomic alterations are frequently found in *Leishmania* parasites that are challenged with stressful conditions such as drug pressure or environmental changes [67, 92].
To identify concomitant genomic alterations possibly compensating for the lack of HSP23, we performed a deep sequencing comparison of the genomes of parental *L. donovani* 1SR or *L. major* 5ASKH wild type parasites and the corresponding HSP23$^{-/-}$ null mutants.

2.5.1.1 Aneuploidy

Based on NGS sequence read coverage data, we first assessed possible changes in the karyotype. The integer or intermediate somy (S) values for each chromosome, referring to full or mosaic aneuploidy, respectively, are graphically represented as heat maps (Fig 17).

L. major

First, we analysed the karyotype of LmjHSP23$^{+/+}$, LmjHSP23$^{+/+}$ Cas9 and the two HSP23$^{-/-}$ clones 1 and 2 of *L. major* promastigotes (Fig 17A). In all samples, most chromosomes were found to be diploid with S values ranging between 1.5 and 2.5. Exceptions were chromosomes 5 and 23, which were triploid, and chromosome 31 which was pentaploid. Notably, while the karyotype of the HSP23$^{-/-}$ cl.1 remained unchanged, we observed marginal differences in the HSP23$^{-/-}$ clone 2 samples for chromosome 1, 2, 3, 5 and 6, demonstrated by a slight increase (+0.4-0.5) of the corresponding S values. In addition, the S value of chromosome 31 decreased from 5.06 in the WT to 4.68 in the HSP23$^{-/-}$ clone 2, while it increased to 5.44 in the LmjHSP23$^{+/+}$ Cas9 sample, indicating mosaic aneuploidy.

L. donovani

In contrast with the overall similar S values among the *L. major samples*, we identified drastic karyotype differences between LdHSP23$^{+/+}$, LdHSP23$^{-/-}$ clones and escape variants as judged by substantial changes in S values (Fig 17B). For instance, a somy score reduction from ~3 to ~2 was observed for chromosomes 12 and 23 in all LdHSP23$^{-/-}$ escape mutants as compared to all other samples demonstrating a change from a trisomic to a disomic state of these chromosomes. In three of the four LdHSP23$^{-/-}$ escape samples we found a mosaic trisomy (2.66-2.71) for chromosome 14 which was disomic in HSP23$^{+/+}$ WT samples

(1.82-2.22). An increase of S values was also observed for chromosomes 8 and 35 in LdHSP23$^{-/-}$ cl.2, cl.3 and LdHSP23$^{-/-}$ esc0-LT, revealing a full or mosaic trisomy for these chromosomes. In keeping with previous reports [199], chromosome 31 was found to be tetraploid (3.88-4.37) in all samples analysed. Dendrogram analysis separates esc0 and its derivatives, esc1 and esc2, from the rest of the strains, but also sets apart LdHSP23$^{-/-}$ clones 2 and 3 from LdHSP23$^{+/+}$ populations.

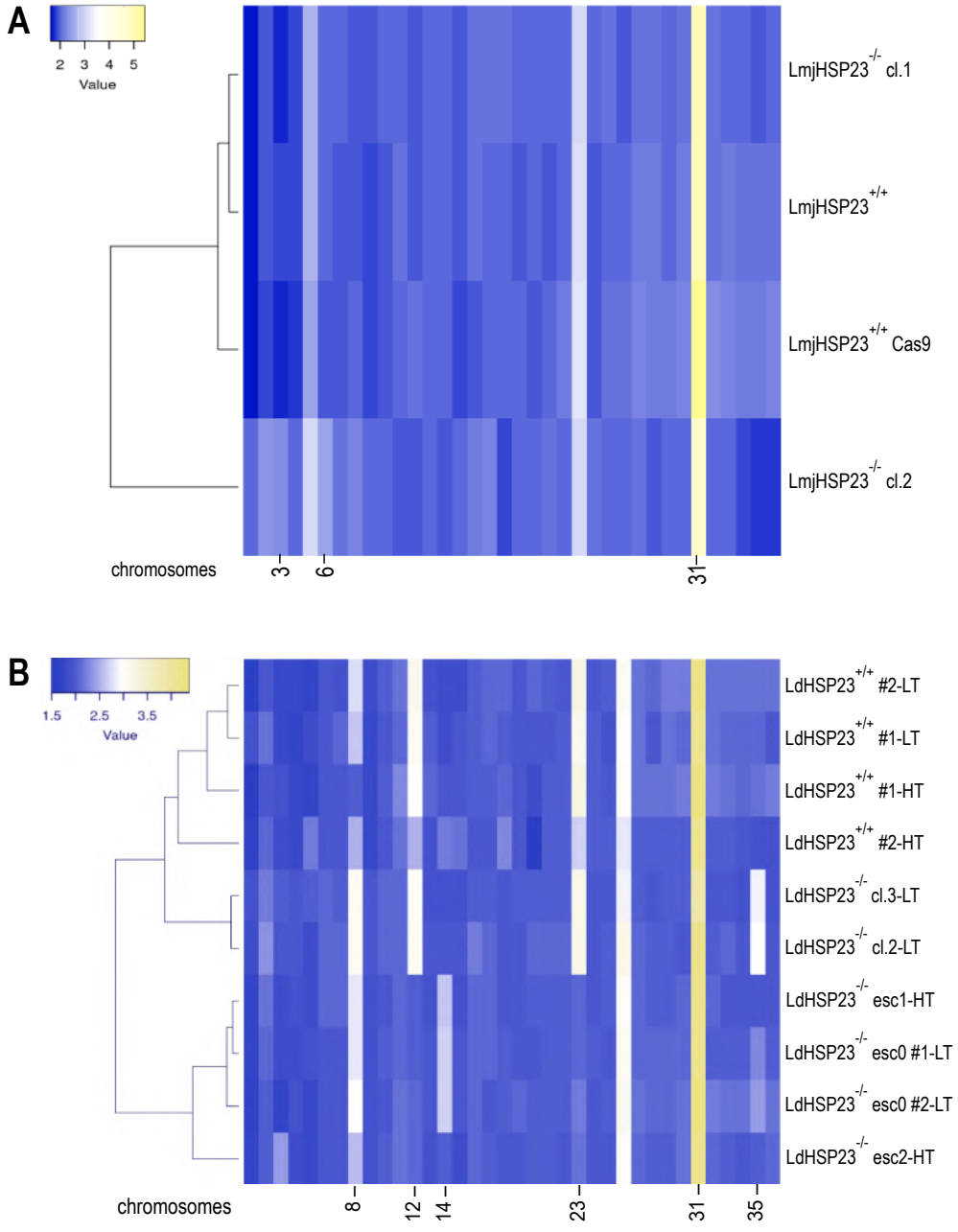

Figure 17 Comparison of chromosomal ploidy profiles. Heat map showing somy levels across all *L. major* (A) and *L. donovani* (B) samples. The x-axis indicates a selected panel of chromosomes showing aneuploidy in HSP23$^{-/-}$. Colour scale indicates low (blue) to high (yellow) somy number. Somy (S) value ranges are as follows: monosomy, $S < 1.5$ (dark blue); disomy, $1.5 \leq S < 2.5$ (light blue); trisomy, $2.5 \leq S < 3.5$ (white); tetrasomy, $3.5 \leq S < 4.5$ (light yellow); pentasomy, $4.5 \leq S < 5.5$ (yellow). The dendrogram (left) was generated by Pearson distance measurements based on similarity of ploidy profiles.

2.5.1.2 Copy Number Variations

Next, we performed a genome-wide analysis of gene copy number variations (CNVs).

L. major

In general, gene copy numbers indeed matched with the observed somy levels. Also, the slightly elevated somy values observed for chromosomes 1, 2, 3, 5 and 6 in the LmjHSP23$^{-/-}$ cl.2 sample (section 2.5.1.1), were reflected by an increase of gene copy numbers.

For chromosome 3 (Fig 18 A-D), which showed an increase in the S value from 1.85 to 2.27 in the LmjHSP23$^{-/-}$ cl.2 sample (Fig 18D), we observed two intrachromosomal amplifications resulting in a 50% increase of gene copy numbers: (i) a 63 kb region from nucleotide position 52154 bp to 115979 bp encompassing 15 genes (LMJLV39_030007300-LMJLV39_030008700) and (ii) a larger application of the 3' half of the chromosome from nucleotide positions 171757 bp to 353290 bp including 41 genes (LMJLV39_030010100-LMJLV39_030014100). Similar results were obtained for chromosome 5 (Fig 18 E-H). Here, the switch from a mosaic (2.53) to a full trisomy (3.04) in the LmjHSP23$^{-/-}$ cl.2 sample (section 2.5.1.1) resulted in a clear increase of gene copy numbers (Fig 18H). In addition, we identified a strong amplification of a single gene (LMJLV39_050015600) in the LmjHSP23$^{-/-}$ cl.2 sample as judged by a 3.5-fold higher gene copy number than the other samples. This gene codes for a hypothetical protein with no orthologues in other organisms. Also, we identified two genes at the 3' telomeric end of chromosome 5, namely LMJLV39_050017700 and LMJLV39_050017900, which were highly amplified (~2-3-fold) in LmjHSP23$^{+/+}$ Cas9 and LmjHSP23$^{-/-}$ cl.1/2, but not in the LmjHSP23$^{+/+}$ sample. Interestingly, in the LmjHSP23$^{-/-}$ cl.2 sample this amplification was even more pronounced leading to up to 5-fold increased GCNs compared to LmjHSP23$^{+/+}$, and additionally comprised at least ten genes of the 3' telomeric end (LMJLV39_050017700-LMJLV39_050018600). Eight of the ten genes code for snoRNAs, suggesting a selective advantage in Cas9 expressing lines.

L. donovani

Comparative bioinformatic analyses revealed 173 genes for which copy numbers changed exclusively in all LdHSP23$^{-/-}$ null mutant samples, but not in the HSP60$^{-/-}$ null mutants used as a control. Again, these changes in CNVs correlated with the observed ploidy alterations. For example, somy reduction from a trisomic to a disomic state, as found for chromosome 12 and 23 in LdHSP23$^{-/-}$ escape mutants (section 2.5.1.1), is reflected by a 50% decrease of gene copy numbers. Similar results were also obtained for chromosome 35 in the LdHSP23$^{-/-}$ clones 2 and 3 (-LT). Gain of chromosome 35 in these lines thereby led to a 50% increase of gene copy numbers compared to the wild type samples (Fig 19 A-D).

However, striking discrepancies between CNVs and somy levels were found for chromosome 35 in the LdHSP23$^{-/-}$ escape variants (Fig 19 E,F).

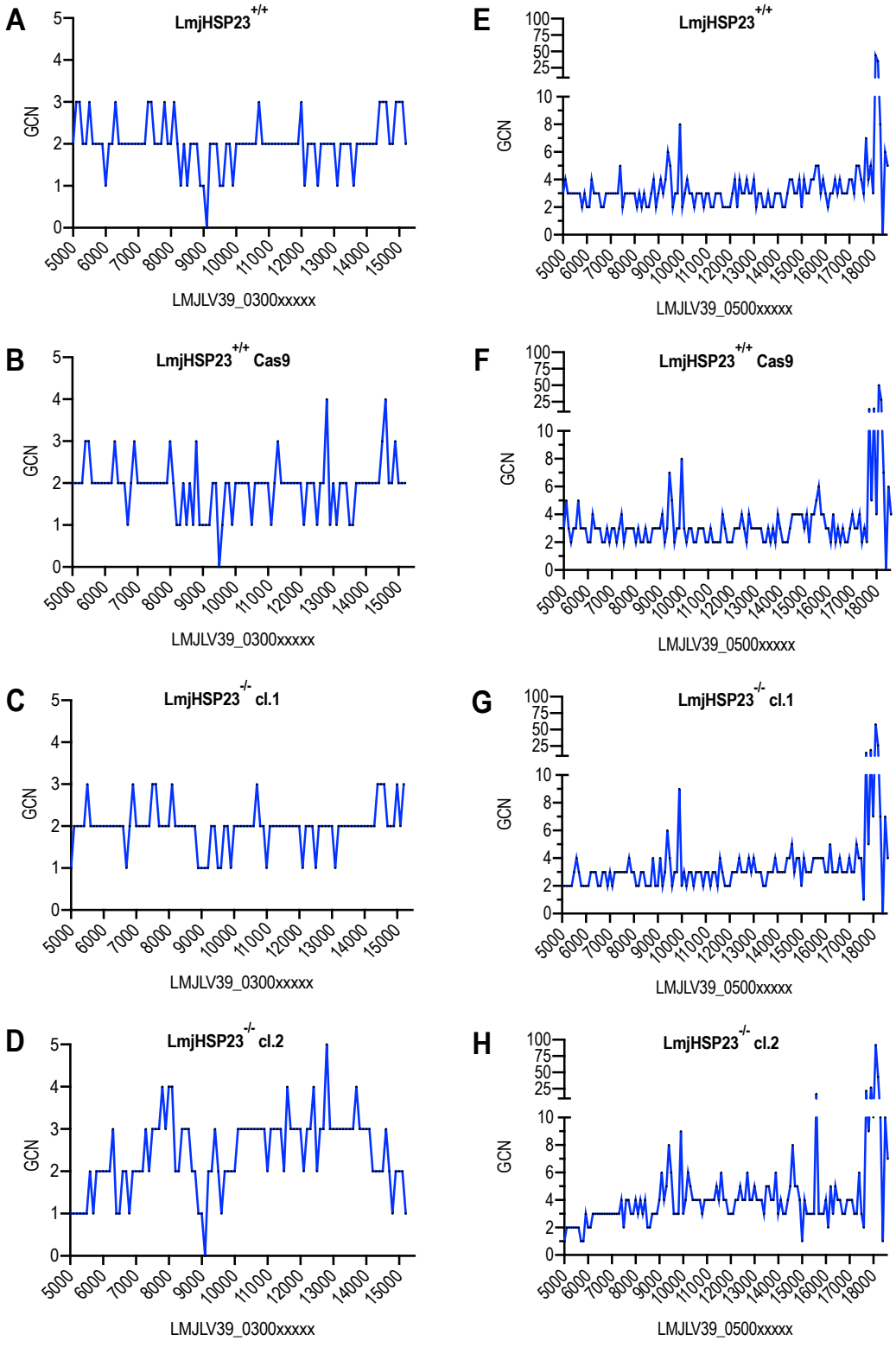

Figure 18 Strain-specific gene-copy number variations in *L. major* HSP23$^{-/-}$. Copy numbers of each gene (LMJV39_0300xxxxx) on chromosome 3 (A-D) and (LMJV39_0500xxxxx) chromosome 5 (E-H) were calculated based on read coverage data and are shown for (A, E) LmjHSP23$^{+/+}$, (B, F) LmjHSP23$^{+/+}$ Cas9, (C, G) LmjHSP23$^{-/-}$ cl.1, and (D, H) LmjHSP23$^{-/-}$ cl.2.

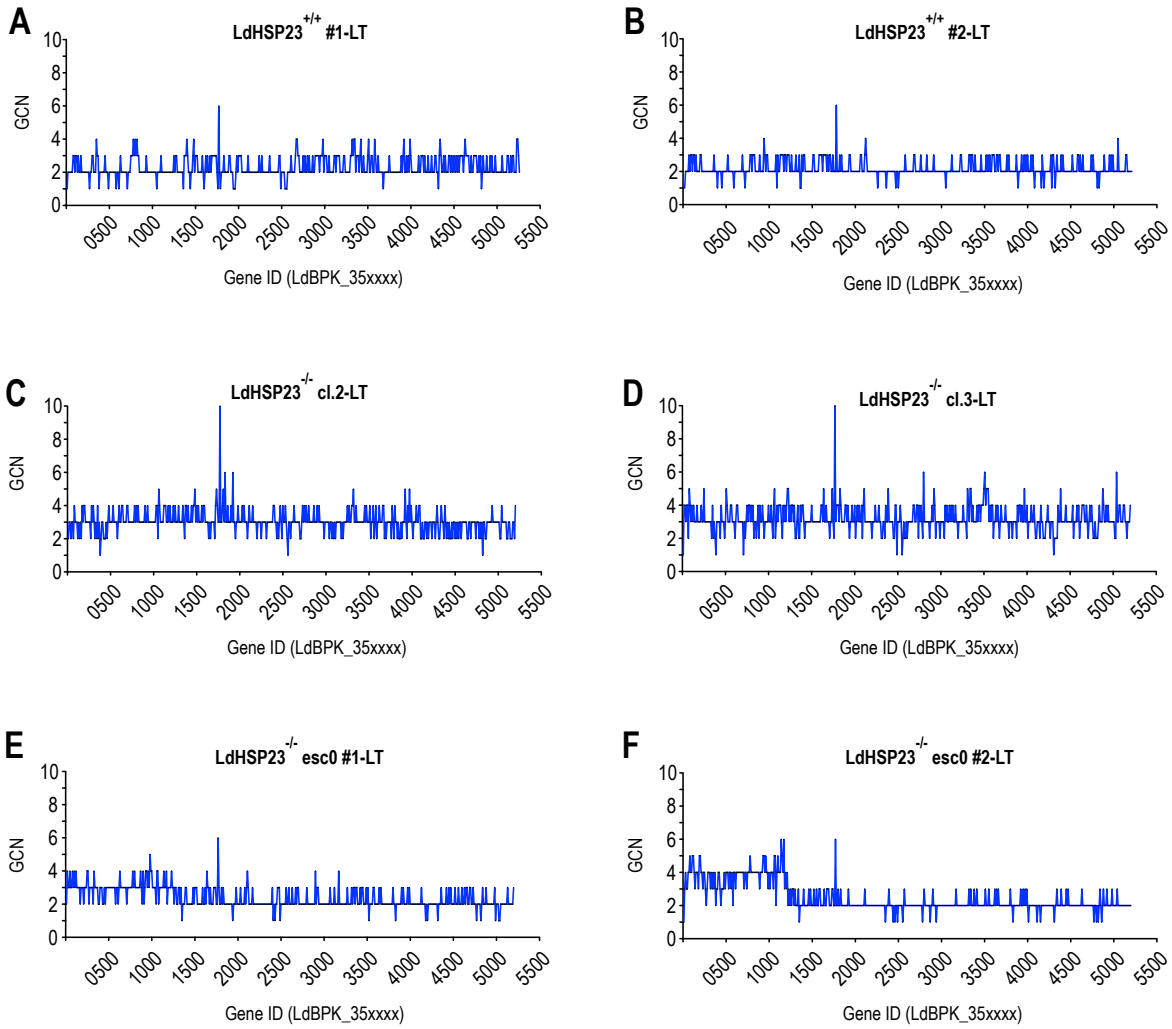

Figure 19 Strain-specific gene copy number variations on chromosome 35 in *L. donovani* HSP23$^{-/-}$ mutants at permissive temperatures. Copy numbers of each gene (LdBPK_35xxxx) on chromosome 35 were calculated based on read coverage data and are shown for (A, B) HSP23$^{+/+}$, (C, D) HSP23$^{-/-}$, and (E, F) HSP23$^{-/-}$ esc0. All strains were selected and grown at 25°C (LT).

While these lines were shown to be predominantly disomic for chromosome 35, an analysis of gene copy numbers revealed a selective amplification of a 0.57 Mb region at the telomeric end of chromosome 35 from nucleotide positions ~4500 bp to 554500 bp and ~4500 bp to ~557500 bp for LdHSP23$^{-/-}$ esc0 #1 and LdHSP23$^{-/-}$ esc0 #2, respectively. The amplified genomic region encompasses 124 or 126 genes and results in a 1.5- to 2-fold increase of gene copy numbers.

Analysis of the temperature-tolerant LdHSP23$^{-/-}$ esc1 and esc2 strains revealed an even more stringent amplification of a cluster of six genes on chromosome 35 (430934…479155 bp) which resulted in 42 to 73 copies per gene (Fig 20 A-D). The amplicon comprised the coding sequence for casein kinase 1.2 (CK1.2) (LdBPK_351030), two CCCH-type zinc finger proteins (LdBPK_351040 and LdBPK_351060), a cupin domain-containing protein (LdBPK_351050), an undefined putative protein kinase (LdBPK_351070) and a hypothetical protein (LdBPK_351080) (Fig 20 E,F).

As previously reported, such DNA amplificates are often induced by DNA rearrangements at the level of repetitive sequences, e.g. inverted and direct repeats or SIDER elements. Literature search [85] indeed turned up documented SIDER2 elements that are present within or delimit the amplified sequence in the temperature-tolerant LdHSP23$^{-/-}$ esc1 and esc2 strain (Fig 20E,F).

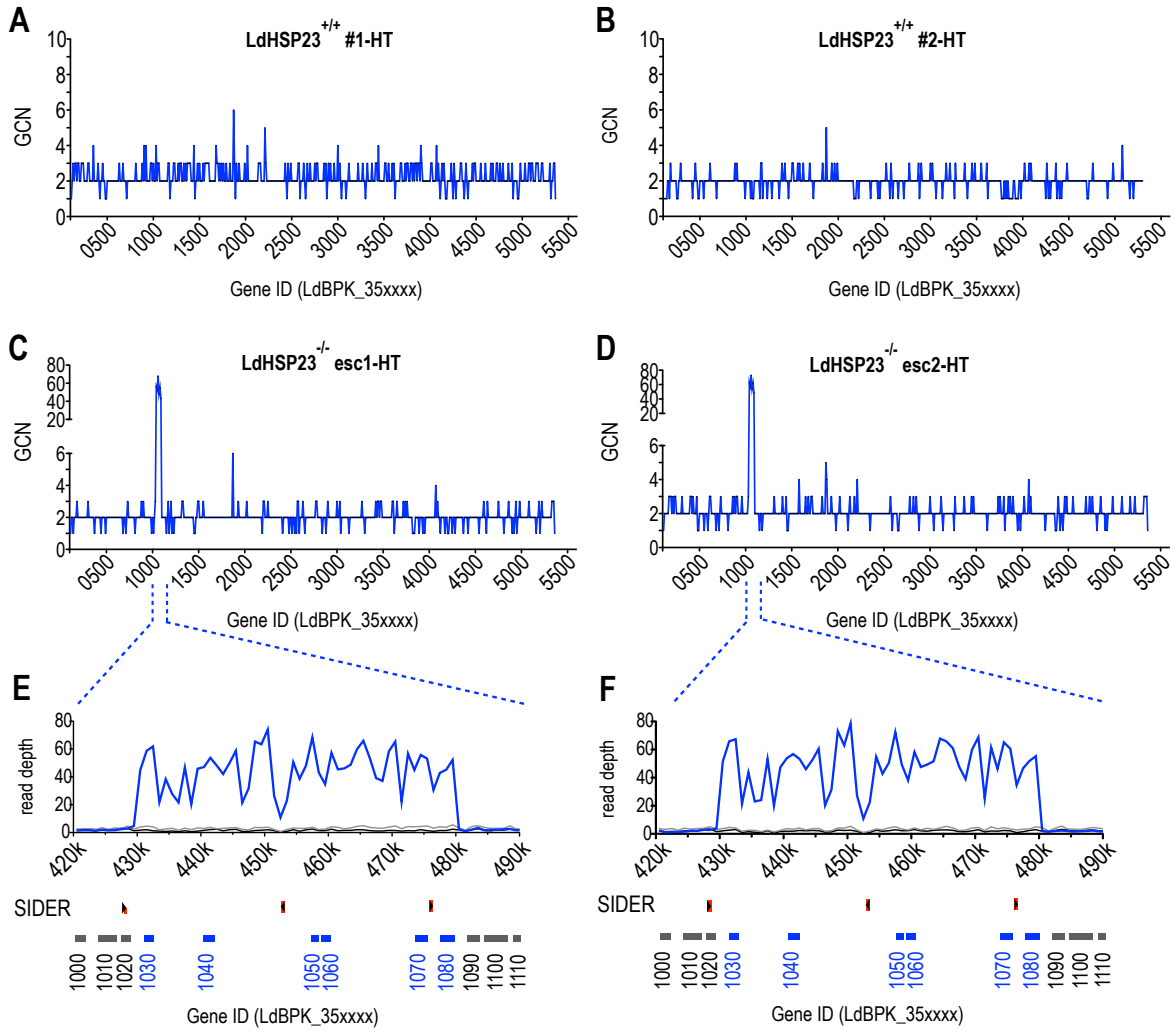

Figure 20 Strain-specific gene copy number variations on chromosome 35 in *L. donovani* HSP23$^{-/-}$ mutants at non-permissive temperatures. Copy numbers of each gene (LdBPK_35xxxx) on chromosome 35 were calculated based on read coverage data and are shown for (A, B) HSP23$^{+/+}$-HT and (C, D) HSP23$^{-/-}$ esc1/2-HT. These strains were selected and grown at HT. (E, F) Enlargement of the amplified region on chromosome 35 between nucleotide positions 420000 and 490000. Sequencing read depth is illustrated for HSP23$^{+/+}$ (LT, black), HSP23$^{-/-}$ esc1/2 (HT, blue) and HSP23$^{-/-}$ cl. 2/3 (LT, grey). Open reading frames and corresponding gene IDs are indicated in grey for non-amplified or blue for amplified CDSs; positions of SIDER2 repeat elements are indicated in red. LT=25°C, HT=37°C.

2.5.1.3 Single Nucleotide Polymorphisms (SNPs)

Next, we conducted a genome-wide SNP analysis comparing the genomes of HSP23$^{+/+}$ and HSP23$^{-/-}$ mutant populations. To identify SNPs potentially involved in the compensation of HSP23, SNPs were filtered according to the following criteria: (i) a valid heterozygous or

homozygous SNP must be present in all analysed HSP23$^{-/-}$ samples, (ii) is not present as a polymorphic allele in the WT sample, and (iii) is not localised in a repetitive DNA sequence.

L. major

The comparative SNP analysis of the genomes of *L. major* HSP23$^{-/-}$ null mutant lines as well as the LmjHSP23$^{+/+}$ Cas9 and LmjHSP23$^{+/+}$ WT samples, revealed a total of 293 missense mutations, among which only three SNPs matched the established criteria (Table 2): (i) a methionine to leucine exchange at position 7 in LMJLV39_080012700 coding for a putative Amastin surface glycoprotein (ii) a heterozygous frameshift mutation at position 475 in LMJLV39_270008800 coding for a putative nucleoporin, and (iii) a homozygous $Ala_{191}Pro$ mutation in LMJLV39_270010000 coding for a hypothetical protein. Orthology and synteny analysis on TriTrypDB revealed sequence similarities of LMJLV39_270010000 with the putative calpain-like cysteine peptidase of several other *Leishmania* spp..

Table 2 Comparative SNP analysis of *L. major* HSP23$^{-/-}$ and HSP23$^{+/+}$ samples.
Chr.= chromosome; fs= frameshift

Chr. #	Gene ID	Protein name	SNP position on chr.	Exchange of base pair	Exchange of amino acid	Type
8	LMJLV39_080012700	amastin surface glycoprotein, putative	306368	A → T	Met_7Leu	Heterozygous
27	LMJLV39_270008800	nucleoporin, putative	106425	TC → TGC	$Phe_{475}fs$	Heterozygous
27	LMJLV39_270010000	hypothetical protein	154493	G → C	$Ala_{191}Pro$	Homozygous

L. donovani

Bioinformatic analyses of LdHSP23$^{-/-}$ cl.2 and cl.3, LdHSP23$^{-/-}$ esc0, esc1 and esc2 as well as two LdHSP23$^{+/+}$ samples revealed a total of 2299 missense mutations. Again only three heterozygous mutations were identified in all four LdHSP23$^{-/-}$ mutant samples, while being absent in the WT samples (Table 3). These included (i) a non-sense mutation at position 494 in LdBPK_070130 coding for the ATP-dependent RNA helicase DBP2B (ii) an aspartic acid to glycine exchange at position 77 in LdBPK_251030 coding for a hypothetical protein and (iii) a $Lys_{477}Glu$ mutation in LdBPK_272520 coding for a putative cystein peptidase (Clan CA, family C2).

Since SNPs are often associated with drug resistance in *Leishmania* parasites, we aimed to investigate whether they also drive the emergence of the temperature-tolerant HSP23$^{-/-}$ escape variants. For this, we compared the genomes of two LdHSP23$^{+/+}$-HT populations and the temperature-tolerant LdHSP23$^{-/-}$ esc1 and esc2 mutants yielding a total of 113 missense mutations. Subsequent filtering resulted in 18 heterozygous SNPs that were exclusively

detected in both LdHSP23$^{-/-}$ esc1 and esc2 samples, but were absent in LdHSP23$^{+/+}$-HT populations (Table 4).

Table 3 Comparative SNP analysis of *L. donovani* HSP23$^{-/-}$ and HSP23$^{+/+}$ -LT samples. Chr.= chromosome, * = stopcodon

Chr. #	Gene ID	Protein name	SNP position on chr.	Exchange of base pair	Exchange of amino acid	Type
7	LdBPK_070130	ATP-dependent RNA helicase DBP2B	58449	T → A	Cys_{494}*	Heterozygous
25	LdBPK_251030	hypothetical protein, conserved	377236	A → G	$Asp_{77}Gly$	Heterozygous
27	LdBPK_272520	cystein peptidase, Clan CA, family C2, putative	201782	A → G	$Lys_{477}Glu$	Heterozygous

Among them, we also identified a frameshift mutation at position 814 in LdBPK_190650 coding for a hypothetical protein, an amino acid deletion of a lysine at position 59 in LdBPK_260570 coding for a putative myosin-like coiled-coil protein and a nonsense mutation at position 475 in LdBPK_351970 coding for a hypothetical protein. Orthology and synteny analysis on TriTrypDB revealed sequence similarities of LdBPK_190650 with the putative suppressor-of-white-apricot splicing regulator of several other *Leishmania* spp., while no results were obtained for LdBPK_351970.

Table 4 Comparative SNP analysis of *L. donovani* HSP23$^{-/-}$ esc1/2 and HSP23$^{+/+}$ -HT samples. Chr.= chromosome, fs = frameshift, *= stopcodon

Chr. #	Gene ID	Protein name	SNP position on chr.	Exchange of base pair	Exchange of amino acid	Type
3	LdBPK_030200	protein kinase, putative	51607	C → T	$Ala_{40}Val$	Heterozygous
3	LdBPK_030490	hypothetical protein, conserved	183862	C → A	$Pro_{838}Thr$	Heterozygous
6	LdBPK_060670	lanosterol synthase, putative	245629	G → T	$Ala_{202}Ser$	Heterozygous
7	LdBPK_070270	Sec7 domain-containing protein, putative	104710	C → G	$Thr_{215}Arg$	Heterozygous
19	LdBPK_190650	hypothetical protein, conserved	289920	GTCGGA → GCACAGC	$Ser_{814}fs$	Heterozygous
23	LdBPK_230580	acetyl-CoA synthetase, putative (fragment)	200625	G → C	$Ala_{263}Pro$	Heterozygous

24	LdBPK_240360	UDP-galactose transporter	117193	ATC → TTA	$Tyr Leu_{121} Phe lle$	Heterozygous
25	LdBPK_250680	epsin, putative	224027	A → G	$Ser_{402} Pro$	Heterozygous
25	LdBPK_251580	protein kinase, putative	595868	GGG → TGC	$His Pro_{20} Gln His$	Heterozygous
26	LdBPK_260570	myosin-like coiled-coil protein, putative	163150	CCTTC → CC	Lys_{59}del	Heterozygous
27	LdBPK_271320	hypothetical protein, conserved	519107	T → A	$Leu_{196} His$	Heterozygous
31	LdBPK_310510	hypothetical protein, unknown function	171688	C → G	$Gly_{477} Ala$	Heterozygous
31	LdBPK_310951	sodium stibogluconate resistance protein, putative (fragment)	357392	AAGAAA → GAGACG or GAGAAG	Phe_{572}Leu or Arg	Heterozygous
31	LdBPK_312060	succinyl-diaminopimelate desuccinylase-like protein	1000388	A → G	$Tyr_{363} His$	Heterozygous
32	LdBPK_323630	uncharacterised protein family UPF0564, putative	1397245	A → G	$Thr_{401} Ala$	Heterozygous
35	LdBPK_351970	hypothetical protein, conserved	788106	G → T	Glu_{475}*	Heterozygous
35	LdBPK_354860	AMP, deaminase	1883760	G → C	$Gly_{896} Arg$	Heterozygous
36	LdBPK_364490	hypothetical protein, conserved	1669258	G → A	$Arg_{85} Gln$	Heterozygous

2.5.2 Analysis of Transcript and Protein Level Changes

Previous works have shown that karyotypic variations correlate with changes in transcript abundance [200]. To investigate whether the observed amplification of the six-gene cluster on chromosome 35 similarly results in differential expression of the associated genes, I first analysed transcript levels by qRT-PCR (Table 5). Indeed, I observed a 10- to 41-fold increased mRNA abundance of the co-amplified genes in the LdHSP23$^{-/-}$ esc1 and esc2 samples compared to the WT (LdHSP23$^{+/+}$). Similarly, mRNA levels were elevated 1.5-to 2-fold in the LdHSP23$^{-/-}$ esc0 strains grown at 25°C, correlating with the partial amplification of the 5' part of chromosome 35 reported before.

Western blot analysis using an antibody raised against the *L. major* CK1.2 [189] further revealed a 3.7- and 2-fold upregulation of CK1.2 protein levels in the LdHSP23$^{-/-}$ esc1 and -esc2 mutants, respectively, confirming the correlation of DNA copy numbers, RNA and protein levels (Fig 21).

Table 5 Comparison of copy numbers (GCNs) and RNA levels of genes co-amplified on chromosome 35 in LdHSP23$^{-/-}$ esc1 and esc2. RNA values are mean ± standard errors of the means (SEM). qRT-PCR data were obtained from three biological and two technical replicates each.

Gene ID: LdBPK	351030		351040		351050		351060		351070		351080	
	GCN	*RNA*	*GCN*	*RNA*	*GCN*	*RNA*	*GCN*	*RNA*	*GCN*	*RNA*	*GCN*	*RNA*
LdHSP23$^{+/+}$ #1-LT	3	1.028 ±0.06	2	1.050 ±0.06	3	1.029 ±0.04	3	0.988 ±0.03	2	0.989 ±0.01	2	0.998 ±0.01
LdHSP23$^{-/-}$ esc0 #1-LT	4	1.445 ±0.05	3	1.908 ±0.07	4	1.798 ±0.16	3	1.505 ±0.19	5	1.64 ±0.17	4	2.253 ±0.17
LdHSP23$^{+/+}$ #1-HT	2	0.915 ±0.05	3	2.487 ±0.32	3	1.120 ±0.11	2	0.787 ±0.11	2	0.953 ±0.06	2	0.922 ±0.15
LdHSP23$^{-/-}$ esc #1-HT	56	15.55 ±1.6	53	35.60 ±1.71	68	29.53 ±3.42	48	10.60 ±0.86	55	28.03 ±2.55	43	40.72 ±1.42
LdHSP23$^{-/-}$ esc #2-HT	63	13.11 ±0.45	58	31.45 ±1.28	73	30.95 ±4.26	54	9.822 ±1.05	62	26.44 ±1.99	48	40.39 ±6.05

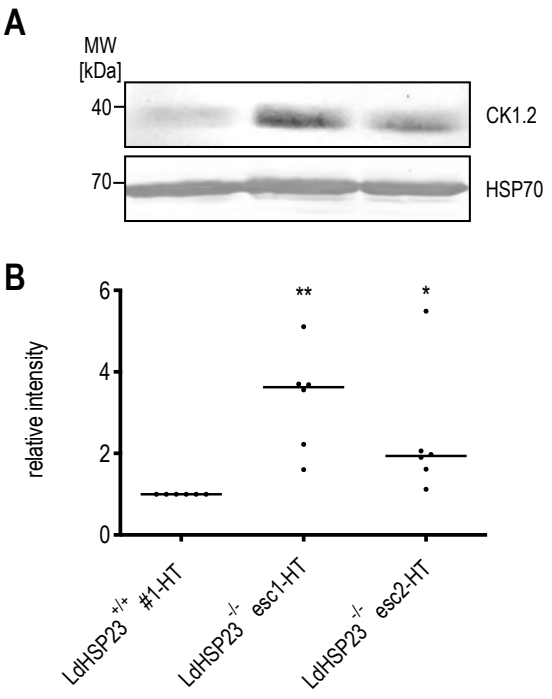

Figure 21 Western blot analysis of CK1.2 protein levels in LdHSP23$^{-/-}$ esc variants. (A) Representative Western blot showing CK1.2 protein levels in cell lysates from LdHSP23$^{-/-}$ esc variants and the LdHSP23$^{+/+}$-HT population. HSP70 was used as loading control. (B) Densitometry analysis for quantification of CK1.2 protein levels using the ImageJ software. Shown are the relative band intensities first normalised to the Coomassie loading control (not shown) and the LdHSP23$^{+/+}$-HT sample (set to 1). Differences were tested for significance using the Kruskal–Wallis test: *=$p < 0.05$, **=$p < 0.01$; (n=6)

2.5.3 Functional Cloning of Stress Tolerance Marker

Next, I tested whether the strain-specific amplification of the six-gene tract on chromosome 35 is responsible for the observed escape mutant phenotype at high temperatures. To this end, TS LdHSP23$^{-/-}$ were co-transfected with a mixture of six different over expression plasmids, bearing the candidate genes from the amplified region (LdBPK_351030 - LdBPK_351080). Transfectants were submitted either to antibiotic selection at LT or to temperature selection at HT without antibiotics (Fig 22A). Indeed, viable over expression lines were obtained both after selection at LT and HT, herein named as LdHSP23$^{-/-}$ [Mix]-LT and LdHSP23$^{-/-}$ [Mix]-HT, respectively, while empty vector-transfected parasites did not survive.

This confirmed that the amplification of the six-gene cluster on chromosome 35 causes the escape mutant phenotype. To further identify the genes associated with survival at HT, I recovered the plasmid DNA from the selected lines and performed PCRs with transgene-specific primers (Fig 22A). As visualised by agarose gel electrophoresis, all six plasmids were still detectable in DNA isolates from LdHSP23$^{-/-}$ [Mix]-LT (Fig 22B, left panels). In contrast, PCR analysis of LdHSP23$^{-/-}$ [Mix]-HT DNA extracts revealed an almost exclusive enrichment of the CK1.2 transgene (Fig 22B, right panels), suggesting a pivotal role of CK1.2 in rescuing the TS phenotype.

Results from the PCR were additionally verified by qRT-PCR analysis (Fig 22C). Indeed, compared to WT samples, LdHSP23$^{-/-}$ [Mix]-HT showed a 60-fold increase of mRNA coding for CK1.2, while mRNA levels of the other transgenes were only slightly increased. In contrast, the selection at LT led to a seven-fold increase of CK1.2 mRNA levels only, similar to that of LdBPK_351050, LdBPK_351070 and LdBPK-351080. The mRNA levels of LdBPK_351040 and LdBPK_351060, coding for two zinc-finger proteins, were not elevated.

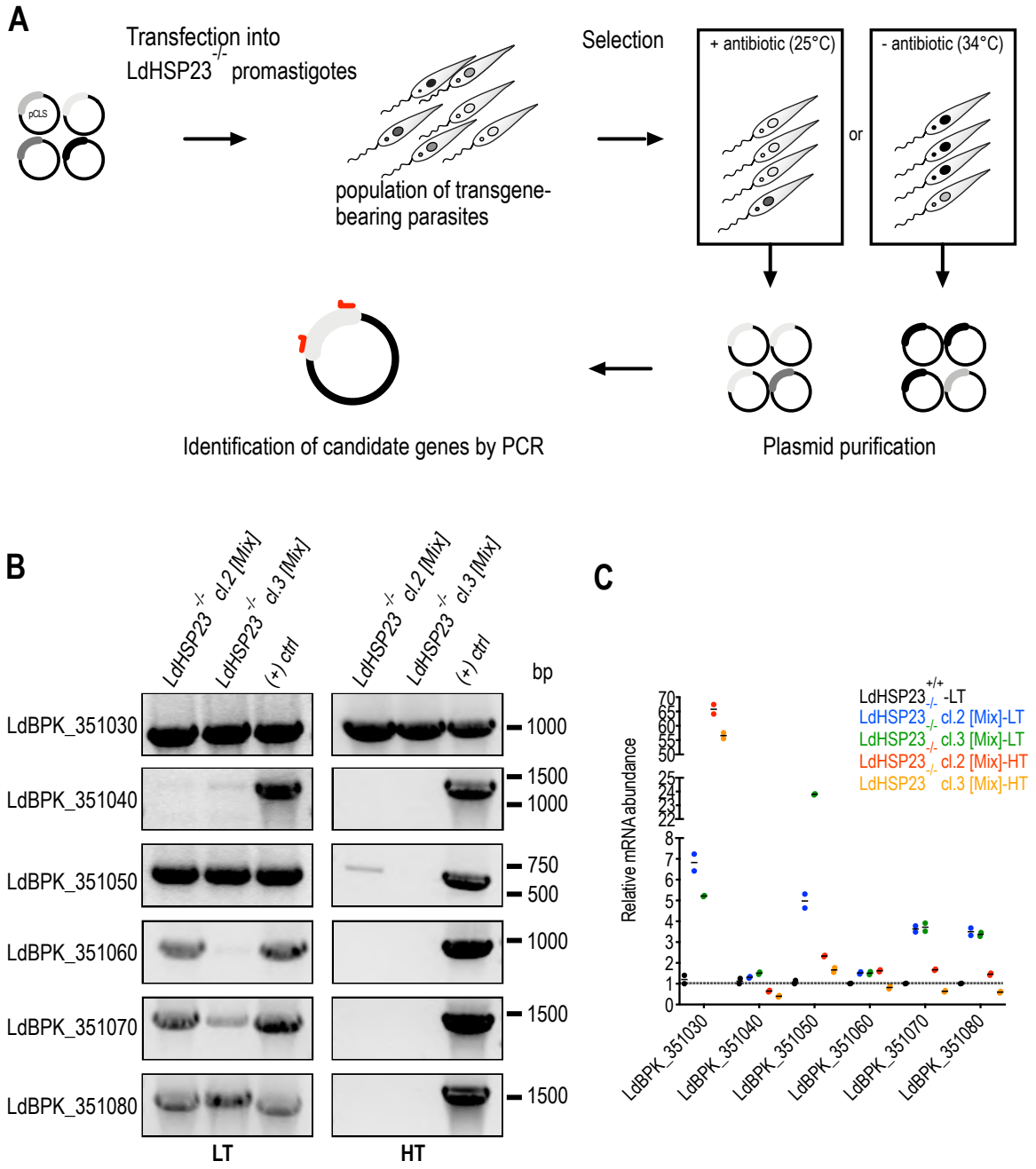

Figure 22 Functional cloning of stress tolerance marker in LdHSP23$^{-/-}$ mutants. (A) Schematic drawing of the transgene selection approach. pCL2S over expression plasmids harbouring the genes of the amplified cluster on chromosome 35 (LdBPK_351030-LdBPK_351080) were co-transfected into the LdHSP23$^{-/-}$ null mutants cl.2 or cl.3. Transfectants were either selected at LT (25°C) with Nourseothricine or at HT (34°C) without antibiotic yielding LdHSP23$^{-/-}$ [Mix]-LT or LdHSP23$^{-/-}$ [Mix]-HT cell populations. The plasmids were re-isolated from the selected parasite lines by phenol-chloroform extraction and DNA isolates were tested for the presence of transgenes by PCR using transgene-specific primers. (B) Results of the analytical PCR. PCR products were visualised by agarose gel electrophoresis and ethidium bromide staining. DNA sizes are indicated in base pairs. The left panel shows the results for low temperature (LT) selected lines, the right panel for high temperature (HT) selected lines. (C) qRT-PCR-analysis of LdHSP23$^{-/-}$ [Mix]-LT or LdHSP23$^{-/-}$ [Mix]-HT cell populations using transgene-specific qPCR primers. mRNA abundance was normalised to the LdHSP23$^{+/+}$-LT sample (set to 1) (n=1).

2.5.3.1 Phenotype Analysis of Over Expression Lines

Our functional cloning approach identified CK1.2 as the likely candidate gene involved in compensating the lack of HSP23. To further validate this finding, I first tested whether over expression of CK1.2 alone can restore growth of the LdHSP23$^{-/-}$ null mutant at HT. Following a similar procedure, two TS LdHSP23$^{-/-}$ clones were transfected with the plasmid harbouring the CK1.2 transgene and selected at LT with antibiotic or at HT without drug pressure. Indeed, I obtained viable antibiotic-resistant lines after LT selection (LdHSP23$^{-/-}$ [CK1.2]-LT), as well as two fully temperature-tolerant transfectants (LdHSP23$^{-/-}$ [CK1.2]-HT) capable of growing at HT. Next, I proceeded to investigate the phenotypes of all transgenic lines (Fig 23A), first monitoring growth at 34°C (Fig 23B). While the parental LdHSP23$^{-/-}$ clones 2 and 3 as well as the empty vector-transfected cells were unable to proliferate as expected, growth was restored in both HT-selected and LT-selected CK1.2 over expression parasites.

Interestingly, growth rates varied substantially depending on the selection condition: While the HT-selected lines, LdHSP23$^{-/-}$ [CK1.2]-HT, reached cell densities comparable to WT cells, LdHSP23$^{-/-}$ [CK1.2]-LT showed only about 25% growth at day 4. This difference became even more apparent at 37°C (Fig 23C). Here, LdHSP23$^{-/-}$ [CK1.2]-HT showed cell densities of about 70-80% compared with wild type cells, while proliferation of LdHSP23$^{-/-}$ [CK1.2]-LT was completely abrogated. This suggests that a preselection at HT is required to allow growth at mammalian tissue temperatures. I also analysed the growth of LdHSP23$^{+/+}$ [CK1.2] cells which were selected at LT with antibiotics. Compared with WT cells, cell densities of LdHSP23$^{+/+}$ [CK1.2] at day 4 were reduced by 10% at 34°C (Fig 23B) and 60% at 37°C (Fig 23C). Thus, while ectopic over expression of CK1.2 appeared to positively affect growth of LdHSP23$^{-/-}$ mutants, resulting in at least partial reversal of the growth phenotype at HT, it substantially reduced the parasite fitness of LdHSP23$^{+/+}$ cells.

In parallel, I also assessed the cell morphology of parasites by immunofluorescence analysis using anti-tubulin antibodies (Fig 23D).

At 34°C, characteristic heat-induced defects such as aggregation and cell rounding were only observed for LdHSP23$^{-/-}$ mutants as well as empty vector control cells, while promastigotes of LdHSP23$^{-/-}$ CK1.2 over expressing lines displayed a normal elongated shape (Fig 23D). In contrast, LdHSP23$^{-/-}$ [CK1.2]-LT subjected to 37°C still showed the original LdHSP23$^{-/-}$ null mutant phenotype, corroborating the results from growth experiments (Fig 23B,C).

In addition, I tested the *in vitro* growth of transgenic lines at LT under different culture conditions. As shown in Fig 23E and 23F, reduced *in vitro* growth of HSP23$^{-/-}$ null mutants under EtOH or hydrogen peroxide challenge was partially or fully restored upon ectopic over expression of CK1.2 in LdHSP23$^{-/-}$ [CK1.2]-LT.

In summary, growth and morphological analysis of transgenic lines confirmed that ectopic over expression of CK1.2 is sufficient to restore stress tolerance both at LT and HT. However, I found that a preselection at HT is required to alleviate the TS phenotype at 37°C.

A

strain #	HSP23	transgene(s)	NT sel.	temp. sel. at
1	+/+	-	-	LT
2	+/+	[CK1.2]	+	LT
3	-/- cl. 2	-	-	LT
4	-/- cl. 3	-	-	LT
5	-/- cl. 2	[CK1.2]	+	LT
6	-/- cl. 3	[CK1.2]	+	LT
7	-/- cl. 2	[CK1.2]	-	HT
8	-/- cl. 3	[CK1.2]	-	HT
9	-/- cl. 2	vector	+	LT

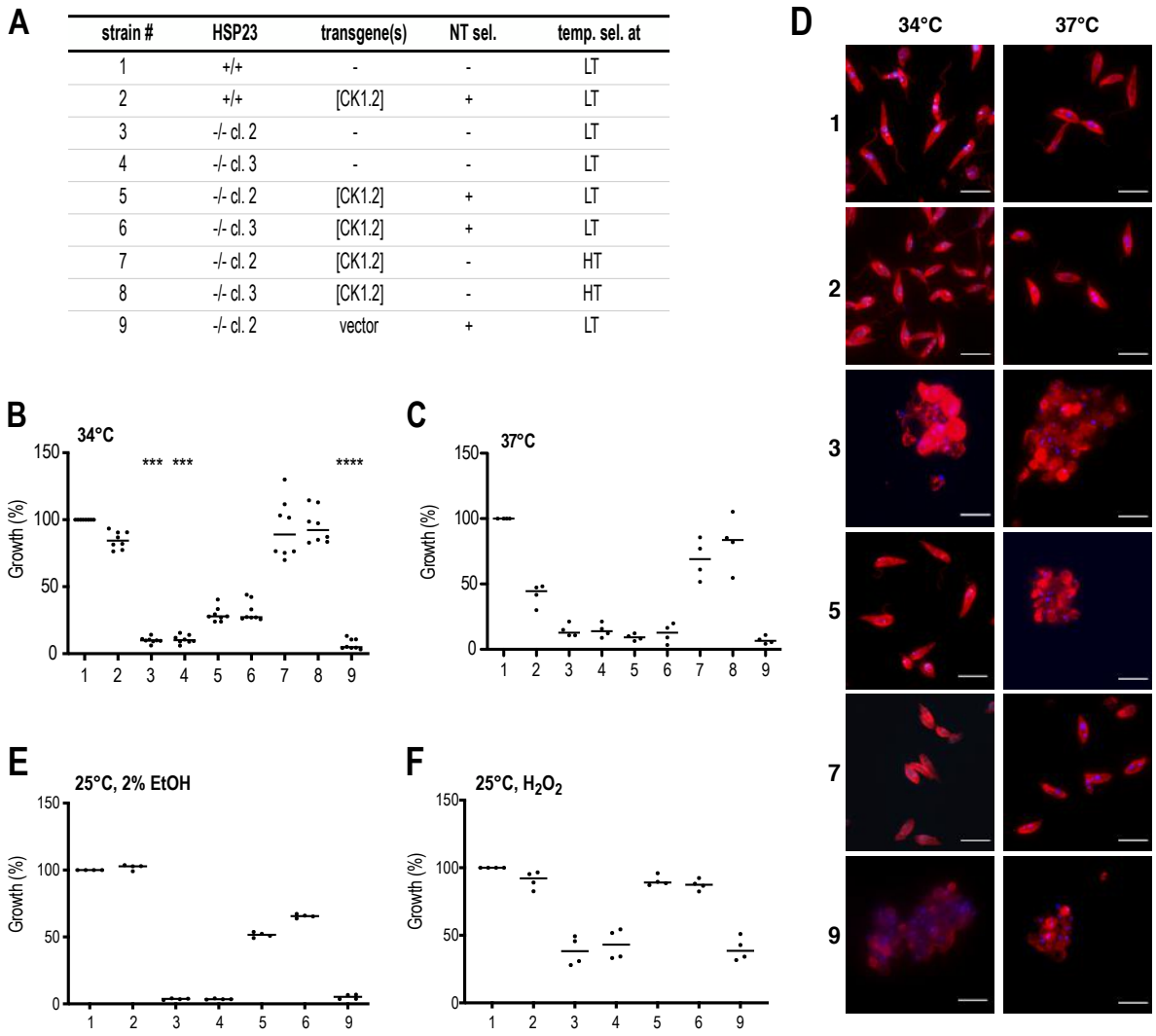

Figure 23 Characterisation of transgenic CK1.2 over expression lines under different culture conditions. (A) List of transgenic parasite cell lines tested. NT sel = selected under nourseothricine; temp. sel. = temperature selection scheme. 5 × 10^6 cells were seeded into 7 mL of complete M199 medium and cultured at 34°C (n=8) (B, D) and 37°C (n=4)(C, D). On day 4 cell density was assessed and is shown normalised to $LdHSP23^{+/+}$ WT growth (set at 100%). Significance was tested using the Kruskal-Wallis test: ***=p < 0.001, ****=p < 0.0001. (D) An aliquot of each parasite lines was fixed on a microscopic slide and stained with mouse anti-α-tubulin antibody (1/4000), anti-mouse-IgG Alexa Fluor 594 (1/500) and DAPI. Images were processed and merged using the ImageJ Fiji Software (Version 2.0.0). Scale bar: 10 µm. Additional growth experiments were performed at ambient temperature. 1 × 10^6 cells were seeded in 7 mL medium containing 2% EtOH (n=4) (E) and 200 nM H_2O_2 (n=4) (F). Cell density is shown on day 4 as percentage relative to WT cells (set at 100%).

2.5.3.2 Analysis of CK1.2 Transcript Levels in Transgenic Parasites

Based on these results, I hypothesised that the discrepancies observed between low and high temperature selection may relate to differences in CK1.2 expression levels. To test this, I compared the CK1.2 encoding transcript as well as protein levels of high temperature selected to low temperature selected lines (Fig 24A). Indeed, high temperature selection resulted in ~10-15-fold higher RNA abundance (Fig 24B) and ~2.5-4-fold higher CK1.2 protein levels (Fig 24C) when compared to low temperature selection.

A

strain #	HSP23	transgene(s)	NT sel.	temp. sel. at
1	+/+	-	-	LT
5	-/- cl. 2	[CK1.2]	+	LT
6	-/- cl. 3	[CK1.2]	+	LT
7	-/- cl. 2	[CK1.2]	-	HT
8	-/- cl. 3	[CK1.2]	-	HT
10	-/- cl. 2/3	mix 351030-80	+	LT
11	-/- cl. 2/3	mix 351030-80	-	HT
12	-/- cl. 2/3	mix 351030-80	+	LT → HT
13	-/- cl. 2/3	[CK1.2]	+	LT → HT

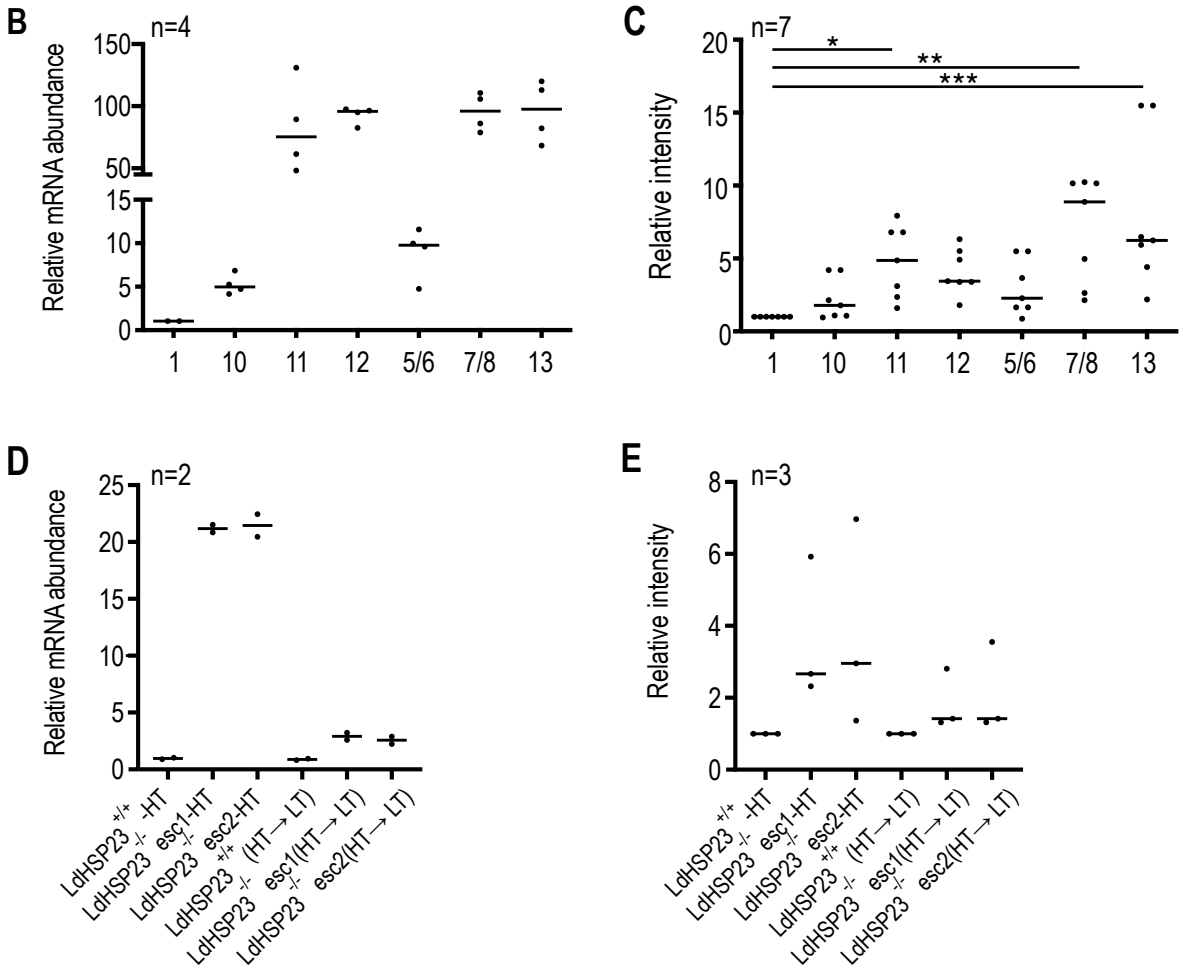

Figure 24 Analysis of CK1.2 mRNA and protein levels in transgenic lines and LdHSP23$^{-/-}$ esc1/2 mutants under different temperatures. (A) List of transgenic parasite cell lines tested. NT sel = selected under nourseothricine; temp. sel. = temperature selection scheme. Analysis of CK1.2 mRNA and protein abundance for CK1.2 over expression lines (B,C) and for LdHSP23$^{-/-}$ esc1/2 mutants (D,E). The latter were selected first at HT (37°C) and were then transferred back to LT (25°C)(HT→LT). mRNA and protein samples were prepared 30 days after shifting the cells to LT conditions. For Western blot analysis, signal intensities were quantified using the Image J Software and were normalised to LdHSP23$^{+/+}$-HT (set to 1). Significance was tested using the Kruskal-Wallis test: *=p < 0.05; **=p<0.01; ***=p < 0.001.

In contrast, an increase of CK1.2 expression levels was not observed for LdHSP23$^{+/+}$ parasites that were transfected with the CK1.2 over expression plasmids and subsequently selected at HT (data not shown).

Next, I analysed CK1.2 mRNA and protein changes in low temperature selected transgenic lines that were later adapted to high temperatures (strains #12 and #13) (Fig 24B,C). Adaptation to high temperatures was achieved by incubating the cells for four days at HT followed by a recovery period at LT. Again, I observed a ~10-19-fold increase of CK1.2 mRNA and ~2-3-fold higher protein levels in high temperature selected lines in comparison to low temperature selection indicating a selective advantage of elevated CK1.2 expression levels at high temperatures.

To further test the impact of temperature on CK1.2 expression levels, I also analysed CK1.2 mRNA and protein abundance in LdHSP23$^{-/-}$ esc1/2 populations that were grown at HT or shifted back for at least 30 days to LT (Fig 24D,E). Compared to high temperature selection, a temperature downshift resulted in an ~8-fold and a ~1.8-fold reduction of CK1.2 mRNA (Fig 24D) and protein (Fig 24E), respectively.

These data demonstrate that there is a strong selective pressure for increased CK1.2 expression levels in LdHSP23$^{-/-}$ mutants and at high temperatures.

2.6 Functional Interactions between CK1.2 and HSP23

L. donovani CK1.2 was previously identified as an essential exo-ectokinase involved in the phosphorylation of HSP90 [186]. Bearing this in mind, I aimed to elucidate whether the kinase may be also functionally linked to HSP23. For this, I conducted an *in vitro* kinase assay with recombinantly expressed proteins.

First, I performed an *in silico* analysis in TriTrypDB (https://tritrypdb.org/tritrypdb/) to search for putative canonical CK1.2 phosphorylation sites (Ser/Thr-X-X-Ser/Thr)[1]. Indeed, the vast majority of protein coding genes in the *L. donovani* genome presented at least one CK1 phosphosite (7705 out of 8136 proteins in total). A deeper sequence analysis revealed two and three CK1.2 consensus motifs within the alpha-crystallin domains of *L. donovani* HSP23 and the structurally related P23, respectively (Fig 25A). An alignment of HSP23 amino acid sequences (Fig 25B) further indicated that the consensus motive SEES$_{(68-71)}$ is conserved in all other *Leishmania* as well as *Trypanosoma* HSP23 homologues. In contrast, the upstream *L. donovani* CK1.2 phosphosite TGVS$_{(31-34)}$ appeared to be more divergent and was even absent in *L. mexicana* and *Trypanosoma* homologues.

[1] Amino acid codes see Abbreviations, X is any amino acid.

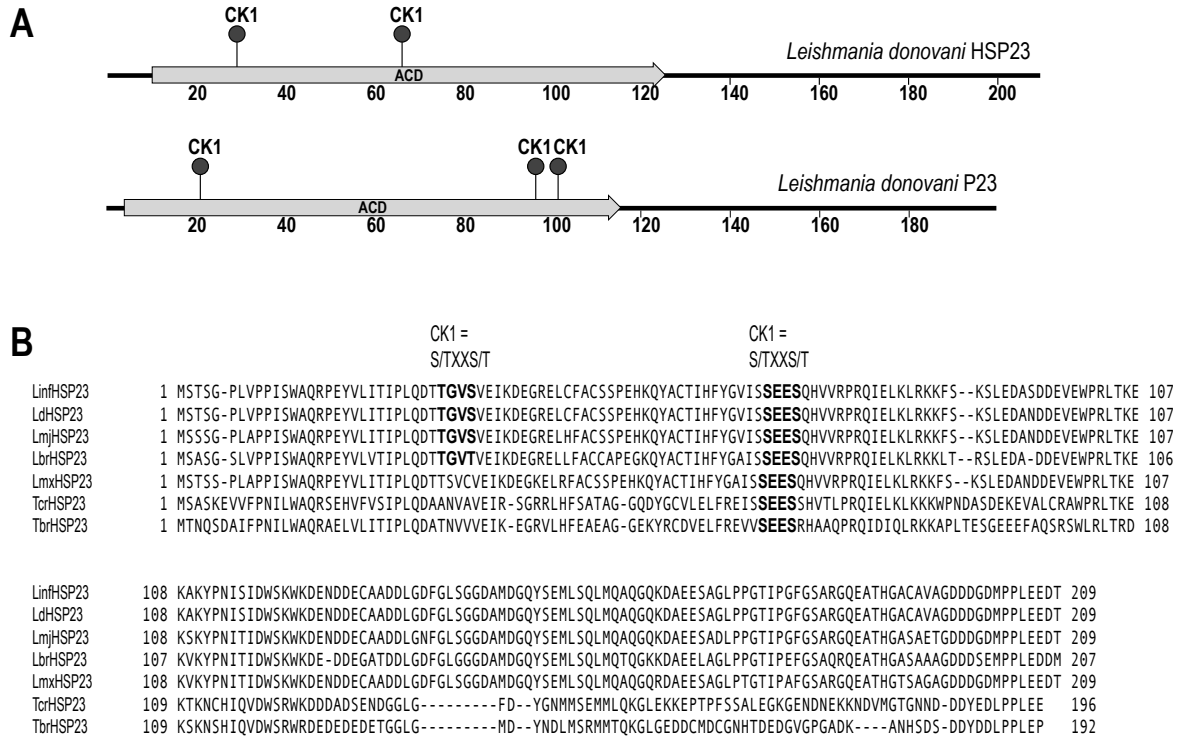

Figure 25 Identification of putative CK1.2 phosphorylation sites in HSP23 and P23. (A) Schematic representation of the putative CK1.2 phosphosites at indicated amino acid positions. ACD = alpha-crystallin domain (B) Sequence alignment of different HSP23 homologues of *Leishmania* and *Trypanosoma* spp.. CK1.2 consensus sequences (Ser/Thr-X-X-Ser/Thr) are marked in bold.

2.6.1 Recombinant Expression of CK1.2, HSP23 and P23 in *E. coli*

For recombinant protein expression, chemocompetent *E. coli* BL21 [pAPlacI^{Q}] were transformed with the protein expression plasmids pJC45 or pJC65, harbouring the genes of interest fused to a $(His)_{10}$-tag coding sequence. Protein expression was induced by 0.4 mM Isopropyl-ß-D-thiogalactopyranoside (IPTG) (= +IPTG), and soluble proteins were purified (= P) from crude cell extracts (= E0) by Ni^{2+} metal chelate chromatography essentially as described [1, 163, 189]. Addition of IPTG allowed induction of all recombinant proteins as demonstrated by the appearance of additional bands at the cognate protein sizes on Coomassie Brilliant Blue-stained SDS-PAGE gels: His_{10}-CK1.2 (41.56 kDa) (Fig 26A), His_{10}-HSP23 (25.94 kDa) (Fig 26B) and His_{10}-P23 (24.11 kDa) (Fig 26C). After cell lysis, soluble proteins were detectable in the supernatant (E0 fraction) and were subsequently purified by Ni^{2+} metal chelate chromatography. While well-defined bands were visible for HSP23 and P23 migrating at a size of 25 kDa, purification of CK1.2 appeared to be less efficient. Hence, I additionally verified CK1.2 expression by Western blot using an anti-CK1.2 antibody (Fig 26A right panel). While CK1.2 protein was not detectable in non-induced samples (-IPTG) as

expected, a band at ~40 kDa was visible in both IPTG-induced and purified samples, confirming the successful purification of recombinant CK1.2.

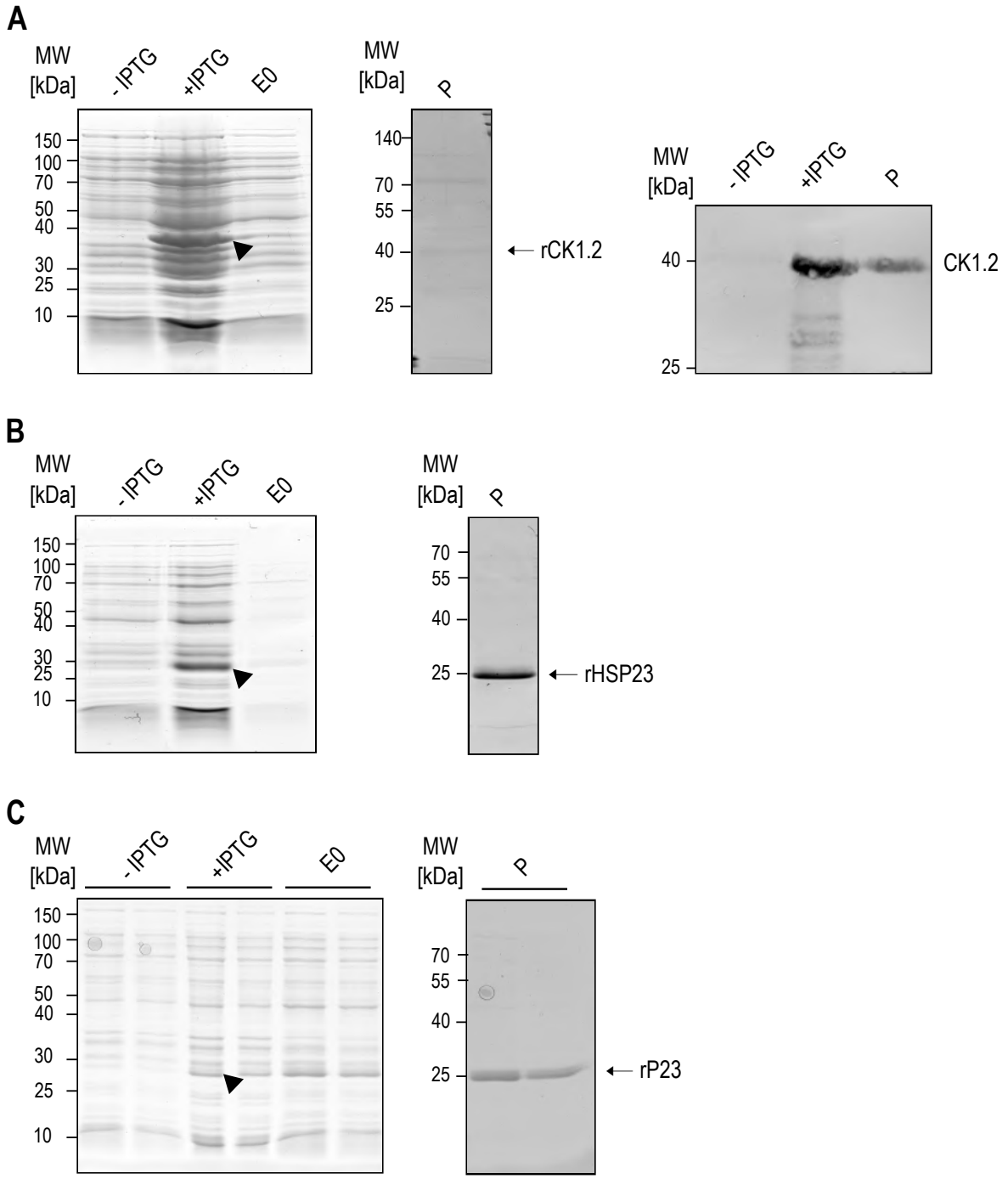

Figure 26 Expression and purification of recombinant proteins in *E. coli*. (A) rLdCK1.2, (B) rLdHSP23 and (C) rLdP23 were expressed in *E. coli* BL21 [pAPlacI^{Q}] cells that were transformed with the protein expression plasmids pJC65-CK1.2, pJC45-HSP23 and pJC45-P23. Single colonies were inoculated in bacterial culture medium and protein expression was induced at an optical density of 0.05 by addition of IPTG (+IPTG) at a final concentration of 0.4 mM. After one hour incubation, cells were lysed in lysis buffer followed by sonication (=E0). Soluble proteins were subsequently purified (=P) from crude cell lysates by Ni^{2+} metal chelate chromatography. All protein fractions were loaded onto an SDS-PAGE gel and were visualised by Coomassie staining. For verification of recombinant CK1.2 expression, additional Western blot analysis was performed using an anti-CK1.2 antibody (1/250) (right panel in A).

2.6.2 *In Vitro* Kinase Assay

To gain insight into possible modulatory interactions of CK1.2 with HSP23, but also P23, I performed *in vitro* phosphorylation assays with recombinantly expressed *L. donovani* CK1.2 using rLdHSP23 or rLdP23 as substrates. To assess CK1.2 general activity, I also tested phosphorylation of the myelin basic protein (MBP), a canonical substrate for CK1.2 [189]. Reactions were incubated for 30 min with [γ-^{32}P]-ATP at 25°C or 37°C in the presence of the CK1.2-specific inhibitor, D4476, or appropriate concentrations of DMSO (drug solvent). Proteins were separated by SDS-PAGE and subsequently blotted onto a polyvinylidene fluoride membrane. Incorporation of [γ-^{32}P]-ATP into proteins was visualised by autoradiography. As a loading control, the same membrane was probed with an anti-CK1.2, anti-HSP23, anti-P23 or stained with Coomassie blue.

As shown in Fig 27A, both rLdHSP23 and MBP were phosphorylated by rLdCK1.2 at LT and to a lesser extent at HT corroborating previous work showing a reduced activity of rLdCK1.2 at elevated temperatures [189]. Addition of the CK1-specific inhibitor D4476 to the reaction mixture reduced [γ-^{32}P]-ATP incorporation, confirming that substrate phosphorylation is specifically due to rLdCK1.2 and not a co-purified bacterial kinase. In line with these results, phosphorylation was neither detectable for HSP23 nor MBP in the absence of rLdCK1.2. I also observed radiolabeling of rLdCK1.2 itself which was inhibited upon addition of D4476, suggesting an intrinsic autophosphorylation activity of the kinase. Also, adding rLdHSP23 substantially enhanced autophosphorylation both at LT and HT.

Following the same experimental procedure, I next analysed the kinase-substrate interaction between CK1.2 and the co-chaperone P23 (Fig 27B). Like HSP23, I found that rLdP23 is a rLdCK1.2 substrate *in vitro,* being phosphorylated to similar degrees at LT and HT. Again, rLdP23 furthered autophosphorylation of rLdCK1.2, in turn leading to reduced MBP phosphorylation. As shown for HSP23, incorporation of [γ-^{32}P]-ATP into P23 and MBP decreased markedly when the samples were treated with D4476. In summary, I was able to show that HSP23 and P23 are *bona fide in vitro* substrates of CK1.2 and have a modulatory impact on CK1.2 activity.

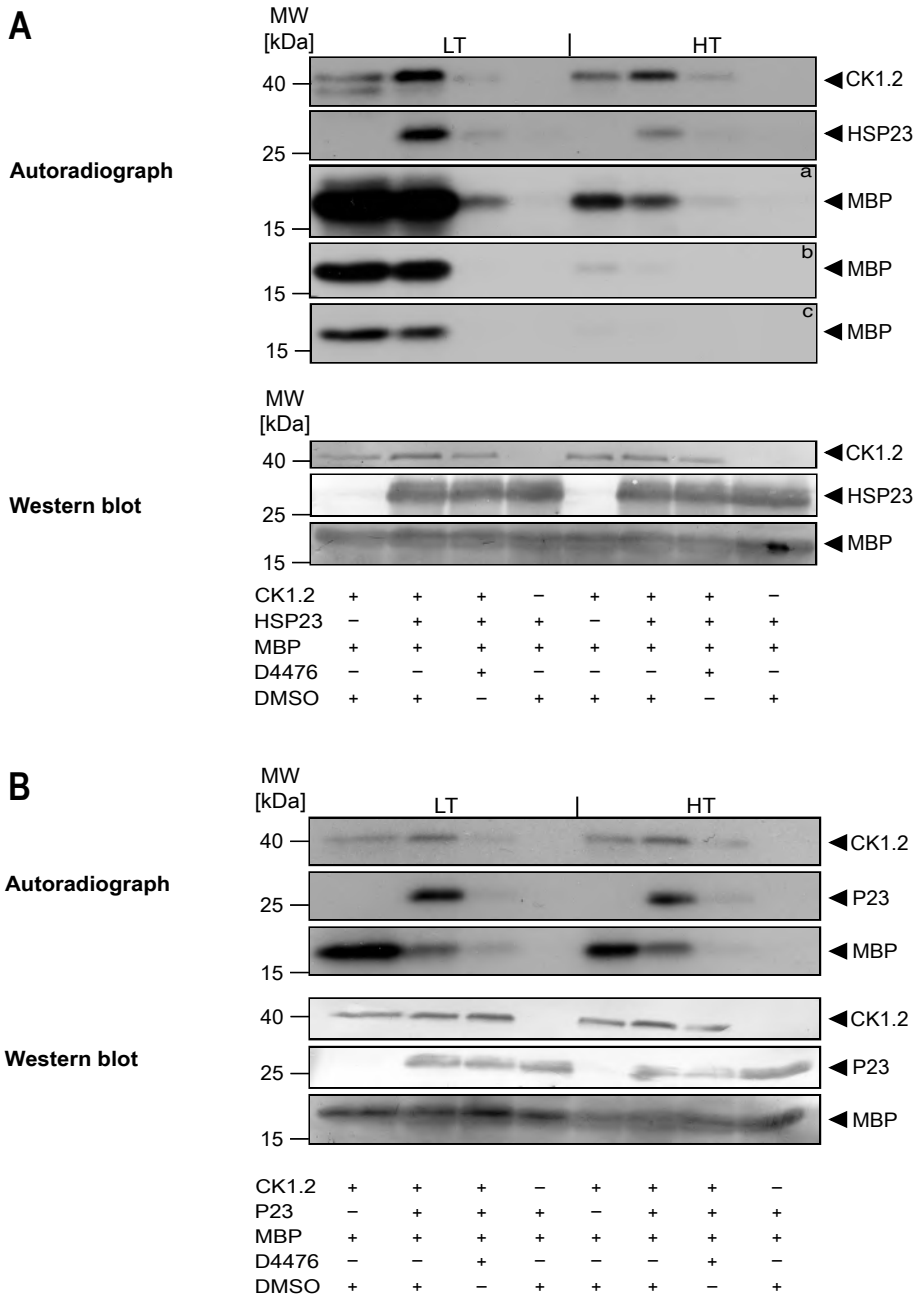

Figure 27 *In vitro* kinase assays using [γ-^{32}P]-ATP. Kinase assays were performed with 0.25 µg recombinant casein kinase 1.2, 3 µg of myelin basic protein (MBP), 1.57 µg of recombinant HSP23 (A) or 1.3 µg P23 (B) in the presence of either 10 µM D4476 inhibitor or equivalent concentrations of DMSO. The reaction samples were incubated at LT (25°C) or HT (37°C) for 30 min and stopped by addition of loading buffer. A reaction without CK1.2 was included to test for possible autophosphorylation of substrates or phosphorylation by bacterial co-purified kinases. Radiolabelled proteins were separated on a 12.5% SDS-PAGE gel followed by Western blot. The incorporation of [γ-^{32}P]-ATP was monitored by autoradiography (upper panels). a = 1 week exposure; b = 24h exposure; c = 12 h exposure of X-Ray films. The blot was probed with an anti-CK1.2 (SY3535) (1/250), HSP23 (1/500) and P23 (1/500) antibody, or stained with Coomassie blue to evaluate loading (lower panels). The figure shows representative autoradiographs and corresponding Western blots from a series (n=4) of experiments.

3 Discussion

3.1 The Function of HSP23 in *Leishmania* and Beyond

During its complex life cycle, *Leishmania* parasites alternate between two morphologically distinct developmental stages: the elongated promastigote inside the insect vector and the ovoid amastigote form inside the mammalian host. The transition from promastigotes to amastigotes is induced by an increase of temperature and acidic pH, which the parasites encounter within the phagolysosome of the host cell macrophages [31]. Not surprisingly, stage conversion is intimately linked to major morphological and metabolic changes. This includes the switch from glycolysis to fatty-acid- and amino-acid-based catabolism, a general downregulation of protein synthesis, but a concomitant upregulation of amastigote-specific genes [201, 202]. During the last years, the identification of essential stage-specific proteins has been the subject of extensive research since they represent potential drug targets. Important insights were gained by comparative proteomics, and more recently by ribosome profiling data, revealing, amongst others, the strong upregulation of the small heat shock protein 23 [127]. Reverse genetic analysis of the HSP23 gene in *L. donovani* indeed revealed that it plays a crucial role in the parasite stress tolerance [1]. The lack of HSP23 abrogates survival at mammalian tissue temperatures and differentiation into axenic amastigotes. *In vitro* infections of bone marrow-derived macrophages further led to a reduced parasite load implicating HSP23 in virulence. This and the fact that no homologues exist in humans identified *L. donovani* HSP23 as a novel, potential drug target for the treatment of leishmaniasis.
In this thesis, I further analysed the suitability of HSP23 as a drug target by addressing two important questions: (i) is the essential function of HSP23 conserved among *Leishmania* and *Trypanosoma* spp. and (ii) are there mechanisms that compensate for the loss of HSP23 at both ambient and mammalian temperatures?

3.1.1 Functional Conservation of HSP23 in Trypanosomatidae

As described in the introduction, small heat shock proteins constitute a group of molecular chaperones that are found in all domains of life (bacteria, archaea, eukaryotes) [203, 204]. In contrast to other HSP protein families such as HSP70 and HSP90, the phylogenetic divergence of sHSPs is rather high given an overall sequence identity of only ≤50% [205]. This is also true for the three *L. donovani* sHSPs HSP20, HSP23 and P23 which only share sequence identities ranging from 6 to 23% [1]. This result suggests an early divergence of sHSPs in evolution which corroborates phylogenetic analyses on ACD proteins in Trypanosomatida [156]. Interestingly, considering each sHSP individually, the sequence conservation of putative homologues among *Leishmania* spp. and related *Trypanosoma* spp.

is much higher. For example, the supposed homologues of *L. donovani* HSP23 in other *Leishmania* and related *Trypanosoma* spp. share between 36% and 99% amino acid sequence identity (see Table 1). The lowest identity was found for the more distantly related *Trypanosoma* spp. as well as for *L. braziliensis*, which, as a member of the subgenus *Viannia,* also shows considerable phylogenetic distance to the Old World species *L. donovani*, *L. infantum*, and *L. major*. The low sequence identity between *L. donovani* and *Trypanosoma* HSP23s may explain the absence of an HSP23 protein signal in Western blot analyses for HSP23$^{-/-}$ [TbrHSP23] and HSP23$^{-/-}$ [TcrHSP23] using an antibody against *L. donovani* HSP23.

Despite the high degree of sequence conservation among sHSP orthologues, functional conservation between the subgenera may not be assumed automatically. In fact, evolutionary adaptation to distinct hostile environments, including differences in the vertebrate host, vector specificity as well as natural climate and ecological pressures may have led to the functional diversification of HSP23 orthologues in distinct *Leishmania* spp.[22]. The latter hypothesis is supported by transcriptomics and proteomics studies showing species and life cycle stage-specific differences [79, 202].

Nevertheless, two lines of evidence point at a functional conservation of HSP23 in *Leishmania* and *Trypanosoma* spp.. Firstly, the *L. donovani* HSP23$^{-/-}$ null mutant phenotype reported by Hombach et al. [1] was reproducible for *L. major* (see Fig 13), and *L. braziliensi*s (Adaui et al. unpublished data). HSP23$^{-/-}$ mutants of three tested *Leishmania* spp. displayed increased sensitivity to sublethal EtOH concentrations and were not viable at mammalian tissue temperatures.

Secondly, the conserved functionality of HSP23 homologues was further confirmed by our complementation studies. Selected *L. donovani* and *L. major* HSP23$^{-/-}$ clones were transfected with episomal *L. donovani, L. infantum*, *L. major*, *L. braziliensis, T. brucei* or *T. cruzi* HSP23 transgenes. Indeed, all trypanosomatid HSP23 homologues, except for TcrHSP23, conferred protection against high temperatures, likely by maintaining protein folding homeostasis in trypanosomatid cells (see Fig 16). The degree of complementation substantially differed for the transgenes in the *L. donovani* HSP23$^{-/-}$ null mutant background, while complete phenotype reversion was observed for all transgenes in the *L. major* HSP23$^{-/-}$ complementation lines. As mentioned previously, the only exception was the HSP23 orthologue of *T. cruzi* whose ectopic over expression partially restored the *L. major* HSP23$^{-/-}$ null mutant phenotype at 34°C, but not that of *L. donovani* HSP23$^{-/-}$ null mutants grown at 37°C.

Although I do not know the reason for the different capacities of HSP23 homologues to complement the HSP23$^{-/-}$ null mutant phenotype in different *Leishmania* spp., several explanations are possible. First, species-specific differences in the sequence and expression level of HSP23 homologues may be a determinant of tissue tropism of *Leishmania* spp. [12]. While viscerotropic *L. donovani* parasites must resist internal body temperatures that exceed 40°C, their dermotropic counterparts are usually more TS with an optimal growth at

28°C-34°C [206]. Previous comparative genomics have identified 19 *L. donovani*-specific genes of which three conferred increased parasite survival in the visceral organs when ectopically expressed in *L. major* [207-211]. However, while over expression of the *L. donovani* HSP23 transgene could fully rescue the TS phenotype in *L. major* HSP23$^{-/-}$ null mutants, it did not increase the general temperature tolerance of *L. major* parasites.
Alternatively, the degree of complementation may be influenced by the varying expression levels observed for the different transgenes (see Fig 15). Notably, genes are not expressed in their natural genetic background, but instead are under the control of non-related sets of UTRs. This marks a major drawback of ectopic over expression, since changes in gene expression may adversely affect protein function and can even cause mutant phenotypes. In other organisms including yeast [212] and *Toxoplasma gondii* [213], the selective over expression of genes was reported to even fully abrogate protein function. This matches our results showing that the non-physiological expression of *L. donovani* HSP23 in LdHSP23$^{-/-}$ null mutants does not completely restore thermotolerance to wild type levels (see Fig 14). Furthermore, it highlights the importance of a balanced expression of HSP23 to guarantee optimal stress tolerance and/or vitality.

3.2 Compensatory Mechanisms for the Loss of HSP23

3.2.1 Genetic Alterations

In lieu of transcriptional control, the high plasticity and mosaic ploidy of the *Leishmania* genome which is characterised by karyotypic fluctuations, stochastic gene amplifications, and nucleotide polymorphisms, provides an important source of phenotypic diversity within natural *Leishmania* populations [85, 92, 214]. Pre-existing, conditionally beneficial genomic alterations can be rapidly selected in response to environmental constraints. The identification of such genomic alterations can therefore indicate specific functions of the corresponding proteins in counteracting these adverse conditions. Recent technical advances in next generation sequencing have revolutionised the analysis of *Leishmania* genomes and allowed to unravel the underlying mechanisms of drug resistance and virulence [200, 215, 216].
Similarly, genetic adaptations may also occur upon depletion of genes by reverse genetics in the laboratory hampering the analysis of mutant phenotypes [217]. Spontaneous reversal of phenotypes has been already described for LPG2$^{-/-}$- and HSP100$^{-/-}$-null mutants of *L. major* [218, 219]; the underlying compensatory mechanisms, however, remain unclear.
In this work, I further report the spontaneous emergence of an LdHSP23$^{-/-}$ escape variant, named LdHSP23$^{-/-}$ esc0. This mutant was characterised by (i) a wild type-like growth at permissive temperatures, (ii) restored tolerance to EtOH and (iii) hydrogen peroxide. The LdHSP23$^{-/-}$ esc0 mutant was further subjected to repeated cycles of permissive and non-permissive temperatures, which allowed selection of two temperature-tolerant LdHSP23$^{-/-}$

mutant populations. While this clarified, contrary to the previous concepts, that the function of HSP23 can indeed be compensated by other means, it does not provide information about the underlying molecular mechanisms. To address this and to identify the proteins involved, we performed a comparative analysis of the genomes that indeed revealed major strain-specific differences presumably associated with the loss of HSP23. We found that all investigated LdHSP23$^{-/-}$ mutant lines either carry a partial or complete, amplification of chromosome 35. The level of acquired stress tolerance appeared to be positively correlated with a step-wise constriction of the sequence length to be amplified and a concomitant increase of relevant gene copy numbers. Hence, stress-sensitive LdHSP23$^{-/-}$ mutants displayed an amplification of the full-length chromosome (trisomy), yielding an average of three copies of the respective genes (see Fig 17). In the identified LdHSP23$^{-/-}$ escape variant, however, the amplification was shown to be restricted to the 5'-terminal third of chromosome 35 (see Fig 19). The amplified region was present either in duplicate or in triplicate, thereby resulting in up to four copies per gene. Even more stringent was the amplification in the temperature-tolerant LdHSP23$^{-/-}$ mutant populations that were selected and maintained under non-permissive temperatures: here, the amplified region was narrowed down to a six-gene cluster with copy numbers ranging between 60-70 (see Fig 20).

Although the nature of this six-gene amplicon remains unknown, such high gene numbers are usually an indicator of linear or circular extrachromosomal rather than intrachromosomal amplicons [85, 200]. Further evidence for this hypothesis is provided by a genome-wide bioinformatic analysis of the *Leishmania* genome in which the authors identified SIDER sequences involved in extrachromosomal DNA amplificates [85]. These were also present either inside or adjacent to the amplified region in the temperature-tolerant LdHSP23$^{-/-}$ mutant lines. Even more interesting was the fact that the amplicon identified in our study coincided with a putative product predicted by Ubeda et al. (Table S3 [85]), thereby highlighting the importance of SIDER-mediated DNA rearrangements in the selection under environmental stress.

It is noteworthy that structural variants of chromosome 35, including large insertions and deletions at the 5' and 3' ends of the chromosome, have been recently identified in several cultured field isolates of *L. donovani* and *L. infantum* [220]. In light of our results, this demonstrates that chromosome 35 is highly prone to DNA rearrangements.

Consistent with previous studies [200, 216], I further confirm that somy and gene copy number variations *per se*, but in particular the massive amplification of the six-gene cluster on chromosome 35 in the temperature-tolerant LdHSP23$^{-/-}$ mutant lines, was reflected at the transcript and protein level (see Fig 21). It is noteworthy that in the absence of temperature -related stress, transcript and protein levels in HSP23$^{-/-}$ temperature-tolerant lines returned to basal levels, suggesting a gradual loss of amplicons (see Fig 24). This has been also observed for extrachromosomal amplificates selected in drug-resistant lines which, upon removal of the drug, were rapidly lost again from the parasite populations [85, 87, 221-224].

Interestingly, while ploidy and gene copy number variations were also observed upon the loss of HSP23 in *L. major*, they affected different chromosomes and were only detected in one of the two *L. major* HSP23$^{-/-}$ clones (see Fig 18). It should be worthwhile to subject the *L. major* HSP23$^{-/-}$ clones to cycles of selection and recovery to observe whether similar adaptive genetic changes can be observed as in *L. donovani.*

In contrast, the contribution of SNPs in compensating for the loss of HSP23 appeared to be comparatively low. Comparative analysis of LdHSP23$^{-/-}$ and LmjHSP23$^{-/-}$ null mutants with HSP23$^{+/+}$ WT cells, revealed mostly heterozygous SNPs. Although I do not know the phenotypic consequences, the effect on protein function may be rather low considering that a WT allele is still present within the populations. Furthermore, the relatively low level of SNP variation in HSP23$^{-/-}$ esc1/esc2 is in keeping with several other studies showing that nucleotide polymorphisms play only a minor role in the early adaptation to changing environmental conditions, while aneuploidy patterns are known to vary within very short time periods [87, 214].

The only homozygous SNP was identified in LmjHSP23$^{-/-}$ samples and resulted in an alanine to proline exchange in the LMJLV39_270010000 gene which showed sequence similarity to the putative cystein peptidase, Clan CA, family C2 (see Table 2). In general, proline residues play a unique role in determining the secondary structure of proteins [225]. Interestingly, insertion of proline residues into the first turn of an α-helix, a β-turn or loop region of a globular protein or into the transmembrane α-helix of membrane proteins have been associated with reduced protein aggregation and increased thermostability [226-229]. It is therefore conceivable that such mutations in HSP23$^{-/-}$ null mutants may allow to overcome stress-induced effects on proteins in the absence of HSP23. Site-directed mutagenesis of selected candidate genes followed by experimental phenotype analyses should be performed to elucidate functionally relevant mutations.

In summary, while I cannot exclude a contributing role of SNPs, our results implicate aneuploidy and CNVs as the predominant mechanism to compensate for the lack of HSP23. Hence, the rapid adaptation of HSP23$^{-/-}$ esc0 to heat stress is mediated through selection of a six-gene cluster on chromosome 35, rather than non-synonymous mutations in protein coding regions.

3.2.2 Functional Cloning of Stress Tolerance Marker

At this point, our data proved compelling evidence for a selective advantage of the six-gene cluster on chromosome 35 in the temperature-tolerant HSP23$^{-/-}$ lines. However, they did not allow to draw conclusions about which and how many proteins coded in the amplicon are involved in compensating for the loss of HSP23. To this end, I performed functional cloning experiments in which the respective transgenes were collectively transfected into TS HSP23$^{-/-}$ mutants. After selection at either permissive or non-permissive temperatures, over expression plasmids were again re-isolated from the selected parasite cultures. The DNA samples were then analysed for the presence of the transgenes by PCR. A similar approach

named Cosmid-Sequencing (Cos-Seq), that combines genome-wide cosmid-based functional screening with NGS has been used in the past to elucidate drug targets and resistance mechanisms in *Leishmania* [230]. Notably, Cos-Seq and over expression only allows the identification of gain-of-function mutations but fails to capture the impact of genetic alterations leading to loss-of-function.

Our screening revealed that over expression of a kinase, namely casein kinase 1.2 (LdBPK_351030), causes a strong gain-of-function effect under non-permissive temperatures and is responsible and sufficient to rescue the TS phenotype of HSP23$^{-/-}$ null mutants (see Fig 23). This was further supported by the fact that the observed gene dosage changes were under tight, temperature-dependent selection (see Fig 24): an increase of temperature translated into increased transcript abundance likely due to selective amplification of plasmid copy numbers.

Although previous studies have already reported the essentiality of this kinase during stage-differentiation and infectivity [189], our results provide the first experimental evidence for a specific function of CK1.2 in temperature tolerance, as shall be discussed later.

In conclusion, by using a combination of whole-genome DNA-sequencing coupled with functional cloning, I was able to identify the primary candidate gene whose over expression lays the ground for the emergence of an HSP23$^{-/-}$ escape variant.

3.2.3 The Role of *L. donovani* CK1.2

Members of the casein kinase 1 family are ubiquitous serine/threonine protein kinases that were first identified in the early 1970s in rat liver extracts [231]. Since that time, casein kinase 1 homologues have been identified in all eukaryotes from protozoan parasites to humans [232]. CK1 enzymes contain a highly conserved N-terminal kinase domain responsible for catalytic activity and non-catalytic domains at the N- and C-terminus [233-235]. The latter are more divergent in terms of length and primary amino acid sequence and are known to have regulatory properties on the kinase activity and localisation.

CK1 phosphorylates acidic serine or threonine residues within a specific consensus sequence (Ser/Thr-X-X-Ser/Thr) which is found in a broad range of substrates [236]. Consequently, they are involved in the regulation of many cellular processes including differentiation, cell cycle control and host-pathogen responses [5–7]. In most organisms including yeast and humans, different isoforms of casein kinase 1 are expressed with non-redundant and essential functions. The *Leishmania* genome codes for at least six casein kinase 1 paralogous proteins, of which only three, namely CK1.1, CK1.2 and CK1.4, have been functionally characterised. LdCK1.1 was shown to be non-essential for the survival of promastigotes as well as amastigotes, though its functions may be linked to the growth regulation during the stationary phase [237]. LdCK1.4 is the only isoform unique to *Leishmania* with no orthologues in other Trypanosomatidae. Over expression studies have shown that LdCK1.4 is released by promastigotes into the extracellular space and may be implicated in virulence [238].

The most studied and also most abundant isoform in *Leishmania*, is CK1.2. The sequence of LdCK1.2 is 58-59% identical to its human orthologues, CK1δ and CK1ε, which appears to be particularly high, given the evolutionary distance between humans and *Leishmania* spp. [189]. A high degree of conservation (99% identity) is also seen between the different *Leishmania* CK1.2 orthologues, underlining the essential functions of this kinase during parasite development. CK1.2 is an ecto-/exokinase and was first identified as part of the secretome of *Leishmania* [114, 138]. In contrast to LdCK1.4, LdCK1.2 is released into the host cell via exosomes that are secreted from the flagellar pocket by external cues such as elevated temperature and acidic pH. Inside the host, the kinase phosphorylates host cell factors such as IFNAR1 (a receptor for alpha/beta interferon), thereby modulating the immune response in favour of parasite survival [138]. A similar immunomodulatory function has been ascribed to the human CK1α and to the *Plasmodium* PfCK1. The latter is released into the host cell where it interacts with components of the host cell protein trafficking machinery [239-241].

Apart from its involvement in parasite-host interaction, the recent identification of a selective ATP-competitive inhibitor of CK1.2, D4476, has paved the way for functional analyses of CK1.2 in parasite biology. Pharmacological inhibition of CK1.2 was found to be cytostatic in promastigotes but cytotoxic in amastigotes revealing an essential role of the kinase during stage differentiation and intracellular survival [189]. Nonetheless, similar to other organisms, the functions of CK1.2 appear to be more pleiotropic than previously anticipated given the high diversity of putative CK1.2 clients and the multiple localisation pattern within the parasites [188, 232].

Therefore, elucidating the role of CK1.2 in compensating the loss of HSP23 was expected to provide additional information about the regulatory network during intracellular parasite survival and stress tolerance.

3.2.4 The Regulatory Interface between sHSPs and CK1.2

The coordinated phosphorylation and dephosphorylation of proteins by kinases and phosphatases represents an additional layer of regulating the parasite stress response, and stage differentiation [242]. The development of a culture-based, host-free differentiation system that mimics the differentiation signal inside the phagolysosome of macrophages (37 °C and pH 5.5) has markedly contributed to the current understanding of stage differentiation in *Leishmania* [243-245]. On this basis, recent proteomic and phosphoproteomic studies have accumulated evidence for important stage-specific differences in protein abundance and phosphorylation between promastigotes and amastigotes [164, 187, 246-248]. In general, while protein translation is reduced [127, 249], an increase of phosphoproteins is observed in axenic amastigotes [187, 250]. This allows the parasite to metabolically adapt to the stage-specific requirements during the amastigote stage [202]. For more than half of the analysed phosphoproteins, changes in phosphorylation did not positively correlate with

changes in protein abundance, indicating a functional regulation of the respective proteins by phosphorylation [248].

CK1.2 represents one of the most abundant and active kinases in *Leishmania*, as judged by an almost 50% reduction of the complete phosphoproteome upon its pharmacological inhibition in both life cycle stages [189]. CK1.2 itself is extensively phosphorylated soon after perception of the differentiation signals, while protein abundance remains constant [248]. This suggests that CK1.2 plays a key role in early differentiation and may activate downstream signalling pathways involved in *Leishmania* transformation. The crucial implication of CK1.2 in the early phase of differentiation was further confirmed by time course inhibition experiments [189].

3.2.4.1 HSP23 and P23 are *in Vitro* Substrates of CK1.2

In general, canonical, but also non-canonical CK1 phosphorylation sites are massively distributed on cellular proteins. To date, more than 140 *in vitro* and *in vivo* CK1 substrates have been reported in diverse organisms [232]. Although our genome-wide *in silico* analysis of CK1.2 phosphosites (Ser/Thr-X-X-Ser/Thr) has identified a large repertoire of putative CK1.2 substrates in *Leishmania* as well, until now, only a few have been identified experimentally. Known substrates are the major chaperones HSP70 and HSP90, both playing essential roles in parasite survival, stress tolerance and stage differentiation [125, 126, 186, 188]. In this work, I showed that the small heat shock proteins HSP23 and the structurally related co-chaperone of HSP90, P23, both contain several canonical consensus motifs for CK1 protein kinases and are *in vitro* substrates of CK1.2 (see Fig 25 and Fig 27). Notably, the human small heat shock protein HspB8 also referred to as Hsp22 and the plant orthologue of P23, were previously shown to be phosphorylated by casein kinase 2 [251, 252] confirming a functional link between sHSPs and kinases. Phosphorylation of human small heat shock proteins is induced by various stresses and affects the oligomerisation state and chaperoning properties [253, 254]. Oligomer formation was also reported for *Leishmania donovani* HSP23 and is enhanced in heat-shocked promastigotes [1]. Whether the phosphorylation of LdHSP23 has an impact on its oligomerisation state and chaperoning function, however, remains to be determined.

3.2.4.2 HSP23 and P23 Modulate CK1.2 Kinase Activity *in Vitro*

Of particular interest was the fact, that both chaperones increased autophosphorylation activity of CK1.2 *in vitro*, in turn leading to a reduced substrate-specific activity (see Fig 27). Indeed, sequence analysis revealed four putative autophosphorylation sites, one within the N-terminal ATP-binding domain, two at the N- and one at the C-terminus (see Fig 25). The inhibitory effect of autophosphorylation on CK1 activity is not unique to *Leishmania* but has been already described in other systems [255-257]. Phosphorylations within the ATP-binding domain may modulate the kinase activity by influencing the proper binding of ATP. This has been previously reported as a mechanism to switch off the kinase activity of Ca^{2+}/calmodulin-

dependent kinase II [258]. Similarly, it was shown that phosphorylation of the C-terminal tail of CK1ε, which shares high sequence similarities with *Leishmania* CK1.2, blocks interactions with binding partners presumably through conformational changes of the enzyme [259].

Apart from autophosphorylation, CK1 activity is known to be modulated by interactions with cellular proteins and by subcellular targeting [188, 260]. Considering this, it is conceivable that both HSP23 and P23 are co-chaperones of CK1.2 *in vivo* thereby influencing its activity and/or localisation during the different life cycle stages. In the absence of HSP23, CK1.2 function may be severely perturbed, possibly due to structural instabilities. Based on this hypothesis, the over expression of CK1.2 in HSP23$^{-/-}$ mutants may represent a possible mechanism to counteract the deregulation of CK1.2 activity, especially under non-permissive temperatures, where proteotoxic stress is increased.

Alternatively, elevated CK1.2 protein levels may alter the phosphorylation state of various client proteins and/or activation of signalling pathways. As mentioned earlier, likely client proteins of LdCK1.2 are the two essential chaperones LdHSP70 and LdHSP90 [186, 188] which are involved in maintaining the cellular protein folding homeostasis. Recent research has demonstrated that post-translational modifications of HSP90 are fundamental for the fine-tuning of the chaperone cycle by modulating the conformation, ATPase activity, interaction with co-chaperones, the recruitment and activation of various client proteins, cell growth, and viability [183, 186, 261]. Thus, differential regulation of HSP70 and/or HSP90 by phosphorylation may be another compensatory mechanism to counteract the increased stress levels observed upon loss of HSP23.

In this context, I also cannot exclude the possibility that the loss of HSP23 directly affects HSP90 function. This is supported by two lines of evidence: first, recombinant *L. braziliensis* HSP23 and P23 inhibit the ATPase activity of HSP90 *in vitro* [160]. While not experimentally verified for HSP23, P23 specifically binds to the middle domain of HSP90 thereby stabilising the closed conformation of the chaperone complex and slowing ATP and substrate turnover [262-267]. Interestingly, the cochaperoning activity of P23 on HSP90 can be hampered by ATP-competitive inhibitors of HSP90 such as geldanamycin (GA) and radicicol [268, 269]. The loss of P23 is thereby associated with a marked hypersensitivity of *Leishmania* promastigotes against these inhibitors confirming the functional link of P23 and HSP90 [163]. Secondly, the fact that over expression of HSP23 in *L. donovani* P23$^{-/-}$ null mutant lines can reverse the hypersensitive phenotype under GA or radicicol [163] indicates overlapping functions of both alpha-crystallin domain-containing proteins and additionally suggests an intrinsic co-chaperone activity of HSP23 on HSP90.

In summary, our data suggest a regulatory network comprising CK1.2, HSP23, P23 and HSP90. This is supported by the following results: (i) HSP23, P23, and HSP90 are *in vitro* substrates of CK1.2 and (ii) HSP23 and P23 affect CK1.2 activity but also HSP90 activity [160].

3.2.4.3 LdCK1.2 and its Role in Temperature Tolerance

In addition, I observed an overall reduction of CK1.2 activity upon temperature shift from 25°C to 37°C indicating that the recombinant CK1.2 enzyme is temperature-sensitive (Fig 27). These results are consistent with published data from Rachidi and colleagues who similarly showed a loss of activity at higher temperatures for the recombinant protein *in vitro* [189]. The authors further suggested that the heat-sensitivity of the recombinant protein may explain the overall reduction of CK1.2 activity in axenic amastigotes. However, results obtained from *in vitro* kinase assays, in which recombinantly expressed proteins are used, should be interpreted with caution since they do not allow to analyse the impact of other kinases, phosphatases and binding partners on the kinase activity in the cellular context.

Another interesting observation was that over expression of the kinase in wild type parasites led to a severe growth defect at 34°C, and even more at 37°C (Fig 23). Not surprisingly, transfection and subsequent selection under non-permissive temperatures did not allow the maintenance of the CK1.2 over expression plasmid in wild type parasites. These results indicate that a balanced and tightly controlled expression of CK1.2, especially at mammalian tissue temperatures, is crucial to guarantee optimal growth.

In conclusion, considering the constitutive expression of CK1.2 throughout the parasite life cycle, a tight regulation of CK1.2 activity by post-translational modifications, interaction partners and subcellular localisation appears to be crucial to meet the parasites' needs during stage differentiation. Although a final proof is still missing *in vivo*, our data provide evidence for a reciprocal interaction between CK1.2 and HSP23.

3.3 HSP23: A Target for Antileishmanial Treatments?

Despite years of research, leishmaniasis is still categorised as one of the most neglected tropical infectious diseases affecting primarily underdeveloped regions of the world. To date, there are no effective vaccines available and existing antileishmanial drugs, e.g. pentavalent antimonials, amphotericin B, paromomycin, miltefosine and sodium stibogluconate, are toxic, teratogenic and/or require long treatment duration and hospitalisation [2]. Furthermore, due to their high costs, most patients in endemic areas cannot afford a complete course of treatment increasing the risk of drug resistance. Thus, the development of new, affordable antileishmanial drugs is of vital importance for future control of the disease.

For many neglected tropical diseases, the discovery of novel drugs relies either on high-throughput screening of compounds with potentially pathogenicidal activity or target-based approaches in which a library of compounds is tested against a specific molecule or protein [270].

Over the past decade, the completion of the genome sequences of many human pathogens, including those of *Leishmania* spp., has greatly contributed to the identification of novel drug

targets. These should be unique to the parasite and essential for their intracellular survival inside the host.

In fact, *Leishmania* parasites, belonging to the order of Trypanosomatida, are evolutionarily very distant from humans and encode a variety of genes that have no homologues in humans. Some of these targets are essential for the parasite, including family members of cysteine proteases [271], metalloproteases [272] and protein kinases [273, 274] [275] or enzymes involved in essential metabolic pathways (e.g. glycolysis [276], thiol metabolism [277], purine salvage [278], and folate metabolism [279]) [280]. A list of potential drug targets is shown in Table 6. However, none of these targets is currently exploited to develop novel antileishmanial treatments.

Furthermore, the *L. donovani* small heat shock protein 23 was recently identified as a promising drug target since it is essential for intracellular survival and has no homologues in humans [1]. Although I could confirm the functional conservation of HSP23 among Trypanosomatidae, which may allow the development of a broad spectrum antileishmanial drug, the emergence of a spontaneous HSP23$^{-/-}$ escape variant argues against the therapeutical use of HSP23 inhibitors. By whole genome sequencing, we found that these escape variants display increased gene copy numbers for casein kinase 1.2 whose over expression was indeed sufficient to compensate for the loss of HSP23. Such genetic variations are not unique to the loss of HSP23, but have been already identified as mechanisms of drug resistance. The high genome plasticity of *Leishmania* parasites thereby poses a major drawback in the development of novel drugs, especially when targeting single molecules or proteins. Similar reasoning can also be applied to the use of live-attenuated *Leishmania* parasites for vaccine purposes [281, 282]. Attenuating genetic modifications may be reversed or compensated through selection from pre-existing, beneficial genetic variants within *Leishmania* populations.

The application of combination therapies may be one possible way to circumvent this issue, but cannot completely exclude the emergence of dual drug resistance.

Since *Leishmania* parasites are known to modulate their host cells in favour of parasite survival [283, 284], another strategy would be to restore the metabolic functions of the host cell. Indeed, targeting host-pathogen interactions for chemotherapeutic intervention has been already recognised for the treatment of viral, bacterial and fungal diseases [285-287]. Also, antileishmanial effects were reported for imiquimod, a Toll-Like Receptor agonist, or the Naloxonazine, which targets the host cell vATPases [288, 289]. In conclusion, new strategies for antileishmanial drug discovery should exploit the parasites' dependence on host-cell metabolism rather than essential parasite-specific proteins.

Table 6 Potential drug targets in *Leishmania* and their known inhibitors. Table was modified from [280].

Pathway	Target proteins	Inhibitors	Suitability as targets
Glycolysis	• glucose 6-phosphate isomerase • trilosephosphate isomerase • GAPDH • pyruvate kinase • aldolase	• 2,5-Anhydro-D-mannose and its analogues • adenosine analogues • N-hydroxy-4-phosphono-butanamide	Selective inhibition is a challenge and only high affinity and competitive inhibitors can be used [276]
Thiol metabolism	• trypanothione reductase • trypanothione synthase	• Crystal violet • polyamine derivatives • naphtoquinone	Absence of these enzymes in mammalian hosts, along with their sensitivity to oxidative stress, makes them a potential target for antileishmanial chemotherapeutics [277]
Cystein- and Metalloproteases	• metacaspases • leishmanolysin	• Aziridine-2,3 dicarboxylate • vinyl sulfones • hydrazides • thiosemicarbazones	CPs are essential for the growth, differentiation, and pathogenicity and play a pivotal role in host-parasite interactions, thus making it a potential target with a promising number of inhibitors in-line [272]
Protein kinases	• cyclin-dependent kinases • MAPKs • glycogen synthase kinase-3 • casein kinases	• Azapurines & purvalanols • thiazoles • paullones • D4476	selective inhibition of CDKs can be achieved and is currently being researched [273]
Purine salvage	• hypoxanthine-guanine phosphoribosyltransferase • adenosine kinase	• Allopurinol • phthalimide derivatives	The parasite has multiple salvage routes, which means that targeting individual enzymes is not effective [278]
Folate and/or pteridine metabolism	• dihydrofolate reductase/ thymidylate synthase • pteridine reductase 1	• 5-Benzyl-2,4-diaminopyrimidines • 8-octyloxy derivatives • 2,4-diaminopteridines	Antifolate therapies against leishmanial DHFR TS have failed because of presence of PTR1, which can reduce pteridebiopterine; It is necessary to design strong inhibitors that can inhibit both enzymes [270]

3.4 Concluding Remarks

Leishmania parasites are the causative agents of a broad spectrum of human diseases. Due to the spreading drug resistance and the lack of vaccines, basic research is of utmost importance to identify new targets for combatting the parasite.

In this work, I analysed the suitability of the small heat shock protein HSP23 as a drug target, the loss of which renders the parasites more sensitive towards chemical stress and incapable to survive at mammalian tissue temperatures. Performing complementation studies, I first showed that over expression of different trypanosomatid HSP23-encoding orthologous genes could functionally complement the TS phenotype of *L. donovani* and *L. major* HSP23$^{-/-}$ null mutants, demonstrating functional conservation of HSP23 homologues among trypanosomatids. However, I found that the loss of the small heat shock protein HSP23 in *Leishmania donovani,* can be complemented by spontaneous or targeted copy number increase of the casein kinase 1.2, a protein kinase previously implicated in the virulence of *L. donovani* parasites. At the same time, these results rule out HSP23 as a drug target against *Leishmania* infections.

In vitro phosphorylation experiments revealed that both HSP23 and the related P23 co-chaperone are *in vitro* substrates and modulators of casein kinase 1.2. Yet, the downstream effects of CK1.2 over expression *in vivo* remain largely unknown. In the future, comparative phosphoproteomics of the wild type, HSP23$^{-/-}$ mutants, and CK1.2 over expressing lines may help to further elucidate the mechanistic details of HSP23 compensation and fill the knowledge gaps left by this study. In addition, such studies may identify novel clients and downstream signalling pathways of CK1.2. In parallel, site-directed mutagenesis of putative CK1.2 phosphosites in HSP23 and P23 should be performed to better understand the relevance of HSP23 and P23 phosphorylation *in vivo* in terms of cell viability and stress tolerance. In conclusion, with the functional characterisation of the small heat shock protein, HSP23, I provide evidence for a crucial link between chaperones and signal transduction protein kinases in *Leishmania*.

4 Materials & Methods

4.1 Materials

4.1.1 Organisms and Strains

4.1.1.1 *Leishmania* Strains

Table 7 List of *Leishmania* strains used in this study.

Strain	Identification number	Origin	Provider
Leishmania donovani 1SR	MHOM/SD/00/1SR	Sudan	Dan Zilberstein, Israel Institute of Technology, Israel
Leishmania major 5ASKH	MHOM/TM/ 1973/5ASKH	Turkmenistan	David Evans, London School of Hygiene and Tropical Medicine, UK

4.1.1.2 Bacterial Strains

Table 8 List of bacterial strains used in this study.

Strain	Properties	Application	Company
E. coli DH5α	*supE44 la- cU169 (80lacZm15) hsdR17 recA1 endA1, gyrA96 thi-1 relA,* chemocompetent	Amplification of plasmids	New England Biolabs, Beverly, USA
E. coli BL21 [pAPlacI^{Q}]	*hsd*S *gal* (λcI*ts*857 *ind* 1 *Sam*7 *nin*5 *lac*UV5-T7 gene 1), [pAPlacI^{Q}], chemocompetent	Expression of recombinant proteins	Sarstedt, Waldbronn, Germany
E. coli XL one Blue	recA endA gyrA96 thi-1 hsdR17 supE44 relA1 lac [F´ proAB lacqZΔM15 Tn10 (Tetr)], electrocompetent	Amplification of plasmids isolated from *Leishmania*	Agilent Technologies, Santa Clara, USA

4.1.2 Plasmids

Table 9 List of plasmids used in this study.

Name	Application	Company/Reference
pUC19	Cloning plasmid	Thermo Fisher Scientific, Waltham, USA

Table 9 List of plasmids used in this study.

Name	Application	Company/Reference
pCL1S	*Leishmania* expression plasmid	[1]
pCL2S	*Leishmania* expression plasmid	[1]
pUC-HSP23-5'puro3'NC	Generation of *L. donovani* HSP23$^{-/-}$ esc0 mutants via homologous recombination	[1]
pUC-HSP23-5'neo3'NC		
pUC-HSP23-5'puro3'NC_new	Generation of *L. donovani* HSP23$^{-/-}$ mutants via homologous recombination	this thesis
pUC-HSP23-5'neo'NC_new		
pCL1S-LdHSP23	Over expression of *L. donovani* HSP23	[1]
pCL1S-LmjHSP23	Over expression of *L. major* HSP23	this thesis
pCL1S-LbrHSP23	Over expression of *L. braziliensis* HSP23	this thesis
pCL1S-LinfHSP23	Over expression of *L. infantum* HSP23	this thesis
pCL1S-TcrHSP23	Over expression of *T. cruzi* HSP23	this thesis
pCL1S-TbrHSP23	Over expression of *T. brucei* HSP23	this thesis
pCL2S-LdBPK_351030	Over expression of LdBPK_351030 (CK1.2)	this thesis
pCL2S-LdBPK_351040	Over expression of LdBPK_351040 (CCCH-type zinc finger protein)	this thesis
pCL2S-LdBPK_351050	Over expression of LdBPK_351050 (cupin domain-containing protein)	this thesis
pCL2S-LdBPK_351060	Over expression of LdBPK_351060 (CCCH-type zinc finger protein)	this thesis
pCL2S-LdBPK_351070	Over expression of LdBPK_351070 (protein kinase)	this thesis
pCL2S-LdBPK_351080	Over expression of LdBPK_351080 (hypothetical)	this thesis
pJC45	Backbone plasmid used for the generation of pJC65	[137]
pJC45-HSP23	Expression of recombinant HSP23 in *E. coli*	[1]
pJC45-P23	Expression of recombinant P23 in *E. coli*	[163]

Table 9 List of plasmids used in this study.

Name	Application	Company/Reference
pJC65	Protein expression plasmid	this thesis
pJC65-CK1.2	Expression of recombinant CK1.2 in *E. coli*	this thesis
pTBlast	Template for amplification of the BlastR replacement construct	[192]
pTPuro	Template for amplification of the PuroR replacement construct	[192]

4.1.3 Oligonucleotides

Table 10 shows the sequence of all oligonucleotides used in this work. Binding sites are depicted in capital, overhangs in small letters. Restriction sites are additionally underlined. Gene targeting sequence of sgRNAs are labelled in bold. All oligonucleotides were ordered at Sigma-Aldrich, Munich, Germany.

Table 10 List of oligonucleotides used in this study.

#	Name	Sequence 5'-3'	Application
			CRISPR/Cas9
1	LmHSP23-UFP	cccgtacacgcccgcgcgttttggtgcagc GTATAATGCAGACCTGCTGC	Amplification of PuroR and BlastR replacement constructs
2	LmHSP23-DRP	tggcgtcgctgcagcggcagagcgccgcca CCAATTTGAGAGACCTGTGC	
3	LmHSP23-5'sgRNA	gaaattaatacgactcactatagg**CTGTCTCTGACATTGACGC**Tgtttt agagctagaaatagc	Amplification of 5' sgRNA or 3' sgRNA template
4	LmHSP23-3'sgRNA	gaaattaatacgactcactatagg**AAGCCTGCTCAATCGACCTG**gttttagagctagaaatagc	
5	G00	AAAAGCACCGACTCGGTGCCACTTTTTCAAGTTGATAACGGACTAGCCTTATTTTAACTTGCTATTTCTAGCTCTAAAAC	

Table 10 List of oligonucleotides used in this study.

#	Name	Sequence 5'-3'	Application
			Plasmid preparation
6	LmHSP23-3'NC-HindIIIb	ggagaagcttatttaaatTTCCCTC ACGTCGTGATGAG	Amplification of *L. donovani* HSP23 3'UTR for generation of pUC19-LdHSP23-5'puro/ neo3'NC_new
7	P23 (2)-3'UTR_BamHI	gggggatccTCACGTGTCCTC CTCGAGC	
8	LbrM_HSP23_BclI_rev	ggagtgatcaTCACATATCGTCC TCGAGCG	Amplification of *L. braziliensis* HSP23 for pCL1S-LbrHSP23
9	LbrM_HSP23_KpnI_fwd	ggagggtaccATGTCGGCCAG CGGTTCATTG	
10	Lmaj_HSP23_BclI_rev	ggagtgatcaTCACGTGTCCTC CTCGAGCG	Amplification of *L. major* HSP23 for pCL1S-LmjHSP23
11	Lmaj_HSP23_KpnI_fwd	ggagggtaccATGTCCAGCAGC GGCCCATTG	
12	Tb_HSP23_BclI_rev	ggagtgatcaTTACGGTTCGAG AGGAGGCAG	Amplification of *T. brucei* HSP23 for pCL1S-TbrHSP23
13	Tb_HSP23_KpnI_fwd	ggagggtaccATGACGAATCAG TCGGACGC	
14	Tc_HSP23_BclI_rev	ggagtgatcaTTACTCCTCTAAA GGAGGAAG	Amplification of *T. cruzi* HSP23 for pCL1S-TcrHSP23
15	Tc_HSP23_KpnI_fwd	ggagggtaccATGTCCGCGAGT AAAGAAGTC	
16	p23.2_5'KpnI	gggggtaccATGTCCACCAGC GGCCCATTG	Amplification of *L. donovani* HSP23 and *L. infantum* HSP23 for pCL1S-LdHSP23 and pCL1S-LinfHSP23
17	p23.2_3'BamHI	gggggtaccTCACGTGTCCTC CTCGAGC	
18	Link-pJC65+	CATGGGCCATCATCATCATC ATCATCATCATCATCACGGT GGTACCA	Generation of the protein expression plasmid pJC65
19	Link-pJC65-	AGCTTGGTACCACCGTGAT GATGATGATGATGATGATGA TGATGGCC	
20	351030_KpnI_fwd	ggagggtaccATGAACGTGGAA CTGCGCGTC	Amplification of *L. donovani* CK1.2 for pCL2S-LdBPK_351030
21	351030_NdeI_rev	ggagcatatgCTACTGCTGTTC TTGCGCAC	
22	351040_KpnI_fwd	ggagggtaccATGCACACGCCA CCCCTCTC	Amplification of *L. donovani* LdBPK_351040 for pCL2S-LdBPK_351040
23	351040_NdeI_rev	ggagcatatgTCACATGAAGCG AGCCGCCA	
24	351050_KpnI_fwd	ggagggtaccATGACCTCCCCG GCAGCCGC	Amplification of *L. donovani*

Table 10 List of oligonucleotides used in this study.

#	Name	Sequence 5'-3'	Application
25	351050_NdeI_rev	ggagcatatgCTAGATTCCTGTTGTCTGTAAG	LdBPK_351050 for pCL2S-LdBPK_351050
26	351060_NdeI_fwd	ggagcatatgATGACGAGCCAGTCGCACGTG	Amplification of *L. donovani* *LdBPK_351060* for pCL2S-LdBPK_351060
27	351060_BglII_rev	ggagagatctTTAGGGCTCCATCACCATCG	
28	351070_KpnI_fwd	ggagggtaccATGACCGTTCTGCCACCCAAG	Amplification of *L. donovani* LdBPK_351070 for pCL2S-LdBPK_351070
29	351070_NdeI_rev	ggagcatatgTCACTTGCGCAAAGCGTCGG	
30	351080_KpnI_fwd	ggagggtaccATGGGTAAGCGAAACGAAAG	Amplification of *L. donovani* LdBPK_351080 for pCL2S-LdBPK_351080
31	351080_NdeI_rev	ggagcatatgCTACATGGATGCGACCACGC	
			Sequencing
32	M13-24F	CCAGGGTTTTCCCAGTCACG	Used for sequencing of pUC19 derived plasmids
33	M13-24R	CGGATAACAATTTCACACAGG	
34	pIR-p-fwd2	GGCTCTGCGTTTCACTTGC	Used for sequencing of pCL1S or pCL2S derived plasmids
35	pIR-p-rev	GCGAACTGGTCGTAGAAATC	
36	pJC45_fwd	GGATAACAATTCCCCTCTAG	Used for sequencing of pJC45 and pJC65 derived plasmids
37	pJC45_rev	CTAGTTATTGCTCAGCGGTG	
			qRT-PCR
38	Lbr_HSP23_qPCR_fwd	CTGCGGAAAAAGCTAACAAGGTC	Quantification of *L. braziliensis* HSP23 mRNA
39	Lbr_HSP23_qPCR_rev	CGTCATCCTCGTCTTTCCACTTA	
40	LmjHSP23_qPCR_fwd	CGGAAGAAGTTCTCCAAGTCACT	Quantification of *L. major* HSP23 mRNA
41	LmjHSP23_qPCR_rev	GTCTTTCCACTTAGACCAGTCGA	
42	Tbruc_HSP23_qPCR_fwd	GAATCAGTCGGACGCGATATTTC	Quantification of *T. brucei* HSP23 mRNA
43	Tbruc_HSP23_qPCR_rev	CTTTATCTCCACCACAACGTTCG	

Table 10 List of oligonucleotides used in this study.

#	Name	Sequence 5'-3'	Application
44	Tcruzi_HSP23_qPCR_fwd	GATAGCGAAAACGATGGTG GTCT	Quantification of *T. cruzi* HSP23 mRNA
45	Tcruzi_HSP23_qPCR_rev	CTCTTTCTTCTCAAGCCCCT TCT	
46	p23.2-F42	CCATTCCTGGATTTGGCTC GG	Quantification of *L. donovani* or *L. infantum* HSP23 mRNA
47	p23.2-B36	GCATATCGCCGTCGTCATCT CC	
48	RT-actin-F1	TGGCACCATACCTTCTACAA CG AG	Quantification of *Leishmania* actin mRNA used as reference gene
49	RT-actin-B2	CGTCATCTTCTCACGGTTCT GC	
50	LdBPK_351030.1_fwd	CACGTGTACATCATCGACTT TGG	Quantification of *L. donovani C*K1.2 mRNA
51	LdBPK_351030.1_rev	CTCTTGCCTTCCTTGTATGG GAT	
52	LdBPK_351040.1_fwd	ACACTCTCCCTTCGCATTAT CAG	Quantification of *L. donovani* LdBPK_351040 mRNA
53	LdBPK_351040.1_rev	CTCGATGAAGTAGATCGGT TGCT	
54	LdBPK_351050.1_fwd	TTTTGGATTAAGCGCCTGC AAC	Quantification of *L. donovani* LdBPK_351050 mRNA
55	LdBPK_351050.1_rev	GAAAGTAAATGGTCGTGTA GGCG	
56	LdBPK_351060.1_fwd	CAGTACTACACACACAACC CGTA	Quantification of *L. donovani* LdBPK_351060 mRNA
57	LdBPK_351060.1_rev	CGACAACTTCTTGGTAGAC TGGA	
58	LdBPK_351070.1_fwd	TAGTCTTCTACGTGCTTCTC TGC	Quantification of *L. donovani* LdBPK_351070 mRNA
59	LdBPK_351070.1_rev	GTGATTTGGGTTGAAGAGG ACAC	
60	LdBPK_351080.1_fwd	CGAGTACGGCAACTTCAAC GATA	Quantification of *L. donovani* LdBPK_351080 mRNA
61	LdBPK_351080.1_rev	CCGGTCGTCTATGTCATCTT CTT	

4.1.4 Chemicals

Table 11 List of chemicals used in this study.

Name	Company or composition
1,10-Phenanthroline	Sigma Aldrich, Munich, Germany
2-[4-(2-hydroxyethyl)piperazin-1-yl]ethanesulfonic acid (HEPES)	Carl Roth, Karlsruhe, Germany
4′,6-Diamidin-2-phenylindol (DAPI)	Sigma Aldrich, Munich, Germany
β-glycerophosphate	Merck, Darmstadt, Germany
[γ-^{32}P]-ATP	Hartmann Analytics, Braunschweig, Germany
Acetic acid	Carl Roth, Karlsruhe, Germany
Acetone	Carl Roth, Karlsruhe, Germany
Acrylamide/Bis-acrylamide (40%) (37.5:1)	Carl Roth, Karlsruhe, Germany
Agarose	Biozym, Hessisch Oldendorf, Germany
Albumin fraction V (BSA)	Carl Roth, Karlsruhe, Germany
Ammonium chloride	Fluka, Munich, Germany
Ammonium persulfate (APS)	Carl Roth, Karlsruhe, Germany
Adenosinetriphosphate (ATP)	Carl Roth, Karlsruhe, Germany
5-bromo-4-chloro-3-indolyl-phosphate (BCIP)	Biomol, Hamburg, Germany
Bromophenolblue	Merck, Darmstadt, Germany
Calciumchloride ($CaCl_2$)	Merck, Darmstadt, Germany
Cesiumchloride	Biomol, Hamburg, Germany
Coomassie blue R250	Carl Roth, Karlsruhe, Germany
D4476	Merck, Darmstadt, Germany
D(+)-Glucose	Sigma Aldrich, Munich, Germany
Deoxynucleoside triphosphate (dNTP)	Sigma Aldrich, Munich, Germany
Dimethyl sulfoxide (DMSO)	Carl Roth, Karlsruhe, Germany
Dipotassium hydrogenphosphate (K_2HPO_4)	Merck, Darmstadt, Germany
Disodiumphosphate (Na_2HPO_4)	Merck, Darmstadt, Germany
Dithiothreitol (DTT)	Biomol, Hamburg, Germany
Dodecylsulfate-Na-salt pellets (SDS)	Carl Roth, Karlsruhe, Germany
Ethanol (EtOH)	Carl Roth, Karlsruhe, Germany

Table 11 List of chemicals used in this study.

Name	Company or composition
Ethidium bromide (Etbr)	Carl Roth, Karlsruhe, Germany
Ethylenediaminetetraacetic acid (EDTA)	Carl Roth, Karlsruhe, Germany
Ethylene glycol-bis β-aminoethyl ether-tetraacetic acid (EGTA)	Fluka, Munich, Germany
Glycerine	Carl Roth, Karlsruhe, Germany
Hydrochloric acid (HCl)	neoLab Migge GmbH, Heidelberg, Germany
Hydrogen peroxide (H_2O_2)	Carl Roth, Karlsruhe, Germany
Imidazole	Fluka, Munich, Germany
Isopropanol	Carl Roth, Karlsruhe, Germany
Magnesium chloride ($MgCl_2$)	Carl Roth, Karlsruhe, Germany
Methanol (MeOH)	Carl Roth, Karlsruhe, Germany
Milk powder	Carl Roth, Karlsruhe, Germany
Mowiol 488	Carl Roth, Karlsruhe, Germany
Nickel sulfate ($NiSO_4$)	Carl Roth, Karlsruhe, Germany
Phenylmethylsulfonylfluorid	Carl Roth, Karlsruhe, Germany
Potassium acetate (CH_3CO_2K)	Sigma Aldrich, Munich, Germany
Potassium chloride (KCl)	Merck, Darmstadt, Germany
Sodium chloride (NaCl)	Carl Roth, Karlsruhe, Germany
Sodium dihydrogen phosphate (NaH_2PO_4)	Merck, Darmstadt, Germany
Sodium dodecyl sulfate (SDS) pellets	Carl Roth, Karlsruhe, Germany
Sodium hydroxide (NaOH) pellets	Carl Roth, Karlsruhe, Germany
Sodium orthovanadate (Na_3VO_4)	Merck, Darmstadt, Germany
Tetramethylethylendiamine (TEMED)	Carl Roth, Karlsruhe, Germany
Tris-Hydroxymethyl-aminomethan	Biomol, Hamburg, Germany
Triton-X-100	Merck, Darmstadt, Germany
Tween-20	Sigma Aldrich, Munich, Germany

4.1.5 Buffers and Solutions

Table 12 List of buffers and solutions used in this study.

Buffer	Company or composition
6× DNA-Loading buffer	Thermo Fisher Scientific, Waltham, USA

Table 12 List of buffers and solutions used in this study.

Buffer	Company or composition
Alkaline phosphatase (AP) buffer	100 mM Tris-HCl (pH 9.5) 100 mM NaCl 10 mM $MgCl_2$
B5 buffer	20 mM Tris-HCl (pH 8.0) 0.5 M KCl, 5 mM imidazole
B100 buffer	20 mM Tris-HCl (pH 8.0) 0.5 M KCl, 100 mM imidazole
B1000 buffer	20 mM Tris-HCl (pH 8.0) 0.5 M KCl, 1 M imidazole
Blocking buffer (Immunofluorescence)	2% w/v BSA 0.1% Triton X-100 ad 1× PBS (pH 7.0)
Blocking buffer (Western blot)	5% w/v milk powder 0.1% Tween-20 1× TBS ad ddH_2O
Blotting buffer (semidry)	48 mM Tris 39 mM glycine 0.037% SDS 20% MeOH ad ddH_2O
CASYton	OLS OMNI Life Science, Bremen, Germany
Coomassie brilliant blue staining solution	40% EtOH 10% acetic acid 1 g/l Coomassie blue R250 50% ddH_2O
Coomassie brilliant blue destaining solution	40% EtOH 10% acetic acid 50% ddH_2O
Electroporation buffer	21 mM HEPES (pH 7.5) 137 mM NaCl 5 mM KCl 0.7 mM Na_2HPO_4 6 mM glucose

Table 12 List of buffers and solutions used in this study.

Buffer	Company or composition
Electroporation buffer Roditi (3×)	3× Roditi: 200 mM Na_2HPO_4 70 mM NaH_2PO_4 15 mM KCl 150 mM HEPES (pH 7.3) Concentration used for transfection: 1× Roditi: 600 µL ddH_2O 350 µL 3× Roditi buffer 100 µL 1.5mM $CaCl_2$
Extraction buffer 0	20 mM Tris-HCl (pH 8.0) 100 mM KCl 5 mM imidazole 10% glycerol 1 mM 1,10-Phenanthroline 0.1 mM DTT
Kinase buffer	40 mM HEPES (pH 7.5) 130 mM KCl 15 mM $MgCl_2$ 0.5 mM 1,10-Phenanthroline 25 mM ß-glycerophosphate 1 mM PMSF 0.1 mM sodium orthovanadate 1 mM EGTA
SDS-PAGE sample buffer (2×)	100 mM Tris 4% SDS 0.1% bromophenolblue 20% glycerine ad ddH_2O
Mounting medium	25% glycerine 0.1 M Tris-HCl (pH 8.5) 10% Mowiol 488
Phosphate buffer saline (PBS) (1×)	0.137 M NaCl 10.14 mM Na_2HPO_4, 2.68 mM KCl 1.76 mM K_2HPO_4 (pH 7.4)
Permeabilisation solution (Immunofluorescence)	0.1% Triton X-100 50 mM NH_4Cl ad 1× PBS
Plasmid preparation buffer 1	50 mM glucose 25 mM Tris-HCl 10 mM EDTA (pH 8.0)
Plasmid preparation buffer 2	0.2 N sodium hydroxide 1% SDS (pH 14)
Plasmid preparation buffer 3	3 M potassium acetate 2 M acetic acid (pH 5.5)

Table 12 List of buffers and solutions used in this study.

Buffer	Company or composition
SDS running buffer (1×)	25 mM Tris 250 mM glycine 0.1% SDS ad ddH_2O
Separating gel (10%)	375 mM Tris-HCl (pH 8.8) 10% acrylamide-bisacrylamide (37.5:1, 40%) 0.1% SDS 0.1% APS 0.1% TEMED
Stacking gel (5%)	125 mM Tris-HCl (pH 6.8) 5% acrylamide-bisacrylamide (37.5:1, 40%) 0.1% SDS 0.1% APS 0.1% TEMED
TAE buffer (1×)	40 mM Tris-Acetate 1 mM EDTA (pH 8.0)
TBS (1×)	150 mM NaCl
TE (Tris-EDTA) buffer	10 mM Tris-HCl 1 mM EDTA (pH 8.0)
TE-RNase-buffer	10 µg/mL RNaseA in TE buffer
Washing buffer (Immunofluorescence)	0.1% Triton X-100 in 1× PBS
Washing buffer (Western blot)	0.02% Tween-20 1× TBS ad ddH_2O

4.1.6 Cell Culture Media and Supplements

Table 13 List of cell culture media and supplements used in this study.

Name	Company and/or composition
Cycle Grow LB-agar plates	2% LB 1.5% LB-agar
Cycle Grow LB-liquid medium	2% LB
Freezing solution	50% FCS (heat-inactivated) 30% M199$^+$-medium 20% DMSO Storage at -20°C
Medium 199 with Earle’s salts	Sigma-Aldrich, Munich, Germany

Table 13 List of cell culture media and supplements used in this study.

Name	Company and/or composition
Parasite culture medium (pH 7.4)	1× M199 20% FCS (heat-inactivated) (Sigma-Aldrich, Munich, Germany) 40 mM HEPES 10 mg/L haemin (Sigma-Aldrich, Munich, Germany) 0.1 mM adenine 5 µM 6-Biopterin (Biomol, Hamburg, Germany) 2 mM glutamine 100 U penicillin 100 µg/mL streptomycin Storage at 4°C

4.1.6.1 Antibiotics

Table 14 List of antibiotics used in this study.

Antibiotic	Final concentration	Company
Ampicillin	100 µg/mL in ddH_2O	Carl Roth, Karlsruhe, Germany
Blasticidin S Hydrochloride	5 µg/mL in 1× PBS	Carl Roth, Karlsruhe, Germany
Hygromycin B	50 µg/mL in 1× PBS	Carl Roth, Karlsruhe, Germany
L-Glutamine Pen/Strep (Penicillin/Streptomycin)	2 mM L-glutamine 100 U penicillin 0.1 mg/mL streptomycin	Sigma Aldrich, Munich, Germany
Geneticin (G418)	50 µg/mL	Carl Roth, Karlsruhe, Germany
Nourseothricine (cloNAT)	150 µg/mL in ddH_2O	Werner BioAgents GmbH
Pen/Strep (Penicillin/ Streptomycin)	100 U penicillin 0.1 mg/mL streptomycin	Sigma Aldrich, Munich, Germany
Puromycin Dihydrochloride	25 µg/mL in 1× $M199^+$	AppliChem, Darmstadt, Germany

4.1.7 Antibodies

Table 15 List of antibodies used in this study.

Antibody	Application	Concentration	Company/Reference
Primary antibodies			
anti-HSP23 IgY (polyclonal, chicken)	WB	1/500	[1]

Table 15 List of antibodies used in this study.

Antibody	Application	Concentration	Company/Reference
anti-HSP70 IgY (polyclonal, chicken)	WB	1/1000	[137]
anti-DYKDDDDK Epitope (FLAG) IgG (polyclonal, rabbit)	WB	1/500	Biolegend, San Diego, USA
anti-LmjCK1.2 IgG (SY3535) (polyclonal, rabbit)	WB	1/250	[189]
anti-P23 IgY (polyclonal, chicken)	WB	1/500	[163]
anti-α-tubulin-IgG (polyclonal, mouse)	IFA	1/4000	Sigma Aldrich, Munich, Germany
Secondary antibodies			
anti-mouse Alexa Fluor® 594 IgG (polyclonal, goat)	IFA	1/250	Thermo Fisher Scientific, Waltham, USA
anti-chicken-AP IgY (polyclonal, rabbit)	WB	1/1000-1/5000	Dianova, Hamburg, Germany
anti-rabbit-AP IgG (polyclonal, goat)	WB	1/1000	Dianova, Hamburg, Germany

4.1.8 Enzymes & Proteins

Enzymes and proteins are listed in Table 16. Details of their application can be found in the respective method sections.

Table 16 List of enzymes and proteins used in this study.

Name	Company
Myelin basic protein (MBP)	Merck, Darmstadt, Germany
Restriction enzymes	New England Biolabs, Beverly, USA
RNase A	Sigma-Aldrich, Munich, Germany
T4 DNA ligase	New England Biolabs, Beverly, USA
Taq DNA polymerase	Thermo Fisher Scientific, Waltham, USA

4.1.9 Kits

Unless mentioned otherwise, kits listed in Table 17 were used according to the manufacturer instructions.

Table 17 List of commercial kits used in this study.

Name	Company
Agencourt AMPure XP Kit	Beckman Coulter, Fullerton, USA

Table 17 List of commercial kits used in this study.

Name	Company
Biozym Blue S'Green qPCR Kit	Biozym Scientific GmbH, Oldendorf, Germany
Agilent High Sensitivity DNA Kit	Agilent Technologies, Santa Clara, USA
InviTrap® Spin Cell RNA Mini Kit	Started, Birekenfeld, Germany
iProof™ High-Fidelity PCR Kit	Bio-Rad, Munich, Germany
ISOLATE II Genomic DNA Kit	Bioline, Luckenwalde, Germany
MiSeq® reagent kit v3 (600 cycle)	Illumina, San Diego, USA
Nextera® XT index Kit	Illumina, San Diego, USA
Nextera® XT DNA Library Preparation Kit	Illumina, San Diego, USA
NucleoBond® PC 20 kit	Machery-Nagel, Düren, Germany
NucleoSpin® Gel and PCR clean up Kit	Machery-Nagel, Düren, Germany
QuantiTect® Reverse Transcription Kit	Qiagen, Venlo, Netherlands

4.1.10 Size Standards

DNA or protein markers listed in Table 18 were always loaded next to DNA or protein samples to allow size discrimination of the bands.

Table 18 List of size standards used in this study.

Name	Company
Gene Ruler 1kb DNA Ladder	Thermo Fisher Scientific, Waltham, USA
PageRuler unstained Protein Ladder	Thermo Fisher Scientific, Waltham, USA
ProSieve QuadColor Protein Marker	Biozym, Hessisch Oldendorf, Germany

4.1.11 Laboratory Equipment

Table 19 Laboratory equipment.

Name	Company
Amaxa™ Nucleofector™ IIb	Lonza, Basel, Switzerland
2100 Bioanalyzer Instrument	Agilent Technologies, Santa Clara, USA
BioMate™ 3 Spectrophotometer	Thermo Fisher Scientific, Waltham, USA
Biometra UV Band Ecuador	Biometra, Göttingen, Germany
Biorad MicroPulser™	Bio-Rad, Munich, Germany

Table 19 Laboratory equipment.

Name	Company
Branson Ultrasonics™ Sonifier Modell 250 CE	G. Heinemann, Schwäbisch Gmünd, Germany
CASY® Cellcounter & Analyzer	Roche, Mannheim, Germany
Electrophoreses Power Supply-EPS301	Amersham, Buckinghamshire, UK
Eppendorf® Centrifuge 5415 D	Eppendorf, Hamburg, Germany
Eppendorf® Centrifuge 5415 R	Eppendorf, Hamburg, Germany
Mastercycler® Gradient	Eppendorf, Hamburg, Germany
Epson Perfection V700 Photo Scanner	EPSON, Meerbusch, Germany
EVOS® FL Auto Cell Imaging System	Thermo Fisher Scientific, Waltham, USA
EVOS™ XL Cell Imaging System	Thermo Fisher Scientific, Waltham, USA
Biorad Gene Pulser™	Bio-Rad, Munich, Germany
Incubator WTC Binder	Binder, Tuttlingen, Germany
Innova™ 440 incubator shaker	New Brunswick Scientific, New Jersey, USA
J2-21 Centrifuge	Beckman Coulter, Fullerton, USA
J2-HS Centrifuge	Beckman Coulter, Fullerton, USA
Illumina MiSeq® Next Generation Sequencer	Illumina, San Diego, USA
Multisizer™ 3 Coulter Counter®	Beckman Coulter, Fullerton, USA
NanoDrop™	Thermo Fisher Scientific, Waltham, USA
New Brunswick™ Galaxy® 170S	Eppendorf, Hamburg, Germany
Optima XE-90	Beckman Coulter, Fullerton, USA
PerfectBlue™ gel system	Peqlab, Erlangen, Germany
PerfectBlue™ Doppel-Gelsystem Twin M	Peqlab, Erlangen, Germany
pH-Meter Microprocessor pH 211	Hanna Instruments, Kehl am Rhein, Germany
Invitrogen™ Qubit™ 3 Fluorometer	Thermo Fisher Scientific, Waltham, USA
Rotor-Gene™ RG 3000 Instrument	Corbett, Sydney, Australia
Safety cabinet MSC-Advantage™	Thermo Fisher Scientific, Waltham, USA
Spectra/Por Dialysis tubing (MWCO 6-8 kDa)	Spectrum, Rancho Dominguez, USA
Taumel roller shaker CAT RM5	neoLab, Heidelberg, Germany
Trans-Blot SD®	Bio-Rad, Munich, Germany

Table 19 Laboratory equipment.

Name	Company
TrayCell®	Hellma, Müllheim, Germany
Vortexter VF2	IKA-Werke GmbH 6 Co.KG, Staufen, Germany

4.1.12 Disposables

Table 20 List of disposables used in this study.

Name	Company
Amersham™ Hybond™ P 0.45 PVDF	GE Healthcare Life Sciences, Munich, Germany
Cell culture flask T25 cm^2	Sarstedt, Waldbronn, Germany
Cell culture flask T175 cm^2	Sarstedt, Waldbronn, Germany
Cellophane® foil	Carl Roth, Karlsruhe, Germany
Eppendorf DNA LoBind® tubes 0.2mL	Eppendorf, Hamburg, Germany
Eppendorf DNA LoBind® tubes 0.5mL	Eppendorf, Hamburg, Germany
Eppendorf DNA LoBind® tubes 1.5mL	Eppendorf, Hamburg, Germany
Fluted filter (⌀= 185 mm)	Schleicher & Schall, Kassel, Germany
Fujifilm Super RX-N	Fujifilm, Tokyo, Japan
His·Bind® Resin	Novagen, Madison, USA
Gene Pulser® cuvettes (0.1 cm)	Bio-Rad, Munich, Germany
Gene Pulser® cuvettes (0.2 cm)	Bio-Rad, Munich, Germany
Gene Pulser® cuvettes (0.4 cm)	Bio-Rad, Munich, Germany
Microfuge tube	Beckman Coulter, Fullerton, USA
Quick-seal tubes	Beckman Coulter, Fullerton, USA
Ultra-clear centrifuge tubes	Beckman Coulter, Fullerton, USA
Whatman® 3MM paper	Schleicher & Schall, Dassel, Germany

4.1.13 Software, Online tools and Databases

Table 21 List of software, online tools and databases.

Online tools and data bases	Application	Reference
Basic Local Alignment Search Tool (BLAST)	DNA or protein sequence similarity search	https://blast.ncbi.nlm.nih.gov/Blast.cgi

Table 21 List of software, online tools and databases.

Online tools and data bases	Application	Reference
EndNote X9.3.3	Literature library and citation manager	https://endnote.com/downloads/
GraphPad Prism8, Version 8.4.3	Statistical analysis	www.graphpad.com
Heatmapper Online Tool	Analysis of ploidy profiles	[286]
ImageJ, Version 2.0.0	Image processing	https://imagej.nih.gov/ij/
Intaglio™, Version 3.9.5	Figure composition assembly	-
LeishGEdit primer design online tool	Primer design for CRISPR/Cas9 gene editing	http://www.leishgedit.net/Home.html
MacVector, Inc. with Assembler, Version 17.5.4	Sequencing analysis & *in silico* design of plasmids	https://macvector.com/Assembler/assembler.html
Rotor-Gene real-time analysis software 6.1.81	qRT-PCR analysis	-
TriTryp	Gene databases for Trypanosomatidae	https://tritrypdb.org/tritrypdb/
PubMed-NCBI	Literature Research	https://pubmed.ncbi.nlm.nih.gov

4.2 Methods

4.2.1 Molecular Biology

4.2.1.1 Polymerase Chain Reaction (PCR)

PCRs were performed in 50 µL reactions using iProof™ High-Fidelity PCR Kit according to the manufacturer instructions. The reactions consisted of 1 pg - 10 ng template DNA, 1× iProof high-fidelity PCR master mix, 0.4 µM each forward and reverse primers, and 12% DMSO.

Diagnostic PCRs were performed in a final volume of 25 µL using 1 pg - 10 ng DNA as template, 1× *Taq* buffer, 0.2 mM dNTPs, 0.2 µM each forward and reverse primers, 1.5 mM $MgCl_2$, and 1.25U *Taq* DNA polymerase. Cycling conditions are listed in Table 22.

Table 22 Cycling conditions of polymerase chain reactions (PCRs).

Polymerase Application		iProof high-fidelity Preparation of plasmids		*Taq* DNA polymerase Diagnostic PCR	
		Temperature	**Time**	**Temperature**	**Time**
Initial denaturation		98°C	3 min	95°C	5 min
Denaturation	29x	98°C	30 s	95°C	1 min
Annealing		55°C - 65°C	30 s	60°C	30 s
Extension		72°C	30 s/kb	72°C	90s/kb
Final extension		72°C	5 min	72°C	2 min

4.2.1.2 Agarose Gel Electrophoresis

Depending on the DNA fragment size, DNA samples were separated on agarose gels consisting of 0.5 - 2% agarose (w/v) in 1× TAE buffer and approximately 1 µL/mL EtBr using the PerfectBlue™ gel system. DNA samples were mixed with 1/6 volumes of 6× DNA loading dye and loaded next to a standard marker for size determination. Electrophoresis was performed in 1× TAE buffer at 80 – 120 V for approximately 20 to 50 min. DNA was visualised by UV illumination.

4.2.1.3 Purification of PCR Products

For generation of plasmids, DNA fragments were excised and purified using the NucleoSpin® Gel and PCR clean up Kit following manufacturer's instruction and eluted in 20 µL elution buffer.

4.2.1.4 Enzymatic Digest of DNA

Restriction enzymes and corresponding buffers were purchased from NEB. For generation of plasmids, 3 - 7 µg plasmid DNA or 20 µL of purified PCR product, and for analytical digests 0.5 - 1 µg plasmid DNA were digested with 2 - 10 U restriction enzymes in the recommended buffers. Reactions were incubated for 2 - 4 h or O/N at 37 °C unless indicated otherwise.

4.2.1.5 Ligation

All ligation reactions were performed using the T4 DNA ligase. 50 ng of the digested vector and purified inserts were ligated in a molar ratio of 1:3 to 1:5 (backbone to insert) in a total volume of 10 µL. The ligation reaction consisted of 1 µL ligase and 1× supplied ligase buffer and was incubated O/N in an ice-bath. Typically, 5 µL of the ligation mixture was used to transform *E. coli* DH5α via heat-shock.

4.2.1.6 Generation of Recombinant DNA Constructs

Plasmids for *L. donovani* HSP23 Gene Replacement

Since the original HSP23 replacement constructs (pUC-HSP23-5'neo3' and pUC-HSP23-5'puro3') [1] were found to target the 3' adjacent gene of *HSP23* (*EMP24*), new constructs containing a shorter *HSP23* 3'UTR were generated. The 3'UTR of the original plasmids was replaced by a 779 bp fragment that was amplified by PCR from *L. donovani* 1SR genomic DNA using primers P6 and P7. The original plasmids were digested with *BamH*I and *Hind*III, and the newly generated DNA fragments, cut with the same enzymes, were ligated between those sites yielding pUC-HSP23-5'puro-3'NC_new and pUC-HSP23-5'neo-3'NC_new shown in Figure 28. The correct integration of the DNA fragments was analysed by sequencing using primer pair 32/33.

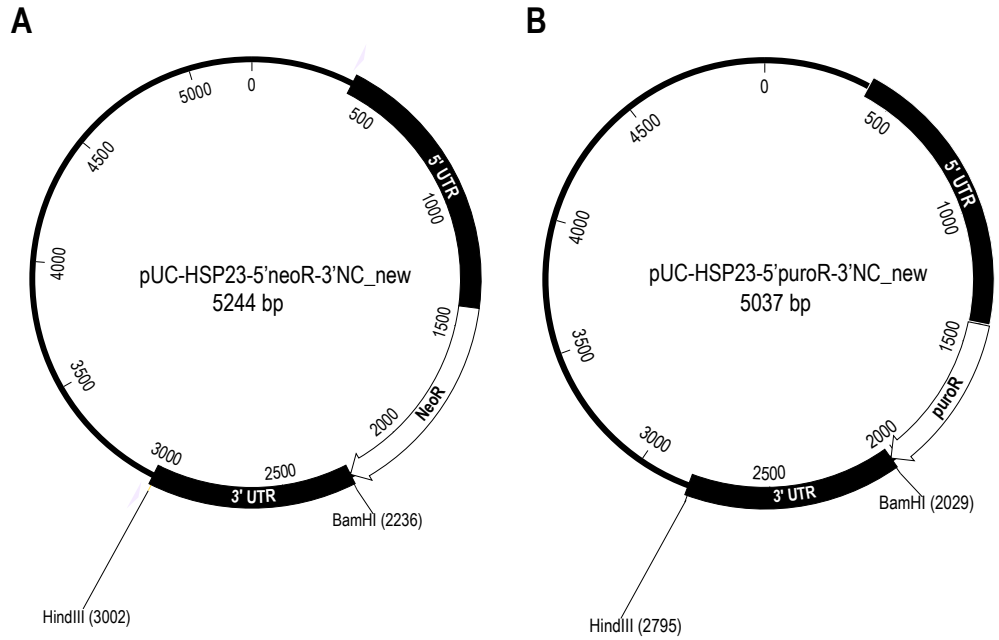

Figure 28 Maps of targeting constructs used for the generation of *L. donovani* HSP23$^{-/-}$ null mutants. The constructs either contain the neomycin (neoR) (A) or puromycin (puroR) resistance gene (B). Nucleotide positions (bp) of restriction sites used for ligation of the respective PCR fragments into the pUC plasmids are shown.

Plasmids for Expression of Transgenes in *Leishmania*

The following transgenes were amplified from species-specific genomic DNA with the indicated primer pairs (Table 10): 1) Putative homologues of *L. donovani HSP23* including *L. braziliensis* (LbrM.20.0220) (P8/P9), *L. major* (LmjF.34.0210) (P10/P11), *L. infantum* (LinJ. 34.0230) (P16/P17), *T. brucei* (Tb927.10.2620)(P12/P13), *T. cruzi* (TcCLB.506407.60) (P14/ P15) and 2) the co-amplified genes on chromosome 35 including LdBPK_351030 (P20/P21), LdBPK_351040 (P22/P23), LdBPK_351050 (P24/P25), LdBPK_351060 (P26/P27), LdBPK_351070 (P28/P29), LdBPK_351080 (P30/P31).

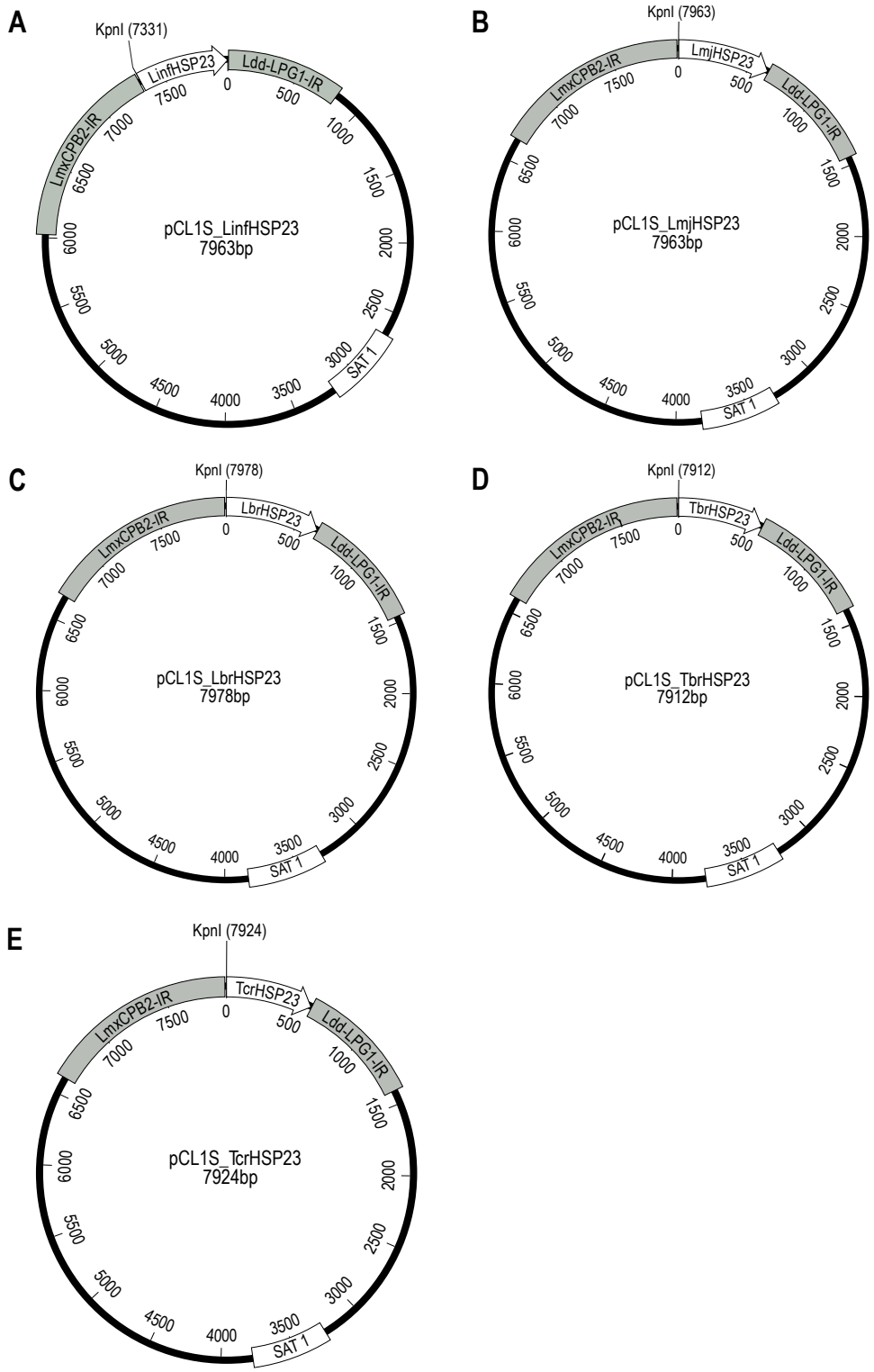

Figure 29 Maps of *Leishmania* expression plasmids harbouring HSP23 transgenes of different *Leishmania* and *Trypanosoma* species. (A) *L. infantum* (B) *L. major* (C) *L. braziliensis* (D) *T. brucei* (E) *T. cruzi* HSP23 transgenes are flanked by the UTR sequences of the *L. mexicana* cysteine protease gene *(LmxCPB2-IR)* and *L. donovani* lipophosphoglycan 1 gene *(Ldd-LPG1-IR).* Robust expression in *Leishmania* is ensured by the nourseothricine (SAT1) resistance marker gene. Nucleotide positions (bp) of restriction sites used for ligation are indicated.

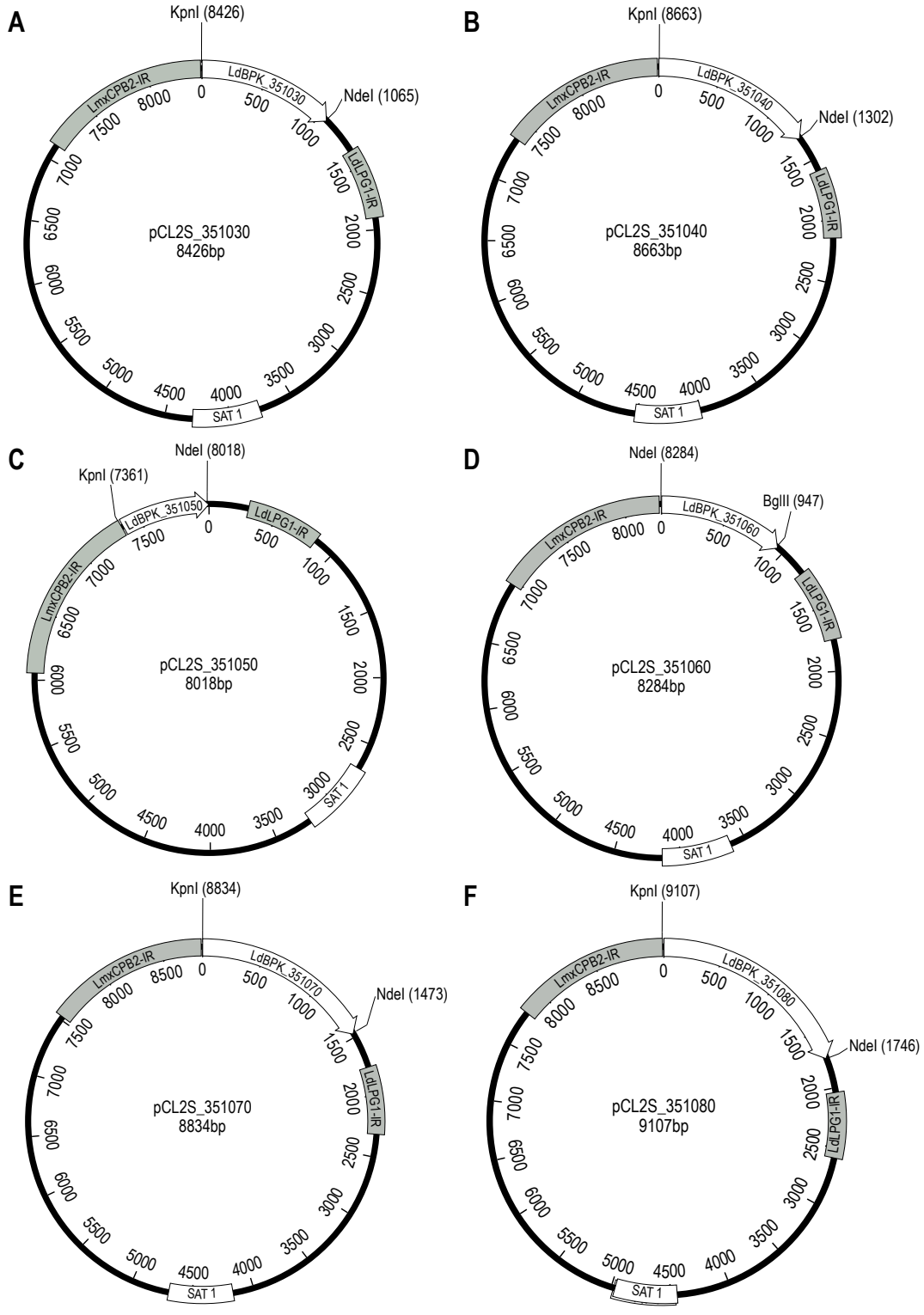

Figure 30 Maps of *Leishmania* expression plasmids used for functional cloning experiments. (A) LdBPK_351030 (B) LdBPK_351040 (C) LdBPK_351050 (D) LdBPK_351060 (E) LdBPK_351070 (F) LdBPK_3510380 are flanked by the UTR sequences of the *L. mexicana* cysteine protease gene *(LmxCPB2-IR)* and *L. donovani* lipophosphoglycan 1 gene *(Ldd-LPG1-IR).* Robust expression in *Leishmania* is ensured by the nourseothricine (SAT1) resistance marker gene. Positions of restriction sites used for ligating the respective PCR fragments into the pCL2S plasmid are indicated.

Purified PCR fragments were subsequently ligated into pCL1S or pCL2S plasmids previously digested with the cognate enzymes. The correct integration of the respective transgenes into the pCL1S or pCL2S plasmid was tested by analytical digest and sequencing using oligonucleotides P34/P35. Maps of all plasmids are shown in Figure 29 and 30.

Protein Expression Plasmids

To create the pJC65 protein expression plasmid, the pJC45 plasmid [137] was modified by introducing a *Kpn*I restriction site into the multiple cloning site. For this, 5 µM oligonucleotides P18 and P19 were annealed in a total volume of 50 µL using 1× NEB2.1 buffer. The reaction was incubated at 95°C for 5 min in a heat block and slowly cooled down to room temperature over 2 to 3 h. 1 µL of the annealed oligonucleotides and 50 ng of the pJC45 plasmid digested with *Nco*I and *Hind*III were ligated for 2 h in a total reaction volume of 10 µL using 1× T4 ligase buffer and 1 µL of the ligase.

For the generation of the CK1.2 protein expression plasmid (pJC65-LdBPK_351030), the open reading frame of *L. donovani* CK1.2 was isolated from the pCL2S_LdBPK_351030 plasmid using *Kpn*I and *BamH*I restriction sites and ligated between the matching sites in pJC65. The correct integration was tested by sequencing using oligonucleotide P36 and P37. Maps of pJC65 and pJC65-LdBPK_351030 are shown in Figure 31.

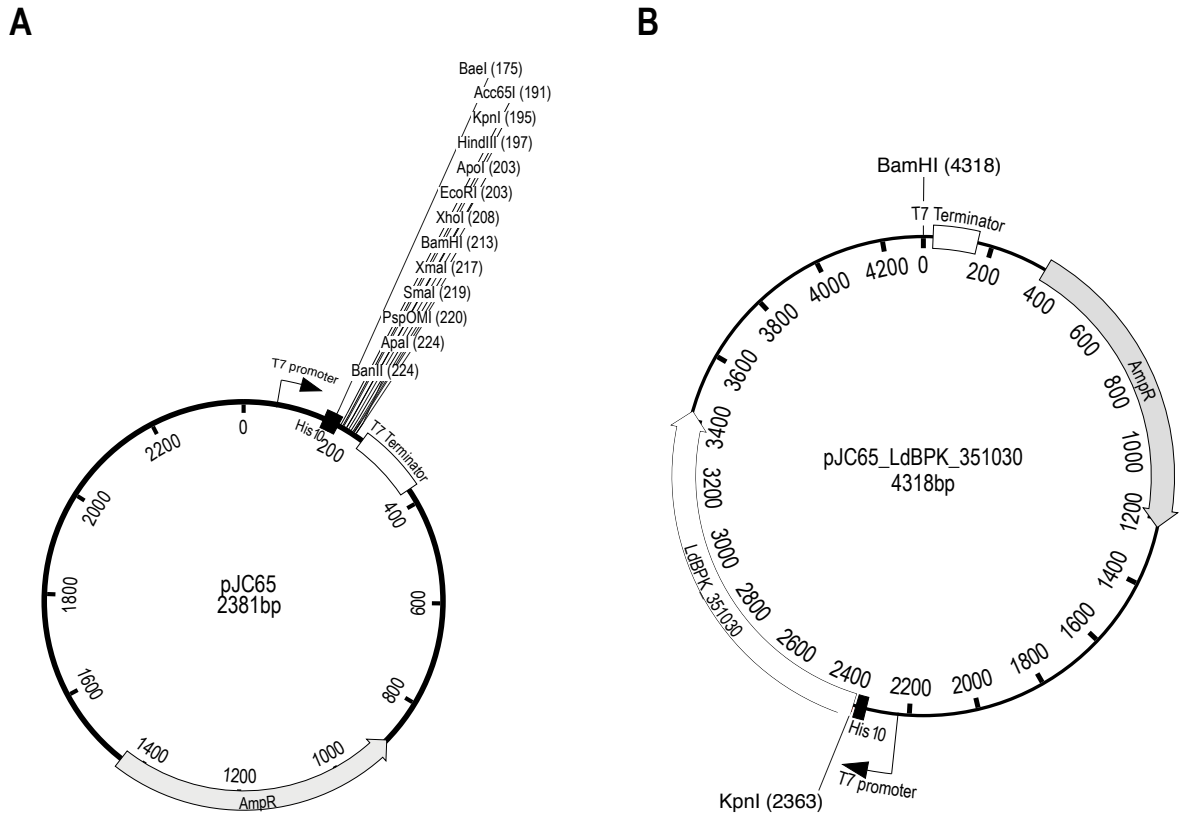

Figure 31 Maps of protein expression plasmids (A) pJC65; the modified multiple cloning site is shown (B) pJC65_LdBPK_351030 used for expression of casein kinase 1.2 in *E. coli* BL21.

4.2.1.7 Transformation of *E. coli*

50 µL of chemocompetent *E. coli* (DH5α or BL21) were thawed on ice and mixed with 5 µL of the ligation reaction or 10 ng plasmid DNA. After incubation on ice for 15 - 30 min, the heat shock was performed for 20 s at 42 °C in a water bath. Cells were placed back on ice for 2 min, resuspended in 950 µL of circle grow medium and allowed to recover for 45 - 60 min at 37°C, shaking. Bacteria were plated on LB agar plates supplemented with the respective antibiotics and incubated O/N at 37 °C. Single colonies were picked for further applications.
50 µL of *E. coli* XL one Blue Electroporation-Competent cells were thawed on ice, mixed with 100 ng of isolated plasmid DNA recovered from *Leishmania* and immediately electroporated in a 0.1 cm Gene Pulser® cuvette applying one pulse with a Biorad MicroPulser™ electroporation device. After addition of 450 µL prewarmed cycle grow medium, the cells were incubated at 37°C for 1 h, shaking. For further applications, transformed bacteria were added to 10 mL cycle grow medium supplemented with ampicillin and grown O/N at 37°C, shaking.

4.2.1.8 Isolation of Plasmid DNA from *E. coli* by Alkaline Lysis

For isolation of plasmid DNA, 2 mL LB medium supplemented with the respective antibiotics were inoculated with an individual colony. Bacteria were grown O/N at 37°C with vigorous shaking at 300 rpm. After centrifugation at 14000 rpm for 2 min (4°C), the supernatant was discarded and the cell pellet was resuspended in 100 µL of ice-cold plasmid preparation buffer 1. Following addition of 200 µL of Plasmid preparation buffer 2, the samples were inverted five times and incubated for 3 min at RT. To stop alkaline lysis, 150 µL of ice-cold plasmid preparation buffer 3 was added to the lysate. The tubes were inverted and incubated for 5 min on ice followed by centrifugation at 14000 rpm for 10 min at RT. Subsequently, the supernatant was transferred to a fresh tube and 1 mL of 96% EtOH was added. After incubation for 5 min at RT, the samples were centrifuged at 14000 rpm for 10 min (RT). The pellet was washed with 70% EtOH and air-dried at RT for approximately 10 min to allow evaporation of the remaining EtOH. The dried DNA pellet was resuspended in 30 µL TE-RNase buffer and incubated for 30 min at 37°C to remove traces of RNA. The final plasmid preparation was stored at 4°C or -20°C.

4.2.1.9 Isolation of High Purity Plasmid DNA from *E. coli*

For isolation of large-scale highly purified plasmid DNA, 200 mL LB-medium containing the appropriate antibiotics were inoculated with a single colony and incubated O/N at 37°C with vigorous shaking at 300 rpm. The bacterial culture was transferred to a 400 mL centrifugation bottle and sedimented at 4000 rpm, 20 min, 4°C. The supernatant was discarded, and the bacterial pellet resuspended in 5 mL of ice-cold plasmid preparation buffer 1. The cell suspension was transferred to a 50mL falcon tube and 10 mL of plasmid preparation buffer 2 were added for lysis. The cell suspension was mixed by repeated gentle inversion and incubated for 5 min at RT on a roller shaker. Alkaline lysis was stopped by addition of 7.5 mL

ice-cold plasmid preparation buffer 3. The lysate was mixed by gentle inversion and subsequently incubated on ice for 10 min. After centrifugation at 8000 rpm for 30 min (4°C), the supernatant was filtrated into a fresh 50mL falcon tube. Following addition of isopropanol at a final concentration of 0.7%, the lysate was mixed, incubated for 20 min at RT and sedimented by centrifugation at 4000 rpm for 20 min (RT). The DNA pellet was washed once with 70% EtOH, let air-dry at RT and resuspended in 4 mL TE-buffer (pH 8.0). After the pellet had completely dissolved, 4.9 g of CsCl and 100 µL of EtBr were added. The sample was vortexed vigorously and transferred to a 5mL QuickSeal tube. Tarred QuickSeal tubes were heat-closed and centrifuged for 8 h, 70000 rpm, 25°C in an Optima XE-90 ultracentrifuge. The plasmid-containing fraction was harvested using a syringe and transferred to a 50mL falcon tube. One Volume of NH_4-acetate saturated isopropanol was added, mixed and the upper phase containing the EtBr and isopropanol was discarded. After a second washing step with 1 Vol. of NH_4-acetate saturated isopropanol, 0.1 Vol. (original volume) of 7.5 M NH_4-acetate, 2 Vol. (latest volume) ddH_2O and 2.5 Vol. (latest volume) 96% EtOH were added. Following incubation for 20 min at RT, the sample was centrifuged for 30 min at 4000 rpm, RT, the supernatant discarded and the pellet air-dry at RT for 15 min. Depending on the pellet size, 100 - 500 µL TE-buffer were added. Plasmid DNA was stored at 4°C or -20°C.

4.2.1.10 Isolation of Genomic DNA from *Leishmania*

Genomic DNA was isolated using the Isolate II Genomic DNA kit. Briefly, 1×10^7 - 1×10^8 parasites were centrifuged at 1250 × g for 10 min at 4°C, washed twice with PBS and resuspended in lysis buffer GL and G3 supplemented with 25 µL Proteinase K. After addition of 210 µL of 100% EtOH, the lysate was transferred to the column and gDNA was isolated according to the manufacturer instructions.

4.2.1.11 Isolation of Plasmid DNA from *Leishmania*

2-4 × 10^9 logarithmic-phase promastigotes, cultivated in T175 cm^2 cell culture flasks, were harvested by centrifugation at 1250 × g for 8 min at 4°C and washed thrice with 1× PBS. Next, plasmid DNA was extracted by alkaline lysis following the protocol described in section 4.2.1.9 and further purified by phenol/chloroform/isoamyl alcohol (25:24:1). For this, 1 Vol. of phenol (Tris-saturated) was added to the extracted plasmid preparation. After gentle mixing by inverting the tube, 1 Vol. chloroform-isoamyl alcohol (24:1) was added. After centrifugation at 3220 × g for 6 min at 20°C, the lower phase was discarded and 1 Vol. chloroform-isoamyl alcohol was added. The tube was inverted and the upper phase was transferred into a new reaction tube. Plasmid DNA was then precipitated by addition of 0.7 Vol. isopropanol followed by centrifugation at 3220 × g for 30 min at RT. The supernatant was discarded and the pellet was dissolved in 400 µL TE-buffer (pH 8.0) for 24 h at 4°C. Plasmid DNA was again precipitated by addition of 0.1 Vol. of 10 M ammonium acetate and 2.5 Vol. 100% EtOH followed by centrifugation. The pellet was dissolved in TE buffer for 24 h. 10 µL (approximately 100 ng) of isolated plasmid DNA was electroporated into *E. coli* XL one Blue

Electroporation-Competent cells as described in section 4.2.1.7. Amplified DNA was isolated using the NucleoBond® PC 20 kit following the manufacturer's instructions and eluted in 20 µL ultrapure ddH_2O.

4.2.1.12 Isolation of RNA

RNA was isolated using the InviTrap® Spin Cell RNA Mini Kit. Briefly, 5 × 10^7 parasites were sedimented (1250 × g, 10 min, 4°C) and washed twice with ice-cold PBS. The supernatant was discarded and *Leishmania* parasites were resuspended in the remaining PBS. 350 µL of lysis solution R was added to the cell suspension that was subsequently transferred to a DNA binding spin filter. RNA was isolated according to the manufacturer instructions and eluted in 40 µL elution buffer R. To remove trace amounts of contaminating DNA, 800 ng of RNA were treated with DNase (gDNA wipe out). Isolated RNA was stored at -80°C.

4.2.1.13 cDNA Synthesis

First strand cDNA synthesis was performed using the QuantiTect® Reverse Transcription Kit with a mixture of random hexamer oligonucleotides and oligo(dT)s. The reaction was performed in a final volume of 20 µL using 14 µL of DNase treated isolated RNA, 5 µL of RT reaction buffer containing the primer mix and 1 µL Reverse Transcriptase. A (-)-RT control without Reverse Transcriptase was included to exclude false-positive results due to gDNA contaminations. The reaction was incubated for 30 min at 42°C followed by 3 min at 95°C. cDNA was directly used for qRT-PCR or stored at -20 °C.

4.2.1.14 Quantitative Real-Time PCR (qRT-PCR)

qRT-PCR was performed on a Rotor Gene real-time PCR cycler (RG 3000) using the Biozym Blue S'Green qPCR Kit. A single reaction consisted of 1 µL cDNA (section 4.2.1.13), 1× qPCR S'Green BlueMix, 0.5 µM forward and reverse primer in a final volume of 20 µL. Actin served as reference gene. The primers used for amplification of the GOI and reference genes are listed in Table 10. Cycling conditions are depicted in Table 23. All reactions were followed by a standard melting curve to test PCR specificity. Data collection and analysis were performed with the Rotor-Gene real-time analysis software 6.1.81.

Table 23 Cycling conditions for quantitative real-time PCR (qRT-PCR)

Polymerase		hot-start DNA polymerase	
		Temperature	**Time**
Initial denaturation		95°C	7 min
Denaturation	34×	95°C	15 s
Annealing		69°C	20 s
Extension		71°C	30 s
Melt analysis		67°C-95°C	Hold 60 s on first step Hold 8 s on next steps

4.2.1.15 DNA Sequencing

Sequencing of DNA samples (e.g. plasmids and PCR products) was carried out by LGC Genomics. Samples for sequencing were prepared with 1 µg of DNA, 2 µL oligonucleotide (10 µM) in a total volume of 14 µL. Analysis of sequences was performed using MacVector, Inc. with Assembler, Version 17.5.4.

4.2.1.16 Next Generation Sequencing

To generate the DNA library, the Nextera® XT library kit and the Nextera® XT index kit were used according to the manufacturer instructions. Briefly, *Leishmania* gDNA was isolated as described previously (section 4.2.1.10) and set to a final concentration of 0.5 ng/µL using the NanoDrop™ and Invitrogen™ Qubit™ 3 Fluorometer for exact measurement of DNA concentrations. One nanogram of gDNA was used in the subsequent transposome-mediated tagmentation step, in which the gDNA is fragmented and adapters ligated to the ends of the DNA fragments. After purification of the DNA library using the Agencourt AMPure XP kit, the size distribution of DNA fragments was determined using a 2100 Bioanalyzer Instrument and the Agilent High Sensitivity DNA Kit. Each sample was further diluted to 4 nM taken into account the average fragment size and sample concentration. A DNA library pool was prepared mixing 5 µL of each diluted sample in an 1.5mL Eppendorf DNA LoBind® tube. To denature the DNA-library, 5 µL of the DNA pool was mixed with 5 µL of freshly prepared 0.2M NaOH. After incubation for 5 min at RT, 990 µL of pre-chilled HT1 buffer was added. The DNA library was further diluted with HT1 buffer to 10 pM in a final volume of 600 µL and supplemented with 6 µL of a denatured PhyX reference library. Prior to loading of the sequencing cartridge, the obtained library was heat-denatured (95°C, 2min) and incubated for 5 min on ice. Sequencing was carried out on a Illumina MiSeq® Next Generation Sequencer.

4.2.2 Protein Biochemistry

4.2.2.1 Preparation of Protein Lysates under Denaturing Conditions

Cells were lysed and prepared for SDS-PAGE according to standard protocols. Briefly, 5 × 10^6 or 1 × 10^7 cells were sedimented at 1000 × g, 8 min, 4°C. The supernatant was discarded and the cells were washed twice with cold 1× PBS. The pellet was resuspended in 10 µL 1× PBS, 9 µL 2× SDS-PAGE sample buffer and 1 µL freshly prepared DTT. The samples were heated to 95°C for 5 min prior to loading onto an SDS-gel.

4.2.2.2 SDS-PAGE

Gel electrophoretic separation of proteins was performed in a discontinuous buffer system according to Laemmli [290]. For this, a 10% - 12.5% separating gel solution was supplemented with freshly prepared APS and TEMED at a final concentration of 0.1% and poured between two glass slides of the electrophoresis chamber. To ensure an even gel surface, the solution was overlaid with isopropanol. After polymerisation and removal of the isopropanol, the 5% stacking gel solution supplemented with APS and TEMED was cast over the top of the separating gel and a comb was inserted into the cassette. The gel was run at 15 V/cm for 1 to 1.5 h in 1× SDS running buffer.

4.2.2.3 Coomassie-brilliant Blue Staining

In-gel visualisation of proteins separated by SDS-PAGE was achieved by staining gels with Coomassie Brilliant Blue R250. Gels were first covered with Coomassie staining solution for 1 h at RT or O/N at 4°C and destained using a destaining solution for 30 min - 2 h at RT. After two washing steps in ddH_2O, gels were scanned for further analysis using an Epson Perfection V700 Photo Scanner and dried between Cellophane® foil for long time storage.

4.2.2.4 Western Blot

5 × 10^6 or 1 × 10^7 cells per lane were loaded onto 10% - 12.5% acrylamide-bisacrylamide gel, ran for 1 h at 100V as described in section 4.2.2.2 and blotted onto a MeOH activated PVDF membrane via semi-dry transfer. For this, a stack consisting of two Whatman® 3MM filter papers, a MeOH activated PVDF membrane, the gel and another two filter papers were soaked in transfer buffer and placed in the described order onto the Trans-Blot SD®. The proteins were transferred onto the membrane by applying 1mA/cm^2 for 1 h.

4.2.2.5 Immunoblot

After blocking in 5% milk/TBST solution (O/N at 4°C or 1 h at RT), the primary antibody (Table 15) was added in blocking solution at the respective concentration and incubated for 1 h at RT. The blot was washed three times for 10 min with washing solution to remove the primary antibody followed by incubation for 1 h at RT with the secondary antibody fused to alkaline phosphatase. After two washing steps and a last one with AP-buffer, blots were

developed using Nitro Blue tetrazolium chloride (NBT) and 5-bromo-4-chloro-3-indolyl phosphate (BCIP). The reaction was stopped by a last wash with ddH_2O. Blots were dried and scanned for further analysis using an Epson Perfection V700 Photo Scanner.

4.2.2.6 Immunofluorescence Assays

1×10^7 *Leishmania* parasites were centrifuged for 5 min at 1500 rpm, washed once with 1× PBS and suspended in 100 µL of 1× PBS. 40 µL aliquots of the cell suspension were applied on a microscopic slide, air-dried and fixed for 3 min in ice-cold MeOH. Cells were gently washed three times and permeabilised for 15 min. After washing, cells were incubated in blocking solution for 1 h at RT. Primary antibodies (Table 15) were added at the respective dilutions in blocking buffer and cells were incubated for 1 h at RT. Cells were washed three times for at least 15 min and then incubated in the dark with the secondary antibodies (Table 15) and DAPI for 1 h. After final washing, stained cells were covered with 20 µL of mounting solution and dried for 24 h at 4°C. Fluorescence microscopy was carried out on an EVOS® FL Auto Cell Imaging System using a 40× objective.

4.2.2.7 Recombinant Protein Expression in *E. coli*

For recombinant protein expression in *E. coli* BL21 (DE3)[pABlaclQ] cells, 1 - 10 ng of the respective plasmids were transformed as described (section 4.2.1.7). A positive colony was picked and added to 400 mL circle grow medium supplemented with 0.2% Glucose, 100 µg/mL ampicillin and 10 µg/mL kanamycin. Cultures were incubated at 37°C, shaking 180 rpm until they reached an OD_{600} of 0.05. Next, protein expression was induced by addition of isopropyl-β-D-thiogalactopyranoside (IPTG) at a final concentration of 0.4 mM for 1 h. One millilitre of the suspension was taken before (-IPTG) and after the induction (+IPTG) and was stored at -70°C for later analysis. Cells were harvested by centrifugation at 5000 rpm, 20 min at 4°C and washed once with ice-cold 1× PBS. Bacterial cells were lysed by ultrasonication (6 × 20 s with 10 s break, on ice) in 20 mL buffer 0. Lysates were centrifuged at 10330 × g for 30 min at 4°C and the supernatant, containing soluble proteins (=E0), was stored at -70°C.

Purification of His-tagged recombinant proteins was performed by Ni^{2+}-chromatography. For this, 2 mL His-Bind Resin (His-beads) were added to a 15mL falcon and sedimented at 200 × g, 4°C for 2 min to remove the storage buffer. The beads were equilibrated with 2 mL of 50 mM $NiSO_4$ solution for 30 min on a roller shaker, sedimented by centrifugation as before and washed once with buffer B5 (30 min, roller shaker). After another centrifugation step, the thawed protein solution (E0) was added to the equilibrated beads and incubated on a roller shaker for 1 h. After centrifugation, the beads were washed once with 10 mL buffer B5 (30 min, roller shaker) and once with 3 mL Buffer B100 (30 min, roller shaker). Proteins were eluted with 2 mL buffer B1000 supplemented with 2 mM EDTA and 10% Glycerol (30 min roller shaker) and were immediately subjected to dialysis.

The expression of recombinant proteins was then analysed by SDS-PAGE. Therefore, an aliquot of the sample E0 was mixed with an equal volume of SDS-PAGE sample buffer (+10% DTT) prior to denaturation at 95°C for 5 min. Samples -IPTG and +IPTG were sedimented at 11300 × g for 5 min, 4°C and washed once with cold 1× PBS. The pellet was suspended in 25 - 100 µL of PBS and prepared for denaturing cell lysis as described.
Recombinant protein samples were separated by SDS-PAGE using the same conditions as described in section 4.2.2.2. The gel was stained with Coomassie blue solution (section 4.2.2.3) for further analysis.

4.2.2.8 *In Vitro* Kinase Assay

To test CK1.2 kinase activity *in vitro*, recombinant proteins were added to 1× kinase buffer supplemented with freshly prepared 0.05 mM ATP, 1 mM DTT and 10 µCi [γ-^{32}P]-ATP in a final volume of 25 µL. Recombinant proteins and substrates were used in the following concentrations: rLdCK1.2: 0.25 µg (6 pmol), rLdHSP23: 1.57 µg (60 pmol), rLdP23: 1.3 µg (60 pmol), myelin basic protein (MBP): 3 µg (162 pmol). CK1.2-specific inhibitor D4476 was used at a concentration of 10 µM in the presence of 0.7% DMSO. Controls were performed with equivalent dilutions of DMSO. After 30 min of incubation at 25°C or 37°C, the reaction was stopped by adding 1 Vol. of 2× SDS-PAGE sample buffer. The samples were incubated for 10 min at 95°C and separated on a 12.5% SDS polyacrylamide gel as described previously (section 4.2.2.2). After Western blot onto a polyvinylidene fluoride (PVDF) membrane (section 4.2.2.4), ^{32}P incorporation was monitored by autoradiography exposing blotted membranes to X-ray films. Exposure times are indicated in the Figure legends.

4.2.3 Cell Biology

4.2.3.1 Cultivation of *Leishmania*

L. donovani strain 1SR and *L. major* strain 5ASKH and its genetically modified derived lines were cultured at 25°C in 10 mL M199$^+$ medium with the respective antibiotics and diluted every three to four days to 1 × 10^5 - 1 × 10^6 cells/mL.

4.2.3.2 Cryopreservation and Thawing of *Leishmania*

For long-term storage, 1 × 10^8 late logarithmic phase (8 × 10^6 cells/mL) promastigotes were sedimented for 10 min at 1000 × g and 4°C. Cells were resuspended in 0.5 mL ice-cold M199$^+$ and 0.5 mL *Leishmania* freezing medium, transferred into a 2 mL cryopreservation tube and cooled down slowly to -70°C in a styrofoam box. One day after, cryovials were transferred to the nitrogen cryogenic tank.
For the thawing of cells, frozen cryovials were removed from the nitrogen tank and rapidly warmed up in a water bath to 37°C. The cell suspension was transferred to a cell culture flask containing 9 mL M199$^+$ supplemented with the required antibiotics. One and two days after, cells were diluted 1/10 and 1/100 to remove traces of DMSO.

4.2.3.3 Determination of *Leishmania* Cell Concentration

Cell concentration of *Leishmania* cultures were determined by automatic cell counting using a CASY® Cell Counter or Multisizer™ 3 Coulter Counter®. For this, 10 µL of cell suspension was added into 10 mL of isotonic buffer.

4.2.3.4 Electroporation of *Leishmania*

Transfection of *Leishmania* parasites was carried out as described previously [291]. In short, 5×10^7 promastigotes from a late-logarithmic phase culture were harvested by centrifugation at 1000 × g for 8 min at 4°C. Parasites were washed twice with ice-cold PBS and once with ice-cold electroporation buffer. After resuspending the cell pellet into 450 µL electroporation buffer, 400 µL of the cell suspension was transferred to a pre-chilled 0.4cm electroporation cuvette already containing either 2 µg linear DNA or 50 µg circular DNA. A mock transfection without DNA was included as control. Parasites were electroporated using a Biorad Gene Pulser™ apparatus applying three pulses at 2.750 V/cm and 25 µF. Following an incubation on ice for 10 min, the cells were transferred into a cell culture flask containing 10 mL $M199^+$ medium supplemented with Pen/Strep and were cultured for 24 h at 25°C. To select for recombinant parasites, antibiotics were added to the culture medium at the respective concentrations. The selection was successful when the mock-transfected population had succumbed to the drug pressure.

4.2.3.5 Gene Editing in *Leishmania* via CRISPR/Cas9

Primer Design

sgRNAs targeting *LmjHSP23* (*LmjF.34.0210*) and primers for the amplification of gene-specific replacement constructs were designed using the LeishGEdit primer design online tool.

5’ and 3’ sgRNA oligonucleotides are composed of a 24-nt sequence encoding the T7 promoter, followed by the 20-nt GOI targeting sequence and a sequence complementary to the 3’-end of the second oligonucleotide, G00, which comprises the sgRNA scaffold.

Upstream forward and downstream reverse primer used for amplification of the replacement constructs consists of 30-nt homology flanks to the 5’UTR or 3’UTR of the GOI, respectively, and a 20-nt sequence corresponding to the primer binding site for amplification of donor DNA from pTBlast and pTPuro plasmids.

Preparation of sgRNA Templates and Replacement Constructs by PCR

sgRNA templates and replacement constructs were PCR-amplified using the iProof™ High-Fidelity PCR Kit essentially as described previously (section 4.2.1.1). sgRNA templates were amplified in a total volume of 20 µL using 1× iProof high-fidelity PCR master mix, 2 µM G00 primer (P5) and 2 µM *LmjHSP23*-specific 5’ sgRNA (P3) or 3’ sgRNA (P4) primer. Cycling conditions were 30 s at 98°C followed by 35 cycles of 10 s at 98°C, 30 s at 55°C, 15 s at 72°C, and a final elongation step of 10 min at 72°C. The replacement constructs were

amplified from 10 ng pTPuro or pTBlast plasmid in 1× iProof mix using 2 µM forward and reverse primers (P1/P2), 3% DMSO in a total volume of 25 µL. PCR steps were 3 min at 98°C followed by 35 cycles of 30 s at 98°C, 30 s at 65°C, 30 s at 72°C, and a final elongation step of 5 min at 72°C. Prior to transfection into Cas9/T7 expressing *Leishmania* cells, PCR products were heat-sterilised at 94°C for 5 min.

Electroporation of sgRNA and Donor DNAs into *Leishmania*

sgRNA templates and replacement constructs were pooled and subsequently transfected following the Amaxa protocol described previously for *Leishmania* spp. [192]. Briefly, 1×10^7 promastigotes grown to mid- to late-logarithmic phase were sedimented by centrifugation at 1250 × g for 10 min at RT, washed once with 1 mL 1× Roditi electroporation buffer. The cells were suspended in 150 µL electroporation buffer and mixed with sgRNA templates and replacement constructs (~100 µL) in a 0.2cm gap Gene Pulser® electroporation cuvette. Electroporation was performed with the Amaxa™ Nucleofector™ IIb device using one pulse with program X-001. A mock transfection control without DNA was included to check the real transfection efficiency. The transfected parasites were immediately transferred into 5 mL complete $M199^+$ medium supplemented with Pen/Strep in 25-cm^2 cell culture flasks. After incubation at 25°C for 24 h, the selection antibiotics were added at the respective concentrations.

4.2.3.6 Limiting Dilution

Clonal parasite populations were obtained by limiting dilution of a culture in 96-well plates with an initial inoculum of 0.5 parasites/well. For this, cell concentration of an exponential logarithmic-phase promastigote culture was determined as described previously (section 4.2.3.3). Afterwards, a serial dilution was conducted from 1×10^7 cells/mL to 2.5 cells/mL in a final volume of 50 mL. 200 µL of these suspensions were aliquoted into 96-well plates. The plates were sealed with parafoil and incubated at 25°C. Clonal populations in single wells were detected by microscopy seven to 14 days after seeding. To ensure the selection of clonal populations, the percentage of positive wells should not exceed more than 50 - 60%. Selected clones were transferred to T25 cm^2 culture flasks for freeze-downs and further investigations.

4.2.3.7 *In vitro* Proliferation Studies

Growth of promastigotes was investigated under different cell culture conditions: (i) at 25°C, pH 7.4 (optimal *Leishmania* promastigote growth conditions *in vitro*); (ii) at 25°C, pH 7.4 in the presence of 2% (v/v) EtOH (chemical induction of protein misfolding stress [292], (iii) at 25°C, pH 7.4 in the presence of 400 nM H_2O_2 (oxidative stress), and (iv) at 34°C or 37°C (heat stress for *L. major* or *L. donovani)*, pH 7.4. Cells were seeded at a density of 1×10^5 cells/mL for conditions (i), (ii), (iii) or 5×10^5 cells/mL for (iv) in a final volume of 10 mL

complete M199^{+} medium in 25-cm^{2} cell culture flasks. Cell density was determined at the indicated days using a CASY® Cellcounter & Analyzer.

4.2.4 *In silico* Procedures

In silico design of plasmids, DNA and protein sequence analysis was performed using the MacVector software version 17.x. Image processing was performed using the ImageJ, Version 2.0.0. Assembling of figures was done using the Intaglio software. The heat map was generated using the Heatmapper Online Tool [293].

4.2.4.1 NGS Data Analysis

Gene annotations and reference genomes (version 42) of *L. donovani* BPK and *L. major* LV39c5 were downloaded from the TriTrypDB server. Reads were aligned to the reference genomes using Bowtie2 [294]. Chromosome ploidy was determined using an in-house program: The coverage of each chromosome was estimated to be 2.0. The mean coverage of the positions in the 15th to 85th quantile and the ratio coverage/mean were calculated. Coverages were then updated according to these fractions and the procedure repeated until conversion. For gene coverages, a similar approach was used, with the difference that the copy number was normalised to the previously calculated chromosome ploidies.

4.2.4.2 Statistical Analysis

Statistical analysis was performed using the software GraphPad Prism 5.0. Experiments were performed in biological duplicates or triplicates on separate occasions, with at least two technical replicates. One way ANOVA (Kruskal-Wallis test) followed by Dunn's test was used to determine statistical difference of more than two groups. The statistical analysis used for each data analysis is indicated in the respective figure legend.

5 References

1. Hombach, A., et al., A small heat shock protein is essential for thermotolerance and intracellular survival of Leishmania donovani. J Cell Sci, 2014. **127**(Pt 21): p. 4762-73.
2. Murray, H.W., et al., Advances in leishmaniasis. Lancet, 2005. **366**(9496): p. 1561-77.
3. Mathers, C.D., M. Ezzati, and A.D. Lopez, Measuring the burden of neglected tropical diseases: the global burden of disease framework. PLoS Negl Trop Dis, 2007. **1**(2): p. e114.
4. Alvar, J., et al., Leishmaniasis worldwide and global estimates of its incidence. PloS One, 2012. **7**(5): p. e35671.
5. WHO, Integrating neglected tropical diseases into global health and development: fourth WHO report on neglected tropical diseases. 2017.
6. Guerin, P.J., et al., Visceral leishmaniasis: current status of control, diagnosis, and treatment, and a proposed research and development agenda. Lancet Infect Dis, 2002. **2**(8): p. 494-501.
7. Sundar, S. and M. Rai, Treatment of visceral leishmaniasis. Expert Opin Pharmacother, 2005. **6**(16): p. 2821-9.
8. Berman, J., Visceral leishmaniasis in the New World & Africa. Indian J Med Res, 2006. **123**(3): p. 289-94.
9. Patz, J.A., et al., Effects of environmental change on emerging parasitic diseases. Int J Parasitol, 2000. **30**(12-13): p. 1395-405.
10. Sutherst, R.W., Global change and human vulnerability to vector-borne diseases. Clin Microbiol Rev, 2004. **17**(1): p. 136-73.
11. Burza, S., S.L. Croft, and M. Boelaert, *Leishmaniasis.* Lancet, 2018. **392**(10151): p. 951-970.
12. Callahan, H.L., et al., Leishmania spp: temperature sensitivity of promastigotes in vitro as a model for tropism in vivo. Exp Parasitol, 1996. **84**(3): p. 400-9.
13. Reithinger, R., et al., *Cutaneous leishmaniasis.* Lancet Infect Dis, 2007. **7**(9): p. 581-96.
14. Berman, J.D. and F.A. Neva, Effect of temperature on multiplication of Leishmania amastigotes within human monocyte-derived macrophages in vitro. Am J Trop Med Hyg, 1981. **30**(2): p. 318-21.
15. Werneck, G.L., et al., Prognostic factors for death from visceral leishmaniasis in Teresina, Brazil. Infection, 2003. **31**(3): p. 174-7.
16. Alvar, J., et al., The relationship between leishmaniasis and AIDS: the second 10 years. Clin Microbiol Rev, 2008. **21**(2): p. 334-59, table of contents.
17. Sampaio, M.J., et al., Risk factors for death in children with visceral leishmaniasis. PLoS Negl Trop Dis, 2010. **4**(11): p. e877.
18. Coura-Vital, W., et al., Prognostic factors and scoring system for death from visceral leishmaniasis: an historical cohort study in Brazil. PLoS Negl Trop Dis, 2014. **8**(12): p. e3374.

19. Druzian, A.F., et al., Risk Factors for Death from Visceral Leishmaniasis in an Urban Area of Brazil. PLoS Negl Trop Dis, 2015. **9**(8): p. e0003982.
20. Le Rutte, E.A., E.E. Zijlstra, and S.J. de Vlas, Post-Kala-Azar Dermal Leishmaniasis as a Reservoir for Visceral Leishmaniasis Transmission. Trends Parasitol, 2019. **35**(8): p. 590-592.
21. Mondal, D., et al., Quantifying the Infectiousness of Post-Kala-Azar Dermal Leishmaniasis Toward Sand Flies. Clin Infect Dis, 2019. **69**(2): p. 251-258.
22. Akhoundi, M., et al., A Historical Overview of the Classification, Evolution, and Dispersion of Leishmania Parasites and Sandflies. PLoS Negl Trop Dis, 2016. **10**(3): p. e0004349.
23. Quinnell, R.J. and O. Courtenay, Transmission, reservoir hosts and control of zoonotic visceral leishmaniasis. Parasitology, 2009. **136**(14): p. 1915-34.
24. Killick-Kendrick, R., The biology and control of phlebotomine sand flies. Clin Dermatol, 1999. **17**(3): p. 279-89.
25. Samy, A.M., L.P. Campbell, and A.T. Peterson, Leishmaniasis transmission: distribution and coarse-resolution ecology of two vectors and two parasites in Egypt. Rev Soc Bras Med Trop, 2014. **47**(1): p. 57-62.
26. Cunze, S., et al., Leishmaniasis in Eurasia and Africa: geographical distribution of vector species and pathogens. R Soc Open Sci, 2019. **6**(5): p. 190334.
27. Killick-Kendrick, R., The life-cycle of Leishmania in the sandfly with special reference to the form infective to the vertebrate host. Ann Parasitol Hum Comp, 1990. **65**(Suppl 1): p. 37-42.
28. Bogdan, C. and M. Rollinghoff, How do protozoan parasites survive inside macrophages? Parasitol Today, 1999. **15**(1): p. 22-8.
29. Peters, N.C., et al., In vivo imaging reveals an essential role for neutrophils in leishmaniasis transmitted by sand flies. Science, 2008. **321**(5891): p. 970-4.
30. Kautz-Neu, K., et al., Langerhans cells are negative regulators of the anti-Leishmania response. J Exp Med, 2011. **208**(5): p. 885-91.
31. Zilberstein, D. and M. Shapira, The role of pH and temperature in the development of Leishmania parasites. Annu. Rev. Microbiol., 1994. **48**: p. 449-470.
32. Sacks, D.L. and P.V. Perkins, Development of infective stage Leishmania promastigotes within phlebotomine sand flies. Am J Trop Med Hyg, 1985. **34**(3): p. 456-9.
33. Sunter, J. and K. Gull, Shape, form, function and Leishmania pathogenicity: from textbook descriptions to biological understanding. Open Biol, 2017. **7**(9).
34. Schlein, Y., Jacobsen, R.L., and Messer, G., Leishmaniainfections damage the feeding mechanism of the sandfly vector and implement parsite transmission by bite. Proc. Natl. Acad. Sci. USA, 1992. **89**: p. 9944-9948.
35. Volf, P., et al., Blocked stomodeal valve of the insect vector: similar mechanism of transmission in two trypanosomatid models. Int J Parasitol, 2004. **34**(11): p. 1221-7.

36. Serafim, T.D., et al., Sequential blood meals promote Leishmania replication and reverse metacyclogenesis augmenting vector infectivity. Nat Microbiol, 2018. **3**(5): p. 548-555.
37. Serafim, T.D., E. Iniguez, and F. Oliveira, *Leishmania infantum.* Trends Parasitol, 2020. **36**(1): p. 80-81.
38. Wyllie, S., M.L. Cunningham, and A.H. Fairlamb, Dual action of antimonial drugs on thiol redox metabolism in the human pathogen Leishmania donovani. J Biol Chem, 2004. **279**(38): p. 39925-32.
39. Haldar, A.K., P. Sen, and S. Roy, Use of antimony in the treatment of leishmaniasis: current status and future directions. Mol Biol Int, 2011. **2011**: p. 571242.
40. Sundar, S., Drug resistance in Indian visceral leishmaniasis. Trop Med Int Health, 2001. **6**(11): p. 849-54.
41. Jha, T.K., Evaluation of diamidine compound (pentamidine isethionate) in the treatment resistant cases of kala-azar occurring in North Bihar, India. Trans R Soc Trop Med Hyg, 1983. **77**(2): p. 167-70.
42. Saha, A.K., T. Mukherjee, and A. Bhaduri, Mechanism of action of amphotericin B on Leishmania donovani promastigotes. Mol Biochem Parasitol, 1986. **19**(3): p. 195-200.
43. Davidson, R.N., et al., Short-course treatment of visceral leishmaniasis with liposomal amphotericin B (AmBisome). Clin Infect Dis, 1996. **22**(6): p. 938-43.
44. Croft, S.L. and V. Yardley, *Chemotherapy of leishmaniasis.* Curr Pharm Des, 2002. **8**(4): p. 319-42.
45. Bhargava, P. and R. Singh, Developments in diagnosis and antileishmanial drugs. Interdiscip Perspect Infect Dis, 2012. **2012**: p. 626838.
46. Mondal, D., et al., Efficacy and safety of single-dose liposomal amphotericin B for visceral leishmaniasis in a rural public hospital in Bangladesh: a feasibility study. Lancet Glob Health, 2014. **2**(1): p. e51-7.
47. Sundar, S., et al., Single-dose indigenous liposomal amphotericin B in the treatment of Indian visceral leishmaniasis: a phase 2 study. Am J Trop Med Hyg, 2015. **92**(3): p. 513-7.
48. Sundar, S., et al., Effectiveness of Single-Dose Liposomal Amphotericin B in Visceral Leishmaniasis in Bihar. Am J Trop Med Hyg, 2019. **101**(4): p. 795-798.
49. Sundar, S., et al., Short-course of oral miltefosine for treatment of visceral leishmaniasis. Clin Infect Dis, 2000. **31**(4): p. 1110-3.
50. Paris, C., et al., Miltefosine induces apoptosis-like death in Leishmania donovani promastigotes. Antimicrob Agents Chemother, 2004. **48**(3): p. 852-9.
51. Rakotomanga, M., M. Saint-Pierre-Chazalet, and P.M. Loiseau, Alteration of fatty acid and sterol metabolism in miltefosine-resistant Leishmania donovani promastigotes and consequences for drug-membrane interactions. Antimicrob Agents Chemother, 2005. **49**(7): p. 2677-86.
52. Rakotomanga, M., et al., Miltefosine affects lipid metabolism in Leishmania donovani promastigotes. Antimicrob Agents Chemother, 2007. **51**(4): p. 1425-30.

53. Bryceson, A., A policy for leishmaniasis with respect to the prevention and control of drug resistance. Trop Med Int Health, 2001. **6**(11): p. 928-34.
54. Perez-Victoria, F.J., et al., Mechanisms of experimental resistance of Leishmania to miltefosine: Implications for clinical use. Drug Resist Updat, 2006. **9**(1-2): p. 26-39.
55. Dorlo, T.P., et al., Failure of miltefosine in visceral leishmaniasis is associated with low drug exposure. J Infect Dis, 2014. **210**(1): p. 146-53.
56. Liu, L.X. and P.F. Weller, *Antiparasitic drugs.* N Engl J Med, 1996. **334**(18): p. 1178-84.
57. Wiwanitkit, V., Interest in paromomycin for the treatment of visceral leishmaniasis (kala-azar). Ther Clin Risk Manag, 2012. **8**: p. 323-8.
58. Sundar, S. and J. Chakravarty, Paromomycin in the treatment of leishmaniasis. Expert Opin Investig Drugs, 2008. **17**(5): p. 787-94.
59. Sundar, S., et al., Short-course paromomycin treatment of visceral leishmaniasis in India: 14-day vs 21-day treatment. Clin Infect Dis, 2009. **49**(6): p. 914-8.
60. Eustice, D.C. and J.M. Wilhelm, Mechanisms of action of aminoglycoside antibiotics in eucaryotic protein synthesis. Antimicrob Agents Chemother, 1984. **26**(1): p. 53-60.
61. Fourmy, D., S. Yoshizawa, and J.D. Puglisi, Paromomycin binding induces a local conformational change in the A-site of 16 S rRNA. J Mol Biol, 1998. **277**(2): p. 333-45.
62. Bhattacharjee, A., et al., Co-administration of glycyrrhizic acid with the antileishmanial drug sodium antimony gluconate (SAG) cures SAG-resistant visceral leishmaniasis. Int J Antimicrob Agents, 2015. **45**(3): p. 268-77.
63. Hendrickx, S., et al., Combined treatment of miltefosine and paromomycin delays the onset of experimental drug resistance in Leishmania infantum. PLoS Negl Trop Dis, 2017. **11**(5): p. e0005620.
64. Diro, E., et al., A randomized trial of AmBisome monotherapy and AmBisome and miltefosine combination to treat visceral leishmaniasis in HIV co-infected patients in Ethiopia. PLoS Negl Trop Dis, 2019. **13**(1): p. e0006988.
65. Blum, J.A. and C.F. Hatz, Treatment of cutaneous leishmaniasis in travelers 2009. J Travel Med, 2009. **16**(2): p. 123-31.
66. van Griensven, J., et al., Combination therapy for visceral leishmaniasis. Lancet Infect Dis, 2010. **10**(3): p. 184-94.
67. Downing, T., et al., Whole genome sequencing of multiple Leishmania donovani clinical isolates provides insights into population structure and mechanisms of drug resistance. Genome research, 2011. **21**(12): p. 2143-56.
68. Leprohon, P., et al., Drug resistance analysis by next generation sequencing in Leishmania. Int J Parasitol Drugs Drug Resist, 2015. **5**(1): p. 26-35.
69. Ivens, A.C., et al., The genome of the kinetoplastid parasite, Leishmania major. Science, 2005. **309**(5733): p. 436-42.

70. Britto, C., et al., Conserved linkage groups associated with large-scale chromosomal rearrangements between Old World and New World Leishmania genomes. Gene, 1998. **222**(1): p. 107-17.
71. Wincker, P., et al., The Leishmania genome comprises 36 chromosomes conserved across widely divergent human pathogenic species. Nucleic Acids Res, 1996. **24**(9): p. 1688-94.
72. Clayton, C.E., Life without transcriptional control? From fly to man and back again. Embo J, 2002. **21**(8): p. 1881-8.
73. Myler, P.J., et al., Leishmania major Friedlin chromosome 1 has an unusual distribution of protein-coding genes. Proc Natl Acad Sci U S A, 1999. **96**(6): p. 2902-6.
74. Myler, P.J., et al., Genomic organization and gene function in Leishmania. Biochem Soc Trans, 2000. **28**(5): p. 527-31.
75. LeBowitz, J.H., et al., Coupling of poly(A) site selection and trans-splicing in Leishmania. Genes Dev, 1993. **7**(6): p. 996-1007.
76. Clayton, C. and M. Shapira, Post-transcriptional regulation of gene expression in trypanosomes and leishmanias. Mol Biochem Parasitol, 2007. **156**(2): p. 93-101.
77. Leifso, K., et al., Genomic and proteomic expression analysis of Leishmania promastigote and amastigote life stages: the Leishmania genome is constitutively expressed. Mol Biochem Parasitol, 2007. **152**(1): p. 35-46.
78. Saxena, A., et al., Analysis of the Leishmania donovani transcriptome reveals an ordered progression of transient and permanent changes in gene expression during differentiation. Mol Biochem Parasitol, 2007. **152**(1): p. 53-65.
79. Lahav, T., et al., *Multiple levels of gene regulation mediate differentiation of the intracellular pathogen Leishmania.* FASEB journal : official publication of the Federation of American Societies for Experimental Biology, 2011. **25**(2): p. 515-25.
80. Alcolea, P.J., et al., Stage-specific differential gene expression in Leishmania infantum: from the foregut of Phlebotomus perniciosus to the human phagocyte. BMC Genomics, 2014. **15**(1): p. 849.
81. Clayton, C., Regulation of gene expression in trypanosomatids: living with polycistronic transcription. Open Biol, 2019. **9**(6): p. 190072.
82. Iantorno, S.A., et al., Gene Expression in Leishmania Is Regulated Predominantly by Gene Dosage. mBio, 2017. **8**(5).
83. Beverley, S.M., Gene amplification in Leishmania. Annu Rev Microbiol, 1991. **45**: p. 417-44.
84. Haimeur, A. and M. Ouellette, Gene amplification in Leishmania tarentolae selected for resistance to sodium stibogluconate. Antimicrob Agents Chemother, 1998. **42**(7): p. 1689-94.
85. Ubeda, J.M., et al., Genome-wide stochastic adaptive DNA amplification at direct and inverted DNA repeats in the parasiteLeishmania. PLoS Biol, 2014. **12**(5): p. e1001868.

86. Sterkers, Y., et al., Parasexuality and mosaic aneuploidy in Leishmania: alternative genetics. Trends Parasitol, 2014. **30**(9): p. 429-35.
87. Dumetz, F., et al., Modulation of Aneuploidy in Leishmania donovani during Adaptation to Different In Vitro and In Vivo Environments and Its Impact on Gene Expression. MBio, 2017. **8**(3).
88. Grondin, K., B. Papadopoulou, and M. Ouellette, Homologous recombination between direct repeat sequences yields P-glycoprotein containing amplicons in arsenite resistant Leishmania. Nucleic Acids Res, 1993. **21**(8): p. 1895-901.
89. Navarro, M., et al., Inverted repeat structure and homologous sequences in the LD1 amplicons of Leishmania spp. Mol Biochem Parasitol, 1994. **68**(1): p. 69-80.
90. Bringaud, F., et al., Members of a large retroposon family are determinants of post-transcriptional gene expression in Leishmania. PLoS Pathog, 2007. **3**(9): p. 1291-307.
91. Smith, M., F. Bringaud, and B. Papadopoulou, Organization and evolution of two SIDER retroposon subfamilies and their impact on the Leishmania genome. BMC Genomics, 2009. **10**: p. 240.
92. Rogers, M.B., et al., Chromosome and gene copy number variation allow major structural change between species and strains ofLeishmania. Genome research, 2011. **21**(12): p. 2129-42.
93. Lindquist, S. and E.A. Craig, *The heat-shock proteins.* Annual review of genetics, 1988. **22**: p. 631-77.
94. Li, Y., X. Gao, and L. Chen, GroEL Recognizes an Amphipathic Helix and Binds to the Hydrophobic Side. J Biol Chem, 2009. **284**(7): p. 4324-31.
95. Saio, T., et al., Structural basis for protein antiaggregation activity of the trigger factor chaperone. Science, 2014. **344**(6184): p. 1250494.
96. Clerico, E.M., et al., How hsp70 molecular machines interact with their substrates to mediate diverse physiological functions. J Mol Biol, 2015. **427**(7): p. 1575-88.
97. Kelly, J.W., Amyloid fibril formation and protein misassembly: a structural quest for insights into amyloid and prion diseases. Structure, 1997. **5**(5): p. 595-600.
98. Winkler, J., et al., Chaperone networks in protein disaggregation and prion propagation. J Struct Biol, 2012. **179**(2): p. 152-60.
99. Brehme, M., et al., A chaperome subnetwork safeguards proteostasis in aging and neurodegenerative disease. Cell Rep, 2014. **9**(3): p. 1135-50.
100. Lackie, R.E., et al., The Hsp70/Hsp90 Chaperone Machinery in Neurodegenerative Diseases. Front Neurosci, 2017. **11**: p. 254.
101. Johnson, J.L., Evolution and function of diverse Hsp90 homologs and cochaperone proteins. Biochim Biophys Acta, 2012. **1823**(3): p. 607-13.
102. Perez-Morales, D. and B. Espinoza, The role of small heat shock proteins in parasites. Cell Stress Chaperones, 2015. **20**(5): p. 767-80.
103. Maresca, B. and L. Carratù, The biology of the heat shock response in parasites. Parasitol Today, 1992. **8**(8): p. 260-6.

104. Clos, J., S. Brandau, and C. and Hoyer, Chemical stress does not induce heat shock protein synthesis inLeishmania donovani. Protist, 1998. **149**(2): p. 167-172.

105. Folgueira, C. and J.M. Requena, A postgenomic view of the heat shock proteins in kinetoplastids. FEMS microbiology reviews, 2007. **31**(4): p. 359-77.

106. Requena, J.M., A.M. Montalvo, and J. Fraga, Molecular Chaperones of Leishmania: Central Players in Many Stress-Related and -Unrelated Physiological Processes. BioMed Research International, 2015. **2015**: p. 301326.

107. Hanson, P.I. and S.W. Whiteheart, *AAA+ proteins: have engine, will work.* Nat Rev Mol Cell Biol, 2005. **6**(7): p. 519-29.

108. Barends, T.R., N.D. Werbeck, and J. Reinstein, *Disaggregases in 4 dimensions.* Curr Opin Struct Biol, 2010. **20**(1): p. 46-53.

109. Clos, J., et al., *LeishmaniaHsp100*, in *Guidebook to molecular chaperones and protein folding catalysts*, M.-J. Gething, Editor. 1997, Sambrook and Tooze: Oxford. p. 259-261.

110. Hübel, A., et al., Leishmania major Hsp100 is required chiefly in the mammalian stage of the parasite. Mol Cell Biol, 1997. **17**(10): p. 5987-95.

111. Krobitsch, S., et al., Leishmania donovaniheat shock protein 100: characterization and function in amastigote stage differentiation. J. Biol. Chem., 1998. **273**: p. 6488-6494.

112. Sanchez, Y. and S.L. Lindquist, HSP104 required for induced thermotolerance. Science, 1990. **248**(4959): p. 1112-5.

113. Mishra, R.C. and A. Grover, ClpB/Hsp100 proteins and heat stress tolerance in plants. Crit Rev Biotechnol, 2016. **36**(5): p. 862-74.

114. Silverman, J.M., et al., Proteomic analysis of the secretome of Leishmania donovani. Genome Biol, 2008. **9**(2): p. R35.

115. Silverman, J.M., et al., An exosome-based secretion pathway is responsible for protein export from Leishmania and communication with macrophages. J Cell Sci, 2010. **123**(Pt 6): p. 842-52.

116. Yau, W.L., et al., Phenotypic Characterization of a Leishmania donovani Cyclophilin 40 Null Mutant. J Eukaryot Microbiol, 2016. **63**(6): p. 823-833.

117. Richter, K. and J. Buchner, Hsp90: chaperoning signal transduction. J Cell Physiol, 2001. **188**(3): p. 281-90.

118. Picard, D., Heat-shock protein 90, a chaperone for folding and regulation. Cellular and molecular life sciences : CMLS, 2002. **59**(10): p. 1640-8.

119. Pratt, W.B. and D.O. Toft, Regulation of signaling protein function and trafficking by the hsp90/hsp70-based chaperone machinery. Exp Biol Med (Maywood), 2003. **228**(2): p. 111-33.

120. Dittmar, K.D., et al., The role of DnaJ-like proteins in glucocorticoid receptor.hsp90 heterocomplex assembly by the reconstituted hsp90.p60.hsp70 foldosome complex. J Biol Chem, 1998. **273**(13): p. 7358-66.

121. Larreta, R., et al., Leishmania infantum: gene cloning of the GRP94 homologue, its expression as recombinant protein, and analysis of antigenicity. Exp Parasitol, 2000. **96**(2): p. 108-15.

122. Larreta, R., et al., Antigenic properties of the Leishmania infantum GRP94 and mapping of linear B-cell epitopes. Immunol Lett, 2002. **80**(3): p. 199-205.

123. Whitesell, L., et al., Inhibition of heat shock protein HSP90-pp60v-src heteroprotein complex formation by benzoquinone ansamycins: essential role for stress proteins in oncogenic transformation. Proc Natl Acad Sci U S A, 1994. **91**(18): p. 8324-8.

124. Schulte, T.W., et al., Interaction of radicicol with members of the heat shock protein 90 family of molecular chaperones. Mol Endocrinol, 1999. **13**(9): p. 1435-48.

125. Wiesgigl, M. and J. Clos, Heat Shock Protein 90 Homeostasis Controls Stage Differentiation inLeishmania donovani. Mol Biol Cell, 2001. **12**(11): p. 3307-16.

126. Hombach, A., et al., The Hsp90-Sti1 Interaction is Critical forLeishmania donovaniProliferation in Both Life Cycle Stages. Cell Microbiol, 2013. **15**(4): p. 585-600.

127. Bifeld, E., et al., Ribosome Profiling Reveals HSP90 Inhibitor Effects on Stage-Specific Protein Synthesis in Leishmania donovani. mSystems, 2018. **3**(6).

128. Ommen, G., M. Chrobak, and J. Clos, The co-chaperone SGT ofLeishmania donovaniis essential for the parasite's viability. Cell Stress and Chaperones, 2010. **39**(5): p. **541-546**.

129. Gupta, R.S., G.B. Golding, and B. Singh, HSP70 phylogeny and the relationship between archaebacteria, eubacteria, and eukaryotes. J Mol Evol, 1994. **39**(5): p. 537-40.

130. Flynn, G.C., et al., Peptide-binding specificity of the molecular chaperone BiP. Nature, 1991. **353**(6346): p. 726-30.

131. Rudiger, S., A. Buchberger, and B. Bukau, Interaction of Hsp70 chaperones with substrates. Nat Struct Biol, 1997. **4**(5): p. 342-9.

132. Bukau, B. and A.L. Horwich, The Hsp70 and Hsp60 chaperone machines. Cell, 1998. **92**(3): p. 351-66.

133. Brandau, S., A. Dresel, and J. Clos, High constitutive levels of heat-shock proteins in human-pathogenic parasites of the genus Leishmania. Biochem J, 1995. **310**(Pt 1): p. 225-32.

134. Miller, M.A., et al., Inducible resistance to oxidant stress in the protozoan Leishmania chagasi. J Biol Chem, 2000. **275**(43): p. 33883-9.

135. Xu, Z. and P.B. Sigler, GroEL/GroES: structure and function of a two-stroke folding machine. J Struct Biol, 1998. **124**(2-3): p. 129-41.

136. Sullivan, M.A., et al., Expression and localization of Trypanosoma cruzi hsp60. Mol Biochem Parasitol, 1994. **68**(2): p. 197-208.

137. Schlüter, A., et al., Expression and Subcellular Localization of Cpn60 Protein Family Members inLeishmania donovani. Biochim. Biophys. Acta, 2000. **1491**: p. 65-74.

138. Silverman, J.M., et al., Leishmania exosomes modulate innate and adaptive immune responses through effects on monocytes and dendritic cells. J Immunol, 2010. **185**(9): p. 5011-22.
139. Ito, H., et al., Regulation of the levels of small heat-shock proteins during differentiation of C2C12 cells. Exp Cell Res, 2001. **266**(2): p. 213-21.
140. Van Montfort, R., C. Slingsby, and E. Vierling, Structure and function of the small heat shock protein/alpha-crystallin family of molecular chaperones. Adv Protein Chem, 2001. **59**: p. 105-56.
141. Haslbeck, M., et al., Some like it hot: the structure and function of small heat-shock proteins. Nat Struct Mol Biol, 2005. **12**(10): p. 842-6.
142. Kamradt, M.C., et al., The small heat shock protein alpha B-crystallin is a novel inhibitor of TRAIL-induced apoptosis that suppresses the activation of caspase-3. J Biol Chem, 2005. **280**(12): p. 11059-66.
143. Sun, Y. and T.H. MacRae, The small heat shock proteins and their role in human disease. Febs j, 2005. **272**(11): p. 2613-27.
144. Haslbeck, M. and E. Vierling, A first line of stress defense: small heat shock proteins and their function in protein homeostasis. J Mol Biol, 2015. **427**(7): p. 1537-48.
145. Treweek, T.M., et al., Small heat-shock proteins: important players in regulating cellular proteostasis. Cell Mol Life Sci, 2015. **72**(3): p. 429-451.
146. Horwitz, J., Alpha-crystallin can function as a molecular chaperone. Proc Natl Acad Sci U S A, 1992. **89**(21): p. 10449-53.
147. Collier, M.P. and J.L.P. Benesch, Small heat-shock proteins and their role in mechanical stress. Cell Stress Chaperones, 2020. **25**(4): p. 601-613.
148. Kim, K.K., R. Kim, and S.H. Kim, Crystal structure of a small heat-shock protein. Nature, 1998. **394**(6693): p. 595-9.
149. van Montfort, R.L., et al., Crystal structure and assembly of a eukaryotic small heat shock protein. Nat Struct Biol, 2001. **8**(12): p. 1025-30.
150. Candido, E.P., The small heat shock proteins of the nematode Caenorhabditis elegans: structure, regulation and biology. Prog Mol Subcell Biol, 2002. **28**: p. 61-78.
151. McDonald, E.T., et al., Sequence, structure, and dynamic determinants of Hsp27 (HspB1) equilibrium dissociation are encoded by the N-terminal domain. Biochemistry, 2012. **51**(6): p. 1257-68.
152. Lee, G.J., et al., A small heat shock protein stably binds heat-denatured model substrates and can maintain a substrate in a folding-competent state. Embo j, 1997. **16**(3): p. 659-71.
153. Veinger, L., et al., The small heat-shock protein IbpB from Escherichia coli stabilizes stress-denatured proteins for subsequent refolding by a multichaperone network. J Biol Chem, 1998. **273**(18): p. 11032-7.

154. Ungelenk, S., et al., Small heat shock proteins sequester misfolding proteins in near-native conformation for cellular protection and efficient refolding. Nat Commun, 2016. **7**: p. 13673.

155. Li, Z.W., et al., The small heat shock protein (sHSP) genes in the silkworm, Bombyx mori, and comparative analysis with other insect sHSP genes. BMC Evol Biol, 2009. **9**: p. 215.

156. Costa-Martins, A.G., et al., Genome-wide identification of evolutionarily conserved Small Heat-Shock and eight other proteins bearing α-crystallin domain-like in kinetoplastid protists. PLoS One, 2018. **13**(10): p. e0206012.

157. Montalvo-Alvarez, A.M., et al., The Leishmania HSP20 is antigenic during natural infections, but, as DNA vaccine, it does not protect BALB/c mice against experimental L. amazonensis infection. J Biomed Biotechnol, 2008. **2008**: p. 695432.

158. Schäfer, C., et al., ARM58 Overexpression Reduces Intracellular Antimony Concentration in Leishmania infantum. Antimicrob Agents Chemother, 2014. **58**: p. 1565–1574.

159. Tejera Nevado, P., et al., A Telomeric Cluster of Antimony Resistance Genes on Chromosome 34 of Leishmania infantum. Antimicrob Agents Chemother, 2016. **60**(9): p. 5262-75.

160. Batista, F.A., et al., Identification of two p23 co-chaperone isoforms in Leishmania braziliensis exhibiting similar structures and Hsp90 interaction properties despite divergent stabilities. FEBS J, 2015. **282**(2): p. 388-406.

161. Obermann, W.M., et al., In vivo function of Hsp90 is dependent on ATP binding and ATP hydrolysis. J Cell Biol, 1998. **143**(4): p. 901-10.

162. Panaretou, B., et al., ATP binding and hydrolysis are essential to the function of the Hsp90 molecular chaperone in vivo. Embo J, 1998. **17**(16): p. 4829-36.

163. Hombach, A., et al., Leishmania donovaniP23 protects parasites against HSP90 inhibitor-mediated growth arrest. Cell Stress Chaperones, 2015. **20**(4): p. 673-85.

164. Tsigankov, P., et al., Regulation dynamics of Leishmania differentiation: deconvoluting signals and identifying phosphorylation trends. Mol Cell Proteomics, 2014. **13**(7): p. 1787-99.

165. Marin, R., M. Demers, and R.M. Tanguay, Cell-specific heat-shock induction of Hsp23 in the eye of Drosophila melanogaster. Cell Stress Chaperones, 1996. **1**(1): p. 40-6.

166. Lockwood, B.L., C.R. Julick, and K.L. Montooth, Maternal loading of a small heat shock protein increases embryo thermal tolerance in Drosophila melanogaster. J Exp Biol, 2017. **220**(Pt 23): p. 4492-4501.

167. Montero-Barrientos, M., et al., The heterologous overexpression of hsp23, a small heat-shock protein gene from Trichoderma virens, confers thermotolerance to T. harzianum. Curr Genet, 2007. **52**(1): p. 45-53.

168. Lee, K.W., et al., Overexpression of alfalfa mitochondrial HSP23 in prokaryotic and eukaryotic model systems confers enhanced tolerance to salinity and arsenic stress. Biotechnol Lett, 2012. **34**(1): p. 167-74.

169. Lee, K.W., et al., Transgenic Expression of MsHsp23 Confers Enhanced Tolerance to Abiotic Stresses in Tall Fescue. Asian-Australas J Anim Sci, 2012. **25**(6): p. 818-23.

170. Wu, C., Clos, J., Giorgi, G., Haroun, R.I., Kim, S-J., Rabindran, S.K., Westwood, J.T., Wisniewski, J., and Yim, G., *Structure and regulation of heat shock transcription factor.*, in *The biology of heat shock proteins and molecular chaperones*, R.I. Morimoto, Tissières, A. and Georgopoulos, C., Editor. 1994, Cold Spring Harbor Laboratory Press: Plainview, New York. p. 395-416.

171. Morimoto, R.I., Regulation of the heat shock transcriptional response: cross talk between a family of heat shock factors, molecular chaperones, and negative regulators. Genes Dev, 1998. **12**(24): p. 3788-96.

172. Akerfelt, M., R.I. Morimoto, and L. Sistonen, Heat shock factors: integrators of cell stress, development and lifespan. Nat Rev Mol Cell Biol, 2010. **11**(8): p. 545-55.

173. Zhong, M., A. Orosz, and C. Wu, Direct sensing of heat and oxidation by Drosophila heat shock transcription factor. Mol Cell, 1998. **2**(1): p. 101-8.

174. Bente, M., et al., Developmentally induced changes of the proteome in the protozoan parasite Leishmania donovani. Proteomics, 2003. **3**(9): p. 1811-29.

175. Lee, M.G., The 3' untranslated region of the hsp 70 genes maintains the level of steady state mRNA in Trypanosoma brucei upon heat shock. Nucleic Acids Res, 1998. **26**(17): p. 4025-33.

176. Quijada, L., et al., Identification of a putative regulatory element in the 3'-untranslated region that controls expression of HSP70 in Leishmania infantum. Mol Biochem Parasitol, 2000. **110**(1): p. 79-91.

177. Argaman, M., R. Aly, and M. Shapira, Expression of heat shock protein 83 in Leishmania is regulated post- transcriptionally. Mol Biochem Parasitol, 1994. **64**(1): p. 95-110.

178. Zilka, A., et al., Developmental regulation of HSP83 in Leishmania: transcript levels are controlled by the efficiency of 3? RNA processing and preferential translation is directed by a determinant in the 3' UTR. J Biol Chem, 2001. **11**: p. 11.

179. David, M., et al., Preferential translation of Hsp83 in Leishmania requires a thermosensitive polypyrimidine-rich element in the 3' UTR and involves scanning of the 5' UTR. RNA, 2010. **16**(2): p. 364-74.

180. Li, J., K. Richter, and J. Buchner, Mixed Hsp90-cochaperone complexes are important for the progression of the reaction cycle. Nat Struct Mol Biol, 2011. **18**(1): p. 61-6.

181. Li, J., J. Soroka, and J. Buchner, The Hsp90 chaperone machinery: Conformational dynamics and regulation by co-chaperones. Biochimica et biophysica acta, 2012. **1823**(3): p. 624-35.

182. Bartsch, K., A. Hombach-Barrigah, and J. Clos, Hsp90 inhibitors radicicol and geldanamycin have opposing effects on Leishmania Aha1-dependent proliferation. Cell Stress Chaperones, 2017. **22**: p. 729-742.

183. Mollapour, M. and L. Neckers, Post-translational modifications of Hsp90 and their contributions to chaperone regulation. Biochimica et biophysica acta, 2012. **1823**(3): p. 648-55.

184. Mollapour, M., et al., Asymmetric Hsp90 N domain SUMOylation recruits Aha1 and ATP-competitive inhibitors. Mol Cell, 2014. **53**(2): p. 317-29.

185. Kaur, P., et al., MAPK1 of Leishmania donovani interacts and phosphorylates HSP70 and HSP90 subunits of foldosome complex. Sci Rep, 2017. **7**(1): p. 10202.

186. Hombach-Barrigah, A., et al., Leishmania donovani 90 kD Heat Shock Protein - Impact of Phosphosites on Parasite Fitness, Infectivity and Casein Kinase Affinity. Sci Rep, 2019. **9**(1): p. 5074.

187. Morales, M., et al., Phosphoproteome dynamics reveals heat shock protein complexes specific to theLeishmaniainfectious stage. Proc Natl Acad Sci U S A, 2010. **107**(18): p. 8381-8386.

188. Martel, D., et al., The low complexity regions in the C-terminus are essential for the subcellular localisation of Leishmania casein kinase 1 but not for its activity. bioRxiv, 2020.

189. Rachidi, N., et al., Pharmacological assessment defines Leishmania donovani casein kinase 1 as a drug target and reveals important functions in parasite viability and intracellular infection. Antimicrob Agents Chemother, 2014. **58**(3): p. 1501-15.

190. Clos, J. and S. Krobitsch, Heat shock as a regular feature of the life cycle ofLeishmaniaparasites. Am. Zool., 1999. **39**: p. 848-856.

191. Hombach, A. and J. Clos, No stress - Hsp90 and the signal transduction in Leishmania. Parasitology, 2014: p. doi:10.1017/S0031182013002151.

192. Beneke, T., et al., A CRISPR Cas9 high-throughput genome editing toolkit for kinetoplastids. R Soc Open Sci, 2017. **4**(5): p. 170095.

193. Beneke, T. and E. Gluenz, LeishGEdit: A Method for Rapid Gene Knockout and Tagging Using CRISPR-Cas9. Methods Mol Biol, 2019. **1971**: p. 189-210.

194. Jinek, M., et al., A programmable dual-RNA-guided DNA endonuclease in adaptive bacterial immunity. Science, 2012. **337**(6096): p. 816-21.

195. Cong, L., et al., Multiplex genome engineering using CRISPR/Cas systems. Science, 2013. **339**(6121): p. 819-23.

196. Zhang, W.W. and G. Matlashewski, CRISPR-Cas9-Mediated Genome Editing in Leishmania donovani. mBio, 2015. **6**(4): p. e00861.

197. Zhang, W.W. and G. Matlashewski, Single-Strand Annealing Plays a Major Role in Double-Strand DNA Break Repair following CRISPR-Cas9 Cleavage in Leishmania. mSphere, 2019. **4**(4).

198. Zirpel, H., The 60 kDa Heat Shock Proteins of Leishmania donovani and their impact on viability, stress tolerance, and virulence. 2018, Hamburg: Bibliothek Hamburg. p. 123.

199. Akopyants, N.S., et al., Demonstration of genetic exchange during cyclical development of Leishmania in the sand fly vector. Science, 2009. **324**(5924): p. 265-8.

200. Ubeda, J.M., et al., Modulation of gene expression in drug resistantLeishmaniais associated with gene amplification, gene deletion and chromosome aneuploidy. Genome biology, 2008. **9**(7): p. R115.

201. Opperdoes, F.R. and G.H. Coombs, Metabolism of Leishmania: proven and predicted. Trends Parasitol, 2007. **23**(4): p. 149-58.

202. Rosenzweig, D., et al., Retooling Leishmania metabolism: from sand fly gut to human macrophage. FASEB J, 2007.

203. Waters, E.R., The molecular evolution of the small heat-shock proteins in plants. Genetics, 1995. **141**(2): p. 785-95.

204. Kappe, G., J.A. Leunissen, and W.W. de Jong, Evolution and diversity of prokaryotic small heat shock proteins. Prog Mol Subcell Biol, 2002. **28**: p. 1-17.

205. de Jong, W.W., G.J. Caspers, and J.A. Leunissen, Genealogy of the alpha-crystallin--small heat-shock protein superfamily. Int J Biol Macromol, 1998. **22**(3-4): p. 151-62.

206. Scott, P., Impaired macrophage leishmanicidal activity at cutaneous temperature. Parasite Immunol, 1985. **7**(3): p. 277-88.

207. Peacock, C.S., et al., Comparative genomic analysis of three Leishmania species that cause diverse human disease. Nat Genet, 2007. **39**(7): p. 839-47.

208. Zhang, W.W., C.S. Peacock, and G. Matlashewski, A genomic-based approach combining in vivo selection in mice to identify a novel virulence gene in Leishmania. PLoS Negl Trop Dis, 2008. **2**(6): p. e248.

209. Zhang, W.W. and G. Matlashewski, Screening Leishmania donovani-specific genes required for visceral infection. Mol Microbiol, 2010. **77**(2): p. 505-17.

210. Zhang, W.W., et al., Expression of a Leishmaniadonovani nucleotide sugar transporter in Leishmaniamajor enhances survival in visceral organs. Exp Parasitol, 2011. **129**(4): p. 337-45.

211. Zhang, W.W. and G. Matlashewski, Screening Leishmania donovani complex-specific genes required for visceral disease. Methods Mol Biol, 2015. **1201**: p. 339-61.

212. Windgassen, M. and H. Krebber, Identification of Gbp2 as a novel poly(A)+ RNA-binding protein involved in the cytoplasmic delivery of messenger RNAs in yeast. EMBO Rep, 2003. **4**(3): p. 278-83.

213. Serpeloni, M., et al., UAP56 is a conserved crucial component of a divergent mRNA export pathway in Toxoplasma gondii. Mol Microbiol, 2016. **102**(4): p. 672-689.

214. Prieto Barja, P., et al., Haplotype selection as an adaptive mechanism in the protozoan pathogen Leishmania donovani. Nat Ecol Evol, 2017. **1**(12): p. 1961-1969.

215. Singh, A.K., B. Papadopoulou, and M. Ouellette, Gene amplification in amphotericin B-resistant Leishmania tarentolae. Exp Parasitol, 2001. **99**(3): p. 141-7.

216. Leprohon, P., et al., Gene expression modulation is associated with gene amplification, supernumerary chromosomes and chromosome loss in antimony-resistantLeishmania infantum. Nucleic acids research, 2009. **37**(5): p. 1387-99.

217. Cruz, A.K., R. Titus, and S.M. Beverley, Plasticity in chromosome number and testing of essential genes in Leishmania by targeting. Proc Natl Acad Sci U S A, 1993. **90**(4): p. 1599-603.

218. Spath, G.F., et al., Identification of a compensatory mutant (lpg2-REV) of Leishmania major able to survive as amastigotes within macrophages without LPG2-dependent glycoconjugates and its significance to virulence and immunization strategies. Infect Immun, 2004. **72**(6): p. 3622-7.

219. Reiling, L., et al., Spontaneous recovery of pathogenicity by Leishmania major hsp100-/- alters the immune response in mice. Infect Immun, 2006. **74**(11): p. 6027-36.

220. Franssen, S.U., et al., Global genome diversity of the Leishmania donovani complex. Elife, 2020. **9**.

221. Mannaert, A., et al., Adaptive mechanisms in pathogens: universal aneuploidy in Leishmania. Trends Parasitol, 2012. **28**(9): p. 370-6.

222. Laffitte, M.N., et al., Plasticity of the Leishmania genome leading to gene copy number variations and drug resistance. F1000Res, 2016. **5**: p. 2350.

223. Cuypers, B., et al., Integrated genomic and metabolomic profiling of ISC1, an emerging Leishmania donovani population in the Indian subcontinent. Infect Genet Evol, 2018. **62**: p. 170-178.

224. Dumetz, F., et al., Molecular Preadaptation to Antimony Resistance in Leishmania donovani on the Indian Subcontinent. mSphere, 2018. **3**(2).

225. MacArthur, M.W. and J.M. Thornton, Influence of proline residues on protein conformation. J Mol Biol, 1991. **218**(2): p. 397-412.

226. Iakobashvili, R. and A. Lapidot, Low temperature cycled PCR protocol for Klenow fragment of DNA polymerase I in the presence of proline. Nucleic Acids Res, 1999. **27**(6): p. 1566-8.

227. Thompson, M.J. and D. Eisenberg, Transproteomic evidence of a loop-deletion mechanism for enhancing protein thermostability. J Mol Biol, 1999. **290**(2): p. 595-604.

228. Samuel, D., et al., Proline inhibits aggregation during protein refolding. Protein Sci, 2000. **9**(2): p. 344-52.

229. Zscherp, C., et al., Effect of proline to alanine mutation on the thermal stability of the all-beta-sheet protein tendamistat. Biochim Biophys Acta, 2003. **1651**(1-2): p. 139-45.

230. Gazanion, E., et al., Cos-Seq for high-throughput identification of drug target and resistance mechanisms in the protozoan parasite Leishmania. Proc Natl Acad Sci U S A, 2016. **113**(21): p. E3012-21.

231. Matsumura, S. and M. Takeda, Phosphoprotein kinases from rat liver cytosol. Biochim Biophys Acta, 1972. **289**(1): p. 237-41.

232. Knippschild, U., et al., The casein kinase 1 family: participation in multiple cellular processes in eukaryotes. Cell Signal, 2005. **17**(6): p. 675-89.

233. Carmel, G., et al., Expression, purification, crystallization, and preliminary x-ray analysis of casein kinase-1 from Schizosaccharomyces pombe. J Biol Chem, 1994. **269**(10): p. 7304-9.
234. Xu, R.M., et al., Crystal structure of casein kinase-1, a phosphate-directed protein kinase. Embo j, 1995. **14**(5): p. 1015-23.
235. Longenecker, K.L., P.J. Roach, and T.D. Hurley, Three-dimensional structure of mammalian casein kinase I: molecular basis for phosphate recognition. J Mol Biol, 1996. **257**(3): p. 618-31.
236. Flotow, H., et al., Phosphate groups as substrate determinants for casein kinase I action. J Biol Chem, 1990. **265**(24): p. 14264-9.
237. Martel, D., et al., Characterisation of Casein Kinase 1.1 in Leishmania donovani Using the CRISPR Cas9 Toolkit. Biomed Res Int, 2017. **2017**: p. 4635605.
238. Dan-Goor, M., et al., Identification of a secreted casein kinase 1 in Leishmania donovani: effect of protein over expression on parasite growth and virulence. PLoS One, 2013. **8**(11): p. e79287.
239. Liu, J., et al., Mammalian casein kinase 1alpha and its leishmanial ortholog regulate stability of IFNAR1 and type I interferon signaling. Mol Cell Biol, 2009. **29**(24): p. 6401-12.
240. Dorin-Semblat, D., et al., Malaria Parasite-Infected Erythrocytes Secrete PfCK1, the Plasmodium Homologue of the Pleiotropic Protein Kinase Casein Kinase 1. PLoS One, 2015. **10**(12): p. e0139591.
241. Batty, M.B., et al., Interaction of Plasmodium falciparum casein kinase 1 with components of host cell protein trafficking machinery. IUBMB Life, 2020. **72**(6): p. 1243-1249.
242. Spath, G.F., S. Drini, and N. Rachidi, A touch of Zen: post-translational regulation of the Leishmania stress response. Cell Microbiol, 2015. **17**(5): p. 632-8.
243. Saar, Y., et al., Characterization of developmentally-regulated activities in axenic amastigotes of Leishmania donovani. Mol Biochem Parasitol, 1998. **95**(1): p. 9-20.
244. Debrabant, A., et al., Generation of Leishmania donovani axenic amastigotes: their growth and biological characteristics. Int J Parasitol, 2004. **34**(2): p. 205-17.
245. Barak, E., et al., Differentiation of Leishmania donovani in host-free system: analysis of signal perception and response. Mol Biochem Parasitol, 2005. **141**(1): p. 99-108.
246. Morales, M.A., et al., Phosphoproteomic analysis ofLeishmania donovanipro- and amastigote stages. Proteomics, 2008. **8**(2): p. 350-63.
247. De Muylder, G., et al., A screen against Leishmania intracellular amastigotes: comparison to a promastigote screen and identification of a host cell-specific hit. PLoS Negl Trop Dis, 2011. **5**(7): p. e1253.
248. Tsigankov, P., et al., Phosphoproteomic analysis of differentiating Leishmania parasites reveals a unique stage-specific phosphorylation motif. J Proteome Res, 2013. **12**(7): p. 3405-12.
249. Cloutier, S., et al., Translational control through eIF2alpha phosphorylation during the Leishmania differentiation process. PLoS One, 2012. **7**(5): p. e35085.

250. Rosenzweig, D., et al., Post-translational modification of cellular proteins during Leishmania donovani differentiation. Proteomics, 2008. **8**(9): p. 1843-50.
251. Kobayashi, T., et al., Regulation of cytosolic prostaglandin E synthase by phosphorylation. Biochem J, 2004. **381**(Pt 1): p. 59-69.
252. Tosoni, K., et al., The p23 co-chaperone protein is a novel substrate of CK2 in Arabidopsis. Mol Cell Biochem, 2011. **356**(1-2): p. 245-54.
253. Ito, H., et al., Phosphorylation of alphaB-crystallin in response to various types of stress. J Biol Chem, 1997. **272**(47): p. 29934-41.
254. Thornell, E. and A. Aquilina, Regulation of αA- and αB-crystallins via phosphorylation in cellular homeostasis. Cell Mol Life Sci, 2015. **72**(21): p. 4127-37.
255. Graves, P.R. and P.J. Roach, Role of COOH-terminal phosphorylation in the regulation of casein kinase I delta. J Biol Chem, 1995. **270**(37): p. 21689-94.
256. Cegielska, A., et al., Autoinhibition of casein kinase I epsilon (CKI epsilon) is relieved by protein phosphatases and limited proteolysis. J Biol Chem, 1998. **273**(3): p. 1357-64.
257. Gietzen, K.F. and D.M. Virshup, Identification of inhibitory autophosphorylation sites in casein kinase I epsilon. J Biol Chem, 1999. **274**(45): p. 32063-70.
258. Yilmaz, M., et al., Phosphorylation at Ser(2)(6) in the ATP-binding site of Ca(2)(+)/ calmodulin-dependent kinase II as a mechanism for switching off the kinase activity. Biosci Rep, 2013. **33**(2).
259. Dahlberg, C.L., et al., Interactions between Casein kinase Iepsilon (CKIepsilon) and two substrates from disparate signaling pathways reveal mechanisms for substrate-kinase specificity. PLoS One, 2009. **4**(3): p. e4766.
260. Cruciat, C.M., et al., RNA helicase DDX3 is a regulatory subunit of casein kinase 1 in Wnt-β-catenin signaling. Science, 2013. **339**(6126): p. 1436-41.
261. Muller, P., et al., C-terminal phosphorylation of Hsp70 and Hsp90 regulates alternate binding to co-chaperones CHIP and HOP to determine cellular protein folding/degradation balances. Oncogene, 2013. **32**(25): p. 3101-10.
262. Fang, Y., et al., SBA1 encodes a yeast hsp90 cochaperone that is homologous to vertebrate p23 proteins. Mol Cell Biol, 1998. **18**(7): p. 3727-34.
263. Felts, S.J. and D.O. Toft, p23, a simple protein with complex activities. Cell Stress Chaperones, 2003. **8**(2): p. 108-13.
264. Richter, K., S. Walter, and J. Buchner, The Co-chaperone Sba1 connects the ATPase reaction of Hsp90 to the progression of the chaperone cycle. J Mol Biol, 2004. **342**(5): p. 1403-13.
265. McLaughlin, S.H., et al., The co-chaperone p23 arrests the Hsp90 ATPase cycle to trap client proteins. J Mol Biol, 2006. **356**(3): p. 746-58.
266. Chua, C.S., et al., Characterization of Plasmodium falciparum co-chaperone p23: its intrinsic chaperone activity and interaction with Hsp90. Cell Mol Life Sci, 2010. **67**(10): p. 1675-86.

267. Echeverria, P.C., et al., The Hsp90 co-chaperone p23 of Toxoplasma gondii: Identification, functional analysis and dynamic interactome determination. Mol Biochem Parasitol, 2010. **172**(2): p. 129-40.
268. Stebbins, C.E., et al., Crystal structure of an Hsp90-geldanamycin complex: targeting of a protein chaperone by an antitumor agent. Cell, 1997. **89**(2): p. 239-50.
269. Forafonov, F., et al., p23/Sba1p protects against Hsp90 inhibitors independently of its intrinsic chaperone activity. Molecular and cellular biology, 2008. **28**(10): p. 3446-56.
270. Gilbert, I.H., Drug discovery for neglected diseases: molecular target-based and phenotypic approaches. J Med Chem, 2013. **56**(20): p. 7719-26.
271. Chen, Y.T., et al., Synthesis of macrocyclic trypanosomal cysteine protease inhibitors. Bioorg Med Chem Lett, 2008. **18**(22): p. 5860-3.
272. Das, P., et al., Protease inhibitors in potential drug development for Leishmaniasis. Indian J Biochem Biophys, 2013. **50**(5): p. 363-76.
273. Naula, C., M. Parsons, and J.C. Mottram, Protein kinases as drug targets in trypanosomes and Leishmania. Biochim Biophys Acta, 2005. **1754**(1-2): p. 151-9.
274. Wyllie, S., et al., Cyclin-dependent kinase 12 is a drug target for visceral leishmaniasis. Nature, 2018. **560**(7717): p. 192-197.
275. Raj, S., et al., Biochemical characterization and chemical validation of Leishmania MAP Kinase-3 as a potential drug target. Sci Rep, 2019. **9**(1): p. 16209.
276. Harris, M.T., W.G. Mitchell, and J.C. Morris, Targeting protozoan parasite metabolism: glycolytic enzymes in the therapeutic crosshairs. Curr Med Chem, 2014. **21**(15): p. 1668-78.
277. Sharma, N., et al., Evaluation of plumbagin and its derivative as potential modulators of redox thiol metabolism of Leishmania parasite. Parasitol Res, 2012. **110**(1): p. 341-8.
278. Datta, A.K., R. Datta, and B. Sen, Antiparasitic chemotherapy: tinkering with the purine salvage pathway. Adv Exp Med Biol, 2008. **625**: p. 116-32.
279. Gilbert, I.H., Inhibitors of dihydrofolate reductase in Leishmania and trypanosomes. Biochim Biophys Acta, 2002. **1587**(2-3): p. 249-57.
280. Rajasekaran, R. and Y.P. Chen, Potential therapeutic targets and the role of technology in developing novel antileishmanial drugs. Drug Discov Today, 2015. **20**(8): p. 958-68.
281. Dey, R., et al., Live attenuated Leishmania donovani p27 gene knockout parasites are nonpathogenic and elicit long-term protective immunity in BALB/c mice. J Immunol, 2013. **190**(5): p. 2138-49.
282. Elikaee, S., et al., Leishmania major p27 gene knockout as a novel live attenuated vaccine candidate: Protective immunity and efficacy evaluation against cutaneous and visceral leishmaniasis in BALB/c mice. Vaccine, 2019. **37**(24): p. 3221-3228.
283. Osorio y Fortéa, J., et al., Transcriptional signatures of BALB/c mouse macrophages housing multiplying Leishmania amazonensis amastigotes. BMC Genomics, 2009. **10**: p. 119.

284. Rabhi, I., et al., Transcriptomic signature of Leishmania infected mice macrophages: a metabolic point of view. PLoS Negl Trop Dis, 2012. **6**(8): p. e1763.

285. Conteduca, V., et al., Therapy of chronic hepatitis C virus infection in the era of direct-acting and host-targeting antiviral agents. J Infect, 2014. **68**(1): p. 1-20.

286. Czyz, D.M., et al., Host-directed antimicrobial drugs with broad-spectrum efficacy against intracellular bacterial pathogens. mBio, 2014. **5**(4): p. e01534-14.

287. Zumla, A., et al., Host-directed therapies for improving poor treatment outcomes associated with the middle east respiratory syndrome coronavirus infections. Int J Infect Dis, 2015. **40**: p. 71-4.

288. Buates, S. and G. Matlashewski, Treatment of experimental leishmaniasis with the immunomodulators imiquimod and S-28463: efficacy and mode of action. J Infect Dis, 1999. **179**(6): p. 1485-94.

289. De Muylder, G., et al., Naloxonazine, an Amastigote-Specific Compound, Affects Leishmania Parasites through Modulation of Host-Encoded Functions. PLoS Negl Trop Dis, 2016. **10**(12): p. e0005234.

290. Laemmli, U.K., Cleavage of structural proteins during the assembly of the head of bacteriophage T4. Nature, 1970. **227**(5259): p. 680-5.

291. Ommen, G., S. Lorenz, and J. Clos, One-step generation of double-allele gene replacement mutants in Leishmania donovani. Int J Parasitol, 2009. **39**(5): p. 541-6.

292. Piper, P.W., The heat shock and ethanol stress responses of yeast exhibit extensive similarity and functional overlap. FEMS Microbiol Lett, 1995. **134**(2-3): p. 121-7.

293. Babicki, S., et al., Heatmapper: web-enabled heat mapping for all. Nucleic Acids Res, 2016. **44**(W1): p. W147-53.

294. Langmead, B., et al., Ultrafast and memory-efficient alignment of short DNA sequences to the human genome. Genome Biol, 2009. **10**(3): p. R25.

6 Publications

1. Kröber-Boncardo, C., J. Grünebast and J. Clos (2020). Heat Shock Proteins in Leishmania Parasites. Prokaryotic and Eukaryotic Heat Shock Proteins in Infectious Disease. Springer**:** in press

2. Kröber-Boncardo, C., et al., Casein Kinase 1.2 Over Expression Restores Stress Resistance to Leishmania donovani HSP23 Null Mutants (2020). Scientific reports: in press

7 Acknowledgements

My PhD thesis would not have been possible without the support of many different people. First of all, I would like to thank my supervisor, Dr. Joachim Clos for his supportive and helpful advice and discussions throughout my whole thesis.

Furthermore, I would like to thank Dr. Tobias Spielmann and Prof. Dr. Iris Bruchhaus for co-supervision and their valuable contributions in my PhD seminars.

My everyday lab life would have been much harder without the support of Anne MacDonald, Annika Bea, Christine Brinker, Dr. Dolores Jiménez Antón, Dorothea Zander-Dinse, Dr. Henner Zirpel, Janne Grünebast, Dr. Vanessa Adaui. You made working in the lab always fun, you were always happy to help out, and to discuss science (among other things).

A special thanks again to those people who have worked on this project and helped me out: Tine for all the cloning work (and the chill out in the garden), Anne MacDonald for all the laborious cell counting at the CASY and my labrotation students Lisa, Preeja and Annika. Also, I would like to thank Valerie Bornholdt for proofreading this thesis.

Furthermore, I am thankful to Dr. Daniel Cadar for the use of the sequencing facility, and Dr. Najma Rachidi for support with the casein kinase assays and for the gift of the anti-CK1.2 antibody. Also, I would like to thank Dr. Stephan Lorenzen for the bioinformatics.

Outside the Lab, I am grateful for the friendship of Sarah, Ka, Kathrin, Franzi, Rosalie. Even if we meet less often than we should, you were always up for a phone call and listened to my complaints when experiments failed.

Zuletzt gebührt mein Dank den Menschen, die schon mein Leben lang hinter mir stehen: Meiner Familie Laura, Leonie, Mama, Papa, Oma und der Rest der Familie. Danke für die Unterstützung, die ich während meines Studiums hatte, und dafür, dass ihr immer für mich da ward!

Zum Schluss möchte ich mich bei meinem Ehemann und größtem Unterstützer, Nicolas, bedanken. Für deine Hilfe und Geduld während der vielen stressigen Phasen im Studium bin ich dir unendlich dankbar!

Language Certificate

I am a native speaker, have read the present PhD thesis and hereby confirm that it complies with the rules of the English language.

Hamburg, 8th September 2020 Valerie Bornholdt